

This document is the unedited Author's version of a Submitted Work that was subsequently accepted for publication in ACS Nano, copyright © American Chemical Society after peer review. To access the final edited and published work see <https://pubs.acs.org/doi/full/10.1021/acsnano.2c01697>.

Access to this work was provided by the University of Maryland, Baltimore County (UMBC) ScholarWorks@UMBC digital repository on the Maryland Shared Open Access (MD-SOAR) platform.

**Please provide feedback**

Please support the ScholarWorks@UMBC repository by emailing [scholarworks-group@umbc.edu](mailto:scholarworks-group@umbc.edu) and telling us what having access to this work means to you and why it's important to you. Thank you.

# Diagnostic Approaches For COVID-19: Lessons Learned and the Path Forward

Maha Alafeef and Dipanjan Pan\*



Cite This: *ACS Nano* 2022, 16, 11545–11576



Read Online

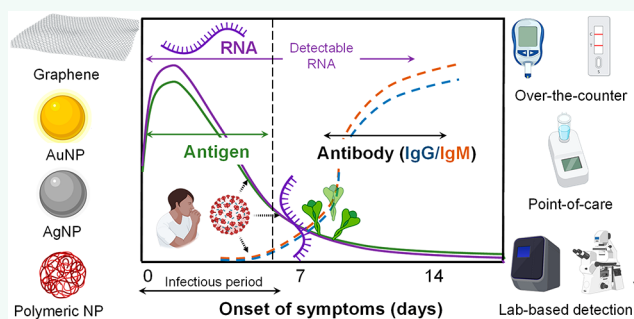
ACCESS |

Metrics & More

Article Recommendations

**ABSTRACT:** Coronavirus disease 2019 (COVID-19) is a transmitted respiratory disease caused by the infection of the severe acute respiratory syndrome coronavirus 2 (SARS-CoV-2). Although humankind has experienced several outbreaks of infectious diseases, the COVID-19 pandemic has the highest rate of infection and has had high levels of social and economic repercussions. The current COVID-19 pandemic has highlighted the limitations of existing virological tests, which have failed to be adopted at a rate to properly slow the rapid spread of SARS-CoV-2. Pandemic preparedness has developed as a focus of many governments around the world in the event of a future outbreak. Despite the largely widespread availability of vaccines, the importance of testing has not diminished to monitor the evolution of the virus and the resulting stages of the pandemic. Therefore, developing diagnostic technology that serves as a line of defense has become imperative. In particular, that test should satisfy three criteria to be widely adopted: simplicity, economic feasibility, and accessibility. At the heart of it all, it must enable early diagnosis in the course of infection to reduce spread. However, diagnostic manufacturers need guidance on the optimal characteristics of a virological test to ensure pandemic preparedness and to aid in the effective treatment of viral infections. Nanomaterials are a decisive element in developing COVID-19 diagnostic kits as well as a key contributor to enhance the performance of existing tests. Our objective is to develop a profile of the criteria that should be available in a platform as the target product. In this work, virus detection tests were evaluated from the perspective of the COVID-19 pandemic, and then we generalized the requirements to develop a target product profile for a platform for virus detection.

**KEYWORDS:** *infectious diseases, pandemic preparedness, COVID-19, diagnostic tests, biosensing, advanced materials, nanotechnology, antigen tests, molecular tests*



## INTRODUCTION

Coronavirus disease 2019 (COVID-19) is a transmitted respiratory disease caused by the infection of the severe acute respiratory syndrome coronavirus 2 (SARS-CoV-2), which was discovered in December 2019 in Wuhan, China.<sup>1,2</sup> With a high rate of infection, the COVID-19 pandemic has pervaded nearly every facet of society, with a lasting impact across the global economy and health care systems.<sup>3,4</sup> Many mandates and regulations were put in place as a part of the effort to slow the spread of the disease. People were asked to intensify their hygiene practices such as handwashing and to practice social distancing by limiting close contact with others, especially in crowded areas. Businesses and schools were forced to close, or vastly reduce in-person contact, transitioning to work remotely. These are life-changing events that could have been avoided by the effective control of the SARS-CoV-2 virus spread. The limited availability of rapid

tests to detect COVID-19 was the major obstacle to containing the spread of the virus.<sup>5–8</sup> In addition, the situation got further out of control because of the way people with stronger “adaptive” immune systems were able to respond to the infection. As some people had a stronger “innate” immune response to the virus, they presented no apparent disease symptoms. The asymptomatic, yet highly infectious subjects represented 17.9% of the infected cases where an infected asymptomatic or presymptomatic patient on average could infect 5.6 other people.<sup>9,10</sup>

**Received:** February 17, 2022

**Accepted:** July 12, 2022

**Published:** August 3, 2022



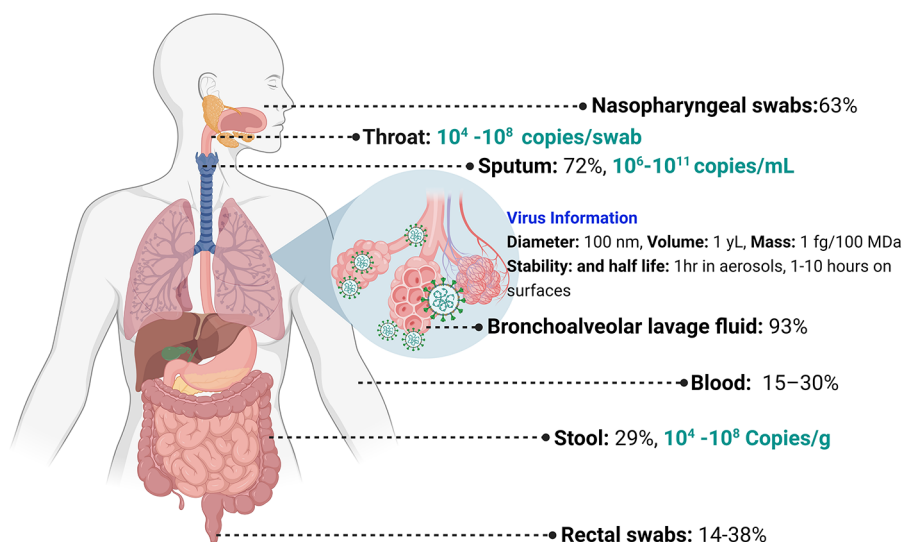


**Figure 1.** Graphical illustration of the distribution of the SARS-CoV-2 viral load in various bodily fluids (green) and the true positive rate (TPR) of a reverse transcription polymerase chain reaction (PCR) test as per specimen source (black). Basic information about the SARS-CoV-2 virus including size, genome, mass, stability, and half-life time is also presented.

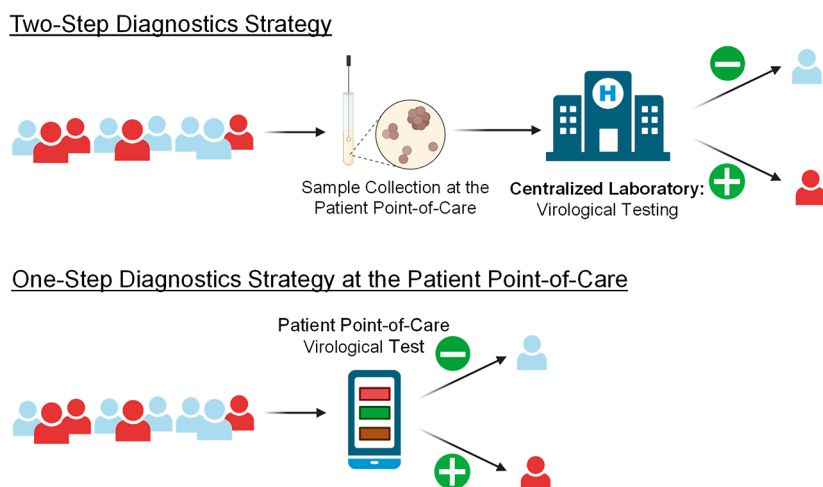


**Figure 2.** COVID-19 testing can be categorized as either a two-step testing method (top) or a one-step method (bottom). The two-step testing strategy involves the collection of the patient sample on site and then transporting the samples to a centralized laboratory to perform the testing; the commonly used test is RT-PCR. In the one-step testing method, the patient's sample is collected and tested on site at the patient's point-of-care side.

Many people have shown no symptoms or mild ones which prevent the identification of the carriers and facilitate its wide spread. Thus, easy access to accurate technologies for the early diagnosis of SARS-CoV-2 is critical to stopping the silent spread of COVID-19. Frequent testing would also allow us to gain a realistic estimation of the actual number of infected subjects. Furthermore, the widespread availability of rapid and accurate COVID-19 tests enables the detection of positive cases on the spot to avoid the unnecessary quarantine of negative cases and allow a physician to take an early step to save the patient's life before they develop severe symptoms.

At the peak of the COVID-19 outbreak, it was estimated that an infected person may carry around one billion to a hundred billion virions, with a total of  $10^6$  to  $10^8$  virions per gram of tissue.<sup>11,12</sup> The total number of produced virions can be estimated using the following equation:

$$N_{\text{virions}} = \frac{I}{t} \quad (1)$$

where  $I$  represents the integral of the viral load curve (virions  $\times$  time), and  $t$  is the time the virus resides in the body which is the reciprocal of the virus recovery rate. The production of the virus is found to be around  $3 \times 10^9$  to  $3 \times 10^{12}$  virions during the whole course of infection, which is about 3–30-fold the virions during the peak of infection.<sup>11,13</sup>

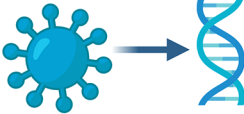
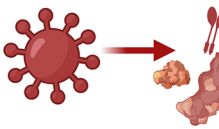
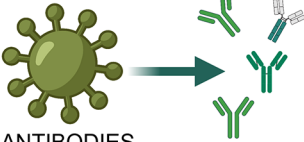
Myriad advancements have been made in biosensing approaches that can aid in the early detection of COVID-19. In this review article, we will present a comprehensive landscape of the various sensing strategies adopted during the pandemic and provide a description, analysis, and interpretation that will allow readers to assess the value of the test. This review will evaluate the strengths and weaknesses of the presented ideas, assess the regulatory guidelines, and outline a target product profile (TPP) with the necessary characteristics of an innovative product to address clinical needs during a future pandemic.

Table 1. Summary of the Tests' Characteristics Performance

| test category                           | nucleic acid tests  |  | antigen tests   |  | serological tests   |          |
|---|---|--|---|--|---|----------|
|   | laboratory-based tests  | home-based and over-the-counter tests (OCT)  | rapid tests   | home use   | home-based tests  | home use |
| target population                       | clinics<br>hospitals<br>intensive care unit (ICU)<br>urgent care<br>immediate care<br>central laboratory<br>diagnostic laboratory<br>skilled personnel<br>nurse<br>physician<br>laboratory technician | home use<br>pharmacy<br>doctor's office<br>urgent care<br>immediate care<br>doctor's office<br>home use<br>layperson<br>skilled personnel<br>nurse<br>physician<br>laboratory technician | clinics<br>hospitals<br>ICU<br>hospitals<br>intensive care unit (ICU)<br>urgent care<br>immediate care<br>layperson and anyone regardless of their level of expertise | pharmacy<br>doctor's office  | home use<br>pharmacy<br>doctor's office                     |          |
| target operator                         |   |  |   |  | layperson and anyone regardless of their level of expertise |          |
| performance characteristics             |   |  |   |  |   |          |
| LOD:                                    | high with minimal value of 1 cp/reaction <sup>22,23</sup>   | good and varies based on the test with a minimum of 900 copies/mL <sup>24,25</sup>   | good with a minimum of $1 \times 10^6$ copies/mL <sup>26,27</sup>   | good but cannot be used to diagnose active infection <sup>2-5</sup>  |   |          |
| sensitivity:                            | high  | good   | low, especially for the samples with Ct > 35 <sup>28,29,30</sup>  | good   |   |          |
| specificity:                            | high  | good, some tests show resistance to mutation   | good  | high   |   |          |
| accuracy:                               | high  | good   | good  | high   |   |          |
| repeatability                           | good  | good   | good  | good   |   |          |
| hysteresis:                             | good  | good   | good  | good   |   |          |
| quantification:                         | yes   | most tests are qualitative   | NA  | yes  |   |          |
| polyvalency:                            | possible  | possible   | possible  | possible   |   |          |
| stability:                              | good  | good   | good  | good   |   |          |
| type of specimen                        | nasal swab, saliva, oral swab, wastewater, stool, urine   | nasal swab, saliva, oral swab.   | nasal swab, saliva, oral swab   | nasal swab, saliva, oral swab  | blood draw and fingerprint                                  |          |
| sample preparation procedure            | RNA extraction, sample transport to the laboratory in viral transport medium (VTM)  | direct analysis of the collected samples through POC column isolation or lysis buffer  | direct analysis of the collected samples using a POC device, chemical lysing  | direct analysis of the collected whole blood sample into a POC device or using whole blood to plasma extraction POC system |   |          |
| required equipment and instrumentations | centrifuge, pipetting, safety cabinet, RNA-extraction tubes, columns, etc.  | minimal instrumentation, battery-operated heating system, electrical reader, etc.  | minimal instrumentation   | minimal instrumentation  |   |          |
| sample-to-assay time                    | hours to days   | minutes to hours   | minutes   | minutes  | minutes   |          |
| test's price                            | expensive to moderate   | affordable   | affordable  | affordable   | affordable  |          |
| power usage                             | high  | low to none  | low to none   | low to none  | low to none   |          |



Table 2. Categories of Available COVID-19 Tests

| TYPE OF THE TEST | DETECTING VIRUS   |   | DETECTING ANTIBODIES  |
|------------------|---|---|---|
|                  | MOLECULAR   | ANTIGEN   | SEROLOGICAL   |
| HOW IT WORKS     |  <p><b>GENETIC</b><br/>Detects the virus genetic materials</p> |  <p><b>PROTEINS</b><br/>Detects the virus proteins</p> |  <p><b>ANTIBODIES</b><br/>Detects the antibodies found in the blood which formed as a response to the virus infection instead of the virus itself.</p> |
| SAMPLE TYPE      | Nasal or nasopharyngeal swab or saliva  | Nasal or nasopharyngeal swab or blood or saliva   | Blood   |
| INFORMATION      | Current or recent infection   | Current or recent infection   | Past infection  |
| ADVANTAGES       | Accurate, detect the infection at its earliest  | Fast and cost effective   | Immunity check  |
| LIMITATIONS      | Cost, time, current infection only  | Less accurate, current infection only   | High false positive rate, not for early detection, not for diagnosis  |

## DISTRIBUTION OF SARS-CoV-2

The SARS-CoV-2 virus is 100 nm in diameter with a mass equivalent to 1 fg and a volume of 1  $\mu\text{L}$ .<sup>11,14,15</sup> The viral load of SARS-CoV-2 was found to be sample-dependent, varying across sputum, serum, stool, and saliva samples (Figure 1).<sup>14</sup>

The level of the cell-specific expression of the angiotensin-converting enzyme-2 (ACE2) receptor was found to be the main factor governing the spread of SARS-CoV-2 from the respiratory tract to the other body organs. During the initial phase of the infection, the amount of SARS-CoV-2 load is high in the respiratory tract, reaching its maximum in the second week, followed by the fast clearance of the virus from the body. On the other hand, in severe cases, SARS-CoV-2 was found to be high in the third and fourth weeks with a long virus-shedding period.<sup>16,17</sup> Furthermore, plasma samples exhibit the highest prevalence of SARS-CoV-2 viral load that is accompanied by lower absolute lymphocyte counts and high level of inflammation biomarkers such as C-reactive protein and interleukin 6 (IL-6).<sup>18–20</sup>

## OVERVIEW OF THE CHARACTERISTIC REQUIREMENTS FOR COVID-19 DIAGNOSTIC TESTS

As the world witnessed the rapid spread of COVID-19, the importance of delivering the test results promptly to slow the spread of the infection became evident. Current active infection can be detected through several approaches depending on the nature of the disease and the causative pathogen. This can be achieved through one- or two-step diagnostics strategies as shown in Figure 2. The two-step diagnostic approach consists of two main stages: first, the collection of the clinical sample at the patient's point-of-care, followed by transporting the sample to a centralized laboratory to run a virological test. However, in the one-step diagnostic strategy, the sample collection, preprocessing, and pathogen detection

take place altogether, namely, by using a point-of-care device, at the patient's bedside.

Table 1 details the performance characteristics of the three main test categories used in COVID-19 diagnosis. Here, the target population refers to people with a medium and high prevalence of the disease under investigation. The target operator discusses the person performing the test, and they vary based on their training level. In the context of the one-step test, optimally the test should be easily performed by a community worker with minimal training. Analytical and clinical performances of the test are correlated with the trust level of the platform. Among some of the important characteristics of the test is the sensitivity or the limit of detection (LOD), which represents the minimum concentration of an analyte that can be detected using a specific analytical method. Sample preparation may vary with the testing strategy. For example, a COVID-19 nucleic acid test that involves an RNA-extraction step is difficult to be performed outside a traditional laboratory setting. Advanced nanomaterials can serve as an important component that helps in reducing the test's complexity by replacing the time-consuming RNA-extraction step with a simple capturing methodology. A test that involves the elution of the virus RNA by chemical (using lysis buffer) or mechanical (using magnetic beads) means can be brought near the patient. The specimen is another test operation characteristic that is critical to the test performance. For example, after the onset of symptoms, the viral load in the sputum samples collected from the throat swabs reaches a peak value of  $10^4$ – $10^7$  copies/mL in 5–6 days. Whereas using real-time polymerase chain reaction (RT-PCR), the test positivity varies with the specimen type and has been found to be 78%, 16%, and 88% for saliva, tears, and blood samples, respectively, as shown in Figure 1.<sup>21</sup>

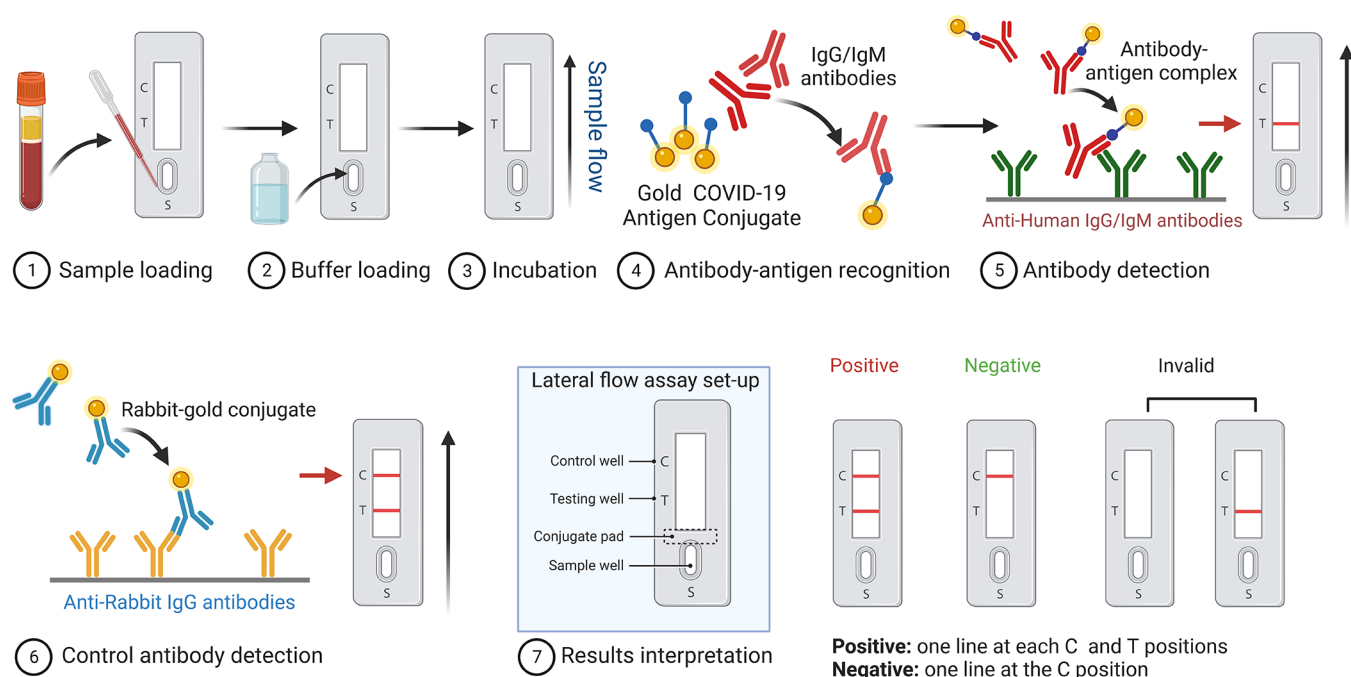


**Figure 3.** Schematic representation of the COVID-19 serological test. The test consists of recombinant antigens specific for the SARS-CoV-2 immobilized onto nitrocellulose paper. Nanoparticles conjugated with mouse anti-human IgM and IgG antibodies immobilized on conjugate pads. The antibodies in the patient sample will be captured using a SARS-CoV-2-specific recombinant antigen. When SARS-CoV-2-specific IgG/IgM is available in the sample, the test band will show color on the test strip, indicating a positive test result.

In the following sections, we will analyze the currently available tests by contrasting the performance alongside the projected performance using the metrics outlined in Table 1.

Currently, there are many tests available commercially for the detection of COVID-19.<sup>30</sup> Some of these tests received approval for emergency use authorization (EUA) from the U.S. Food and Drug Administration (FDA).<sup>31,32</sup> These tests fall into three main categories based on the targeted analyte: nucleic acid–based (NAT or molecular), antigen-based, and antibody-based testing methods. NAT or molecular tests can identify the infected subjects during the acute phase of infection by detecting the presence of viral nucleic acid in the tested sample. These molecular tests involve the use of polymerase chain reaction (PCR)-based techniques<sup>16,23,33</sup> or rely on DNA–RNA hybridization for the detection of SARS-CoV-2 viral RNA.<sup>34</sup> The second category is the antigen tests that involve the detection of the virus proteins either from saliva, nasal, or nasopharyngeal swabs, or even in the blood.<sup>35–39</sup> The third category is the serological or immunological assay which is an indirect method of detecting the virus as the test looks for developed antibodies as a response to the infection rather than detecting the virus itself.<sup>40–42</sup> Serological tests detect the presence of antibodies in the blood when the body is responding to the viral infection. This type of test is important to identify the potential convalescent plasma donors and to monitor the subject's immune status over time.<sup>43–45</sup> Many rapid serological tests were quickly developed,<sup>40–42,46</sup> however, they do not provide information on active infection as the body takes several weeks to develop a detectable level of antibodies following the infection.<sup>47</sup> Table 2 summarizes the differences between the three main testing methods currently employed in the diagnosis of COVID-19.

## SEROLOGICAL TESTS

As discussed briefly, serology tests do not detect the virus itself, but instead, they look for the presence of antibodies produced by the body's immune system as a response to the infection.<sup>16,40,42</sup> For the serological tests to work, the body needs to develop a detectable antibody level which takes 5–7 days.<sup>13,20</sup> Serological tests cannot be used to diagnose acute or active COVID-19 infection.<sup>31,40,41</sup> The performance characteristics of such tests are assessed based on their clinical sensitivity and specificity using a 95% confidence interval. The sensitivity or the true positive rate (TPR) is evaluated based on the ability of the test to identify the samples with antibodies to SARS-CoV-2. Specificity or true negative rate (TNR) refers to the test's ability to identify the samples that lack SARS-CoV-2 antibodies.

The larger the number of data sets used in the test evaluation, the smaller the confidence interval, which means having higher confidence in the estimated sensitivity and specificity. Although serology tests cannot be used to detect acute COVID-19 cases, they play a major role in the fight against COVID-19 by supporting the effort of the healthcare providers in identifying the subjects who have developed an adaptive immune response against the infection.<sup>47</sup> Nanoparticles serve as a component in the serological test, being a key element of the transduction of the antigen–antibodies interaction.<sup>48–50</sup> Gold nanoparticles have been used as a colorimetric label in a lateral flow-based assay for the rapid detection of a serological response to SARS-CoV-2.<sup>48–52</sup> The assay uses gold nanoparticles (AuNPs) conjugated to antigens specific for SARS-CoV-2. The IgG or IgM presented in the loaded samples (either blood or saliva) would bind to the SARS-CoV-2 antigen and antibody, which can be viewed as a clear test band (Figure 3). The assay has a fast turn-around time of 20 min and high accuracy of ~90%.<sup>51</sup> Table 3

Table 3. Summary of the Performance of Selected FDA-Granted EUA Serological Tests<sup>31</sup>

| company name             | test                                   | technology                            | target                 | Ab <sup>a</sup> | sensitivity (PPA); *TP/TP + FN (95% confidence interval) | specificity (NPA); *TN/TN + FP (95% confidence interval) |
|--------------------------|--|---------------------------------------|------------------------|-----------------|--|--|
| Abbott Laboratories Inc. | AdviseDx SARS-CoV-2 IgG II (Alinity)   | semiquantitative high-throughput CMIA | spike                  | IgG             | 98.1%; 51/52 (89.9–99.7%)                                | 99.6%; 2000/2008 (99.2–99.8%)                            |
| Abbott Laboratories Inc. | AdviseDx SARS-CoV-2 IgG II (Architect) | semiquantitative high-throughput CMIA |                        |                 | 98.1%; 52/53 (90.1–99.7%)                                | 99.6%; (1999/2008) (99.2–99.8%)                          |
| Abbott                   | Alinity i SARS-CoV-2 IgG               | high-throughput CMIA                  | nucleocapsid           | IgG             | 100%; 34/34 (89.9–100%)                                  | 99.0%; 99/100 (94.6–99.8%)                               |
| Abbott                   | ARCHITECT SARS-CoV-2 IgG               | high-throughput CMIA                  | nucleocapsid           | IgG             | 100%; 88/88 (95.8–100%)                                  | 99.6%; 1066/1070 (99.0–99.9%)                            |
| Abbott Laboratories Inc. | AdviseDx SARS-CoV-2 IgM (Alinity (i))  | high-throughput CMIA                  | spike                  | IgM             | 95.0%; 38/40 (83.5–98.6%)                                | 99.6%; 2972/2985 (99.3–99.7%)                            |
| Abbott Laboratories Inc. | AdviseDx SARS-CoV-2 IgM (Architect)    | high-throughput CMIA                  | spike                  | IgM             | 95.0%; 38/40 (83.5–98.6%)                                | 99.6%; 2952/2965 (99.3–99.7%)                            |
| Access Bio, Inc.         | CareStart COVID-19 IgM/IgG             | lateral flow                          | spike and nucleocapsid | IgM             | 89.1%; 57/64 (79.1–94.6%)                                | 99.5% (181/182) (97.0–99.9%)                             |
|                          |  |                                       |                        | IgG             | 96.9%; 62/64 (89.3–99.1%)                                | 99.5%; 181/182 (97.0–99.9%)                              |
|                          |  |                                       |                        | combined        | 98.4%; 63/64 (91.7–99.7%)                                | 98.9%; 180/182 (96.1–99.7%)                              |
| ACON Laboratories, Inc.  | ACON SARS-CoV-2 IgG/IgM Rapid Test     | lateral flow                          | spike and nucleocapsid | IgM             | 96.7%; 29/30 (83.3–99.4%)                                | 98.8%; 79/80 (93.3–99.8%)                                |
|                          |  |                                       |                        | IgG             | 100%; 30/30 (88.7–100%)                                  | 97.5%; 78/80 (91.3–99.3%)                                |
|                          |  |                                       |                        | combined        | 100%; 30/30 (88.7–100%)                                  | 96.2%; 77/80 (89.5–98.7%)                                |
| ADVAITE, Inc.            | RapCov Rapid COVID-19 Test             | lateral flow                          | nucleocapsid           | IgG             | 90.0%; 27/30 (74.4–96.5%)                                | 95.2%; 99/104 (89.2–97.9%)                               |

<sup>a</sup>Ab: Antibody, CMIA: chemiluminescent microparticle immunoassay. \*These numbers represent the number of samples used to evaluate each test and calculate the positive predictive value (PPV) and negative predictive value (NPV).<sup>31</sup>

summarizes the performance in terms of sensitivity and specificity of several FDA-granted EUA serological tests.<sup>7,31,44</sup>

## ANTIGEN TESTS

The antigen test is a diagnostic test designed for the rapid, direct detection of the SARS-CoV-2 virus, where a fast turnaround time is the primary advantage.<sup>27,35,36,39,53</sup> The antigen test detects the proteins present in the sample directly but not the genetic material as in the case of molecular tests. Typically, the detection component of the antigen tests are nanoparticles, which make it a valuable diagnostic tool when laboratory facilities are not available.<sup>54</sup> Although the antigen tests are very specific for the virus, they are not as sensitive as molecular PCR tests and cannot detect all of the active cases. It is worth mentioning that getting a negative result by the antigen test does not rule out the infection because of the high chance of a false-negative.<sup>55,56</sup> Furthermore, antigen tests were found to be unable to detect positive COVID-19 samples with a cyclic threshold (Ct) number > 35, weak COVID-19, which may lead to missing some of the active COVID-19 cases.<sup>37</sup>

The immunochromatographic assay (ICA), lateral flow immunochromatographic assay, and chemiluminescent enzyme immunoassay (CLEIA) are three examples of commonly used antigen tests. All of these tests can produce results within a few minutes and enable large-scale population-based field testing.<sup>57,58</sup>

## NUCLEIC ACID AMPLIFICATION TEST (NAAT)

**Reverse Transcription Polymerase Chain Reaction (RT-PCR).** PCR remains the gold standard technique since it can reach a high sensitivity.<sup>22,23,59</sup> The test procedure begins with isolating the RNA from the collected sample, followed by converting the RNA into complementary DNA (cDNA) and then amplifying the target using a polymerase. The discrimination of SARS-CoV-2 from other commonly reported respiratory viruses is also possible using this technique.<sup>60,61</sup> For RT-PCR, typically N, E, and RNA-dependent RNA polymer-

ase (RdRp) genes of SARS-CoV-2 are targeted for detection. The complete genome sequence of SARS-CoV-2 was revealed on January 11, 2020, followed by the design of the primers and probes by the Center for Disease Control and Prevention (CDC). Other countries followed a similar approach and went on to develop their own RT-PCR kits.<sup>16,62</sup> Although RT-PCR is a highly sensitive technique, running the test can take a long, labor-intensive effort using specialized equipment, and the test must be performed by expert personnel. This multistep procedure typically takes 2–4 h to finish, which increases the risk of cross-contamination. Further, the test is usually conducted in hospitals or centralized laboratories based on the aforementioned two-step diagnostic strategy model. In addition, the logistical process of cold chain transportation from the sample collection location to the testing laboratory makes the conventional RT-PCR process slower, taking nearly 48–72 h to send the results back to the patients. To overcome these challenges, nanoenabled approaches have been proposed recently. Cheong *et al.*<sup>63,64</sup> reported the use of gold nanoparticles with a magnetic core to speed up the thermocycling process to detect SARS-CoV-2 using *in situ* fluorescence. The portable device relies on plasmonic heating through magnetoplasmonic nanoparticles (MPNs) to decrease the time needed for the RT-PCR from a few hours to 17 min. This approach is referred to as high-speed nanoPCR, and it consists of three main steps. First, RNA is extracted using a disposable RNA preparation kit with plungers for reagents mixing. Next, RT-PCR is performed with the assistance of magnetoplasmonic thermocycling. Finally, the fluorescence signal is detected to diagnose COVID-19 after applying an external magnetic field to remove the magnetoplasmonic nanoparticles (Figure 4).<sup>63,64</sup>

Recently, a combination of PCR and isothermal nucleic acid amplification known as loop-mediated isothermal amplification (LAMP) techniques was explored.<sup>65</sup> The idea was to introduce the speed of the LAMP techniques and the accuracy of the PCR method in one single platform. It has been shown that



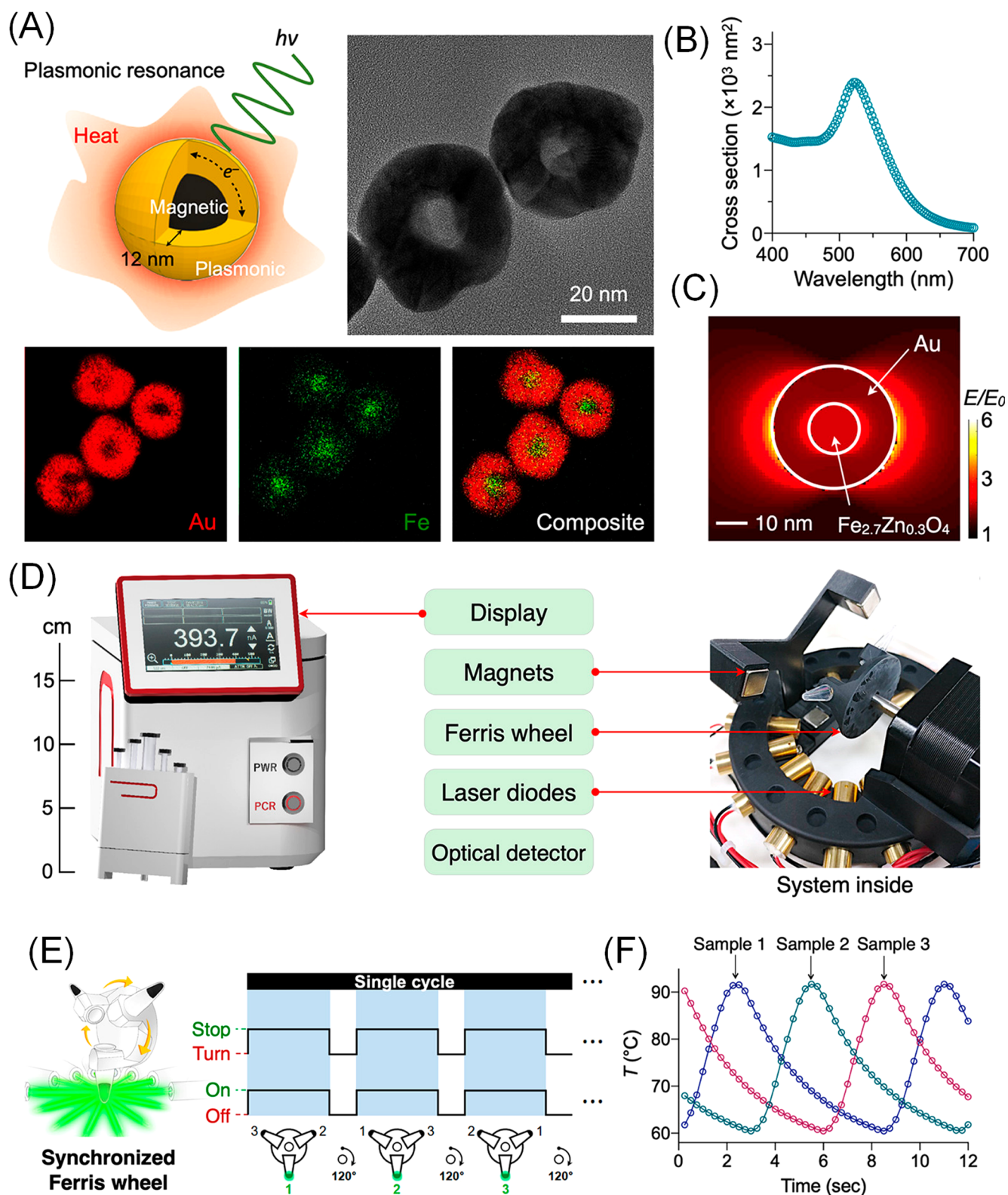


Figure 4. (A) Elemental mapping for gold and iron, schematic, and transmission electron microscopy (TEM) images of MPNs. (B) The absorption spectrum of MPNs reveals a peak at 535 nm. (C) Surface plasmon resonance of the MPN as shown by electric field simulation. (D) Representation of the NanoPCR system and its components. These include a laser for heating steps, a Ferris wheel, optics for output signal detection, and a screen for a result display. (E) Illustration of the laser array used for the plasmonic heating of the sample. The use of the Ferris wheel enables the sample rotation with syncing laser illumination to facilitate multisample processing. (F) The time-series change of the temperature profile of the sample under processing. Reprinted with permission from ref 64. Copyright 2021 American Chemical Society.

combining LAMP and RT-PCR in one assay to develop RT-q(PCR-LAMP) was approximately 100-fold more sensitive than conventional RT-LAMP. Using RT-q(PCR-LAMP) for COVID-19 diagnosis enables the detection of SARS-CoV-2 RNA of as few as five copies per reaction within a short time of 35 min for the amplification step (six cycles of PCR).<sup>65</sup> In another attempt, Shirato *et al.*<sup>66</sup> explored a real-time RT-PCR-based assay for the ultrarapid detection of SARS-CoV-2 using the PCR1100 device. The whole amplification procedure takes less than 20 min and could achieve a sensitivity and specificity comparable to those of conventional real-time RT-PCR performed using thermocycler instruments. The technique is potentially helpful for COVID-19 mass screening and when multiple SARS-CoV-2 testing is required, though the system is capable of testing only one specimen at a time.<sup>66</sup>

Although RT-PCR is the gold standard diagnostic test for COVID-19, it has several limitations in terms of cost, wait time, RNA-extraction procedure, and sample storage. Moreover, the sensitivity of the RT-PCR test is hampered by mutation and virus evolution, resulting in false-negative results. These mutations were seen as a variation in the genetic materials in the population of the circulating viral strains. The genetic mutation is the change of the SARS-CoV-2 genetic sequence when compared to the reference sequence such as the first genetic sequence identified, Wuhan-Hu1, or the one identified in the United States, USA-WA1/2020. The effect of these mutations varies: some have no impact, while others can make the spread of COVID-19 faster. Testing a mutated patient sample for sure will have an impact on the test performance, and it depends on the nature of the mutation, the test design, and the prevalence of the variant. Molecular tests that rely on multiple genetic targets to provide the results are less likely to be impacted by the viral mutation. On the basis of FDA analysis of the viral mutation impact on the test's performance, they identify Accula SARS-CoV-2 Test (Mesa Biotech Inc.) to be slightly affected by genetic mutation at positions 28881–28883 (GGG to AAC) and 28877–28878 (AG to TC) in patient samples. The same holds for other EUA FDA-approved kits as detailed in Table 4.<sup>67</sup>

**SARS-CoV-2 Detection Using Nucleic Acid Isothermal Amplification Tests.** Reverse transcript loop-mediated isothermal amplification (RT-LAMP) is a nucleic acid amplification technique that is carried out at a constant temperature. RT-LAMP-based tests rely on the turbidity or the use of colorimetric or fluorescence dye to indicate the successful amplification of the target.<sup>68–70</sup> The test is simple to perform without the need for complex equipment, and a simple output that can be visualized by the naked eye with no background noise or interferences. The RT-LAMP test can be integrated into a lateral flow strip,<sup>71–73</sup> or it can be made into a lab-on-chip viral diagnostic device using a microfluidic system.<sup>74–76</sup>

The performance of the RT-LAMP-based colorimetric test in detecting SARS-CoV-2 has been evaluated in the presence of several dyes. These dyes have been used to indicate the successful amplification of the SARS-CoV-2 target segment. A sensitivity of 50 virions/reaction has been reported using leucocystal violet (LCV) dye when combined with LAMP because the LCV dye is insensitive to the sample's pH. Further, a two-stage isothermal amplification has been proposed by combining recombinase isothermal amplification (RPA) and RT-LAMP in a close tube reaction. The two-stage approach is

**Table 4. Impact of Virus Mutation on the Test's Performance<sup>67</sup>**

| Test Name   | The mutation impact on the test sensitivity.  |
|---|---|
| Revogene SARS-CoV-2 test (Meridian Bioscience, Inc.)        | A false-negative result is expected for the SARS-CoV-2 omicron variant (B.1.1.529). This is due to the deletion of nine nucleotides at the N-gene (position 28370–28362).   |
| Accula SARS-CoV-2 test (Mesa Biotech Inc.)                  | The test results are expected to be affected slightly due to genetic mutation at positions 28881–28883 (GGG to AAC) and 28877–28878 (AG to TC) in patient samples.  |
| Linea COVID-19 assay kit (Applied DNA Sciences, Inc.)       | B.1.1.7 variant (UK VOC-202012/01) can reduce sensitivity significantly. Further, the test is expected to have false-negative results when testing the SARS-CoV-2 omicron variant (B.1.1.529). This may be attributed to the fact that the test targets cover two mutated regions of the S-gene. The viral target of this test has mutations at nucleotide positions 23599 (from T to G) and 23604 (C to A) with deletions at the amino acid positions 69–70. |
| TaqPath COVID-19 combo kit (Thermo Fisher Scientific, Inc.) | B.1.1.7 variant (UK VOC-202012/01) has a significant reduction in sensitivity.  |
| Xpert Xpress SARS-CoV-2, Xpert Omni SARS-CoV-2 (Cepheid)    | Cepheid tests were found to be susceptible to a single-point mutation.  |

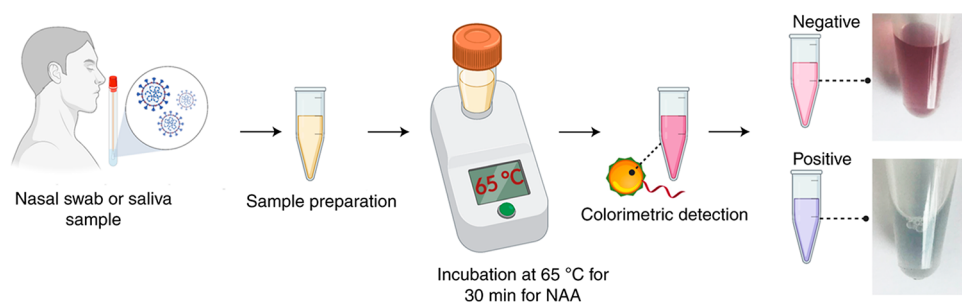


**Figure 5.** Schematic representation of the colorimetric test based on RT-LAMP and AuNPs-capped with ASOs. First, the sample was collected from the subject and added to lysis and NAA reagents. The sample undergoes an isothermal NAA for 30 min at a constant temperature (65 °C). Next, the AuNPs-capped ASOs will be added to the amplification products to induce a color change. The sample changed color from pink to purple in the case of positive COVID-19, whereas negative samples remained pink. Reprinted with permission from ref 79. Copyright 2021 Springer Nature.

referred to as COVID-19 Penn-RAMP, and it exhibited an improved sensitivity of 5 virions/reaction.<sup>77</sup>

Despite the RT-LAMP approach offering many advantages, its applicability is limited by its inherent limitations. Utilizing RT-LAMP tests call for the necessity of skilled laboratory personnel to optimize the running conditions. Despite the simplicity and sensitivity of the RT-LAMP method, it suffers from increased background noise due to contaminants from irrelevant DNA molecules, which lead to a high false-positivity rate due to the spurious amplification byproducts.<sup>78,79</sup>

Nanotechnology may offer a solution to enhance the RT-LAMP specificity by serving as a secondary check.<sup>79</sup> The specificity of the RT-LAMP has improved dramatically through the introduction of AuNPs-coated antisense oligonucleotides (ASOs) due to its dual-targeting approach for SARS-CoV-2 detection. The protocol relies on a synergistic targeting mechanism to compensate for the high false-positivity rate with the standalone RT-LAMP test. The sensitivity of the RT-LAMP test improved due to the use of AuNPs to indicate the presence of SARS-CoV-2 RNA due to the aggregation of the AuNPs as shown in Figure 5.<sup>79</sup> This approach relies on the hypothesis that the aggregation of AuNPs in a colloidal solution changes the surface reflective index (RI) and accordingly shifts in the resonance wavelength because of localized surface plasmon resonance (LSPR). The sensitivity of the test was found to be 10 copies/ $\mu\text{L}$  after adding the nucleic acid amplification (NAA) step with a total sample-to-assay time of  $\sim 35$  min.<sup>79</sup>

Several other isothermal approaches have been also reported, which may overcome the limitations associated with RT-LAMP tests. Carter *et al.*<sup>80</sup> reported the development of the SARS-CoV-2 test with a sample-to-assay time of 10 min using the reverse transcription–free exponential amplification reaction (RTF-EXPAR).<sup>80</sup> The fast turn-around time of the RTF-EXPAR is due to the generation of cDNA while bypassing the slow reverse transcription method and utilizing an exponential amplification process.<sup>80</sup> Woo *et al.*<sup>81</sup> reported the development of a sensitive fluorescence sensor for the detection of multiple viruses and bacteria including SARS-CoV-2, MERS-CoV, *V. vulnificus*, and *E. coli O157:H7* with the ability to multiplex. The test relies on the ligation of promoter probe and reporter probe segments in the presence of the target genetic material.<sup>81</sup> Next, the ligated segment was transcribed using the T7 RNA polymerase leading to the formation of a fluorescent light-up aptamer that binds to fluorogenic dyes to indicate the presence of the target

pathogen. When evaluated using 40 nasopharyngeal COVID-19 samples, the assay showed 95% and 100% of positive and negative predictive values, respectively, with a LOD of 0.1 attomolar. Further, the test was evaluated using a direct samples testing protocol, without RNA extraction. Thermal lysing offers an alternative to conventional RNA-extraction methods.<sup>81</sup> However, the need for specialized heating equipment to reach the high temperature for thermal lysing limited the method's applicability to in-field testing and limited resources.

RNA extraction is a time-consuming, laborious, and expensive procedure that prevents the use of the technology for patient point-of-care use. It requires several centrifugation steps and special reagents, and must be conducted in sterilized conditions to avoid cross-contamination. Although the RNA-extraction step can be replaced by chemically lysing the virus, nanoparticles provide a better alternative to capturing the virus within a complex matrix of interferences. The EasyCOV RT-LAMP-based COVID-19 test is a technology that bypasses the RNA-extraction step to make the detection of SARS-CoV-2 easier and straightforward. The performance evaluation of the EasyCOV test showed a sensitivity of about 73%.<sup>82</sup>

Recently, Lucira COVID-19 All-in-One test kit (Lucira Health, Inc.) received EUA FDA approval as a home-based self-testing device. This test is out in the market, and it utilizes RT-LAMP in a single-use home-based test for COVID-19 diagnosis. The test employs a hand-held battery-powered heating device for isothermal amplification. The test is fast, with 30 min turn-around time and is easy to use by a layperson; however, each test cost around \$85 and is not economically feasible for mass use.<sup>24</sup> Other isothermal amplification techniques were also explored including the nicking enzyme amplification reaction (NEAR),<sup>83,84</sup> transcription-mediated amplification (TMA),<sup>85</sup> transcription reverse-transcription concerted reaction (TRC),<sup>86</sup> and smart amplification process (SmartAmp).<sup>87</sup> The NEAR amplifies DNA exponentially at a constant temperature from 55 to 59 °C. A reverse transcription step is needed to use the NEAR for RNA amplification.<sup>83,84</sup> RNA targets can be amplified using SmartAmp in the presence of optimized ssDNA amplification probes. First, the amplification probes are mixed with the sample, followed by separating the amplification probes–target RNA complex from the unbonded capturing probes–magnetic beads complex.<sup>87</sup> Recently, the RNA-extraction-free test known as “Accula SARS-CoV-2”<sup>88</sup> has been released into the market. Accula eliminates the RNA-extraction step by enabling



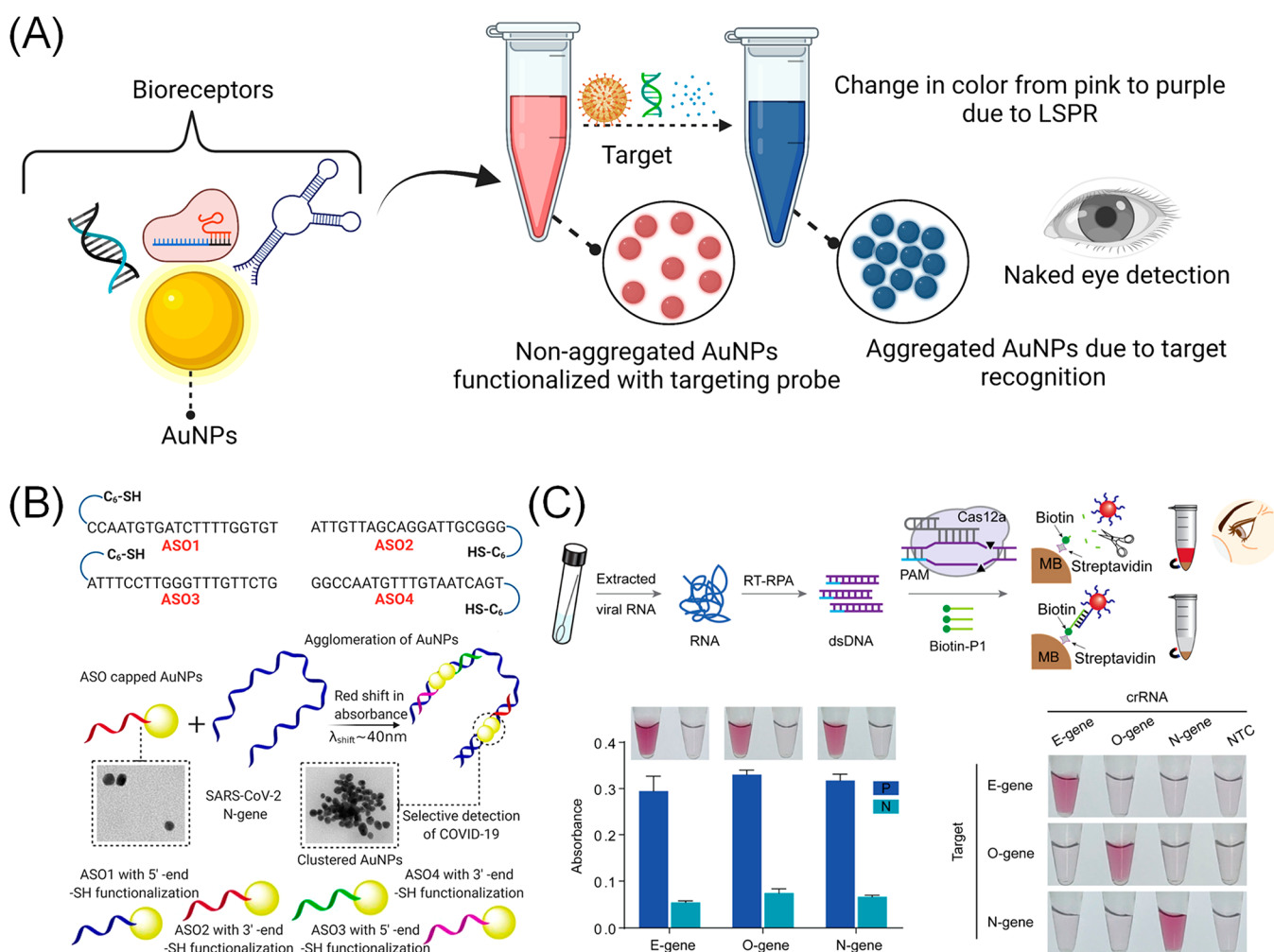


**Figure 6.** (A) Schematic representation of the principle behind the colorimetric tests. Several biorecognition (bioreceptors) elements can be used with the colorimetric tests. These bioreceptors include antibodies, antigens, CRISPR/gRNA complex, aptamers, and ssDNA. (B) The sequences of the ssDNA were used to develop an amplification-free colorimetric test. ASOs-coated AuNPs are used to induce a color change in the presence of the genetic target. Reprinted with permission from ref 34. Copyright 2020 American Chemical Society. (C) Schematic diagram of the workflow used in detecting SARS-CoV-2 using a CRISPR/Cas12a system and representative results of the visual detection of SARS-CoV-2 virus RNA. Reprinted with permission from ref 147. Copyright 2021 American Chemical Society.

the release of virus genetic materials using a proprietary lysis solution, and recently, it has been granted FDA EUA approval. The test addresses the time and complexity limitations associated with the gold standard RT-PCR while maintaining a comparable accuracy and selectivity. Using a proprietary NAA procedure, the test was successful in reducing the thermocycling time and enabling a rapid exponential amplification of the target. Thus, the test has a short turn-around time and a simple readout system using lateral flow strips. The test workflow consists of the following four steps: (1) lysing of the virus, (2) reverse transcription (RT) of viral RNA to complementary DNA (cDNA), (3) nucleic acid amplification, and (4) detection. The test cost is less than \$1, and no refrigeration is required for the reagents. Despite the advantages claimed for the Accula test, the widespread availability of the test is still a limitation.<sup>88</sup> *In-situ* hybridization and immunohistochemistry are commonly used alternatives for the gold standard RT-PCR;<sup>89–94</sup> however, the inability to conduct large sample testing has limited their applicability in clinical practice. Further, the immunohistochemistry results are dependent on the type of antibody used to perform the test.<sup>93</sup>

## DIAGNOSTIC TESTS OF SARS-CoV-2 BASED ON NANOMATERIALS AND 2D MATERIALS

The manipulation of material near the atomic scale allows the development of nanomaterial which exhibits properties superior to the same material in the bulk state.<sup>95,96</sup> Nanomaterials facilitate the development of devices and technologies that may replace the gold standard RT-PCR to accurately detect viruses.<sup>34,50,52,79,97–108</sup> Nanoparticles can play several roles in the sensing platform by acting as capturing elements, signal reporters, or being involved in sample preprocessing. The sample preprocessing protocol for COVID-19 diagnosis involves the extraction of RNA from the clinical sample to perform RT-PCR. Nanoparticles would enable the elimination of the conventional RNA-extraction step by using a magnetic beads-based RNA-extraction technique. Several RNA-extractions kits with magnetic nanoparticles as a capturing agent are available commercially.<sup>109,110</sup>

Nanosensors enable high sensitivity and selectivity and a large surface-to-volume area for the probe-target interaction. Nanosensors rely on a “nano” recognition element which is designed to interact with the target, an event that can be

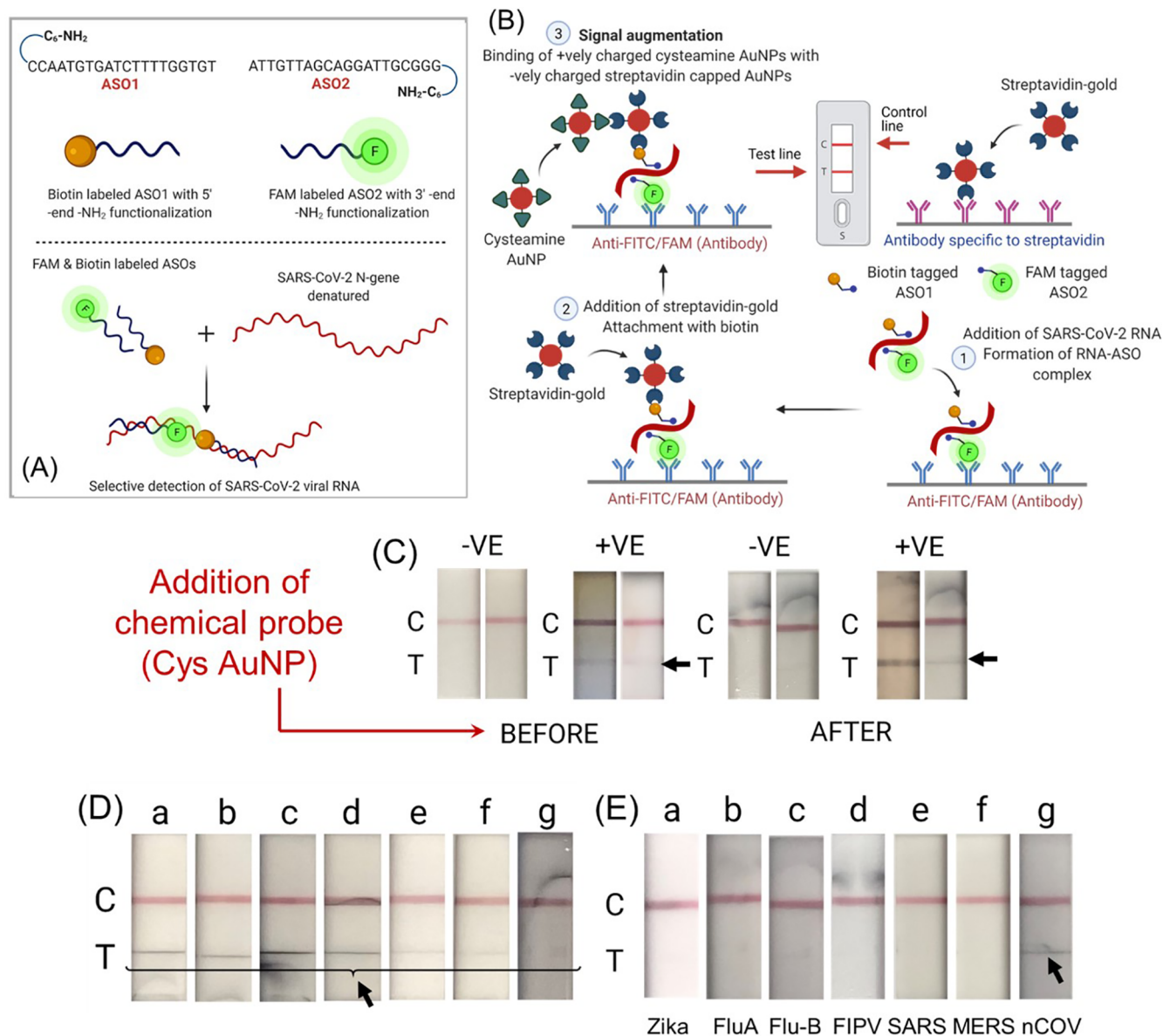


**Figure 7.** (A) The sequences of the ASOs adapted in the LFA test and the differential functionalization of the two strands with FAM and biotin. (B) Targeting principle of the SARS-CoV-2 nucleic acid and the workflow to induce a visible test band in the LFA. (C) Representative results show the appearance of both test and control bands in the presence of the SARS-CoV-2 gene, whereas only the control bands are showing in the absence of the target (i.e., SARS-CoV-2). The images were captured before and after the addition of cysteamine AuNPs. (D) The test line bands as results of responses to different concentrations of SARS-CoV-2 RNA, where a: 67250 copies/ $\mu$ L; b: 3362 copies/ $\mu$ L; c: 168 copies/ $\mu$ L; d: 8 copies/ $\mu$ L; e: 0.42 copies/ $\mu$ L; f: 0.02 copies/ $\mu$ L; and g: 0.001 copies/ $\mu$ L. (E) Evaluation of the proposed LFA cross-reactivity toward genetically related and nonrelated viruses and microorganisms including a: Zika; b: influenza A; c: influenza B; d: feline infectious peritonitis virus (FIPV); e: SARS-CoV; f: MERS-CoV; and g: SARS-CoV-2. Reprinted with permission from ref 101. Copyright 2022 Elsevier.

detected through recording optical, mechanical, electrical, or magnetic signals. These systems are an excellent candidate for analytes sensing with a high LOD, sensitivity, and specificity. Gold nanoparticles,<sup>111–114</sup> carbon nanoparticles,<sup>97,103,115,116</sup> silver nanostructures,<sup>117,118</sup> metal–organic framework,<sup>119,120</sup> covalent organic framework,<sup>121,122</sup> nanoparticles/polymer composite,<sup>123,124</sup> carbon nanotube,<sup>105,125</sup> and quantum dots,<sup>126,127</sup> are examples of nanostructures utilized for nanosensing. The inherent optical, electrical, mechanical, electrochemical, and magnetic properties of the nanoparticles make them favorable to develop nanosensors to compose the patient's molecular profile and enable a high signal-to-noise

ratio (SNR).<sup>128–132</sup> Here, we are focusing on the nanosensor's applications in detecting the presence of a pathogen to establish an effective treatment plan, guarantee early diagnosis, and monitor the infectious disease progression. Nanosensors should be able to detect an extremely low concentration of nucleic acid or whole virus even in the presence of other biological interferences. This is critical because the virus or its genetic materials can be present in ultralow concentrations at very early stages of the infection, where the symptoms have not yet developed, but treatments are still effective. Another important consideration when developing a nanosensor is that the test should be simple, without the necessity of

sophisticated instrumentation or significant technical training. Further, test affordability is important when it is implemented in healthcare systems. The nanosensors should exhibit a short response time, enabling the clinical team to take the necessary steps as soon as possible. The nanomaterial-based sensors can be categorized based on the platform output signal into (1) colorimetric tests, (2) fluorescence tests, (3) electrochemical-based tests, and (4) spectrometry-based tests as detailed in the following sections.

**Sensors With Visual Readout.** Tests which rely on a color change to indicate the presence of the target analyte are easy to use and interpret by a layperson. The test reporter can be a dye or small molecule,<sup>133,134</sup> or nanoparticle;<sup>34,97,135</sup> however, the use of nanomaterial as a reporting agent offers several advantages. Nanomaterials have a high surface-to-volume ratio providing a large surface for the analyte to interact with the capturing probes. Further, these nanomaterials can act as both reporting agents and capture probes simultaneously. Gold nanoparticles (AuNPs) have been studied extensively in colorimetric sensors due to their LSPR.<sup>111,135,136</sup> However, color-based tests with YES/NO answers based on LSPR for COVID-19 are not yet available commercially. This may be attributed to the necessity to find the best binding protocol which can capture the target molecule in a pile of many interferences present in the sample. Examples of the capturing probes which hold a promise to address these challenges include antibodies,<sup>137,138</sup> aptamers,<sup>139,140</sup> peptides,<sup>141,142</sup> and molecularly imprinted polymers (MIPs)<sup>143,144</sup> (Figure 6A).

Several platforms which rely on the detection of the viral RNA have been proposed for COVID-19 diagnosis. The nanosensors consist primarily of two main components: the recognition element and the output reporter. The nanosensor platform translates the hybridization between the target genetic materials and the nanoprobe into a detectable output. Qui *et al.*<sup>145</sup> introduced the use of two-dimensional gold nanoislands (AuNIs) for the detection of SARS-CoV-2. A combination of the localized surface plasmon resonance (LSPR) and plasmon photothermal (PP) effect of the AuNIs has been used for SARS-CoV-2 RNA detection. The AuNIs have been functionalized with DNA probes complementary to the target RNA to enable the detection of the target sequence via RNA–DNA *in situ* hybridization, with high sensitivity and a high limit of detection (0.22 pM).<sup>145</sup> However, the necessity of specialized equipment to measure the LSPR limited the applicability of this technology.<sup>146</sup> The overarching goal is to develop a home-care device that offers quick reliable information about the infectious pathogen and to make the device accessible for everyone. Moitra and Alafeef *et al.*<sup>34</sup> showed that gold nanoparticles capped with an antisense oligonucleotide (ASO) can be used to develop a naked-eye-based test for the detection of COVID-19.<sup>34</sup> The technology was successful in detecting the presence of the SARS-CoV-2 within ~10 min and a LOD of 0.18 ng/mL without nucleic acid amplification.<sup>34</sup> Figure 6B shows the ASO's sequences used for the SARS-CoV-2 targeting and the aggregation of the AuNP-capped ASOs as confirmed using transmission electron microscopy (TEM). The AuNPs form a large aggregate in the presence of the SARS-CoV-2 gene due to the hybridization of the SARS-CoV-2 RNA (N-gene) strand with the Au-ASO mix. Using a thermostable RNase H, a color change was observed in the sample due to the recognition and cleavage of the phosphodiester bonds in SARS-CoV-2 RNA (N-gene)

nanoconjugate, while the ASO strands are left intact. The RNase H influences the agglomeration propensity among the AuNPs for an immediate color change in the tested sample.<sup>34</sup>

In another work, a colorimetric test has been proposed to detect COVID-19 with a LOD of 50 copies per reaction using Cas12 protein/guide RNA complex.<sup>147</sup> The test uses the collateral cleavage activity of the Cas12 protein/guide RNA complex to facilitate the detection process. To begin with, SARS-CoV-2 RNA has been extracted from the clinical sample followed by an isothermal amplification using recombinase polymerase amplification (RPA). Next, the successfully amplified segment is recognized by the Cas12/gRNA complex and thus activates the trans-cleavage mechanism. Two complementary probes have been used in this assay, biotinylated probes and their complementary sequence conjugated to AuNPs. In the presence of the target, the trans-cleavage activity of the CRISPR complex cleaves the probes and thus prevents their hybridization. On the other hand, in the absence of the target (i.e., SARS-CoV-2 RNA), the CRISPR complex will be inactivated, and thus the AuNP probes will be hybridized with the biotinylated probe (Figure 6C). Magnetic nanoparticles with streptavidin coating help in pulling the biotin/AuNPs assembly to aggregate, shifting the LSPR and changing the color from pink to purple.<sup>147</sup> CRISPR technology can also be integrated into lateral flow strips for the molecular diagnosis of pathogens. For example, DETECTR is a lateral flow sensing technology that relies on Cas12 to diagnose COVID-19.<sup>72</sup>

Using ASOs instead of antibodies as capturing probes,<sup>101,148</sup> a lateral flow-based molecular test has been developed for the diagnosis of COVID-19.<sup>101</sup> This can be achieved by first capturing the target segment of SARS-CoV-2 on the test line by ASOs labeled with either biotin/fluorescein amidites (FAM) (Figure 7A). These ASOs are designed to recognize and bind two consecutive regions of the SARS-CoV-2 genome and bind to the anti-FAM antibodies immobilized on the test line, leaving biotin exposed to the surface. Streptavidin-conjugated AuNPs or plasmonic particles then bind to the exposed biotin and aggregate to show color on the test line (Figure 7B). This approach has been validated using 60 COVID-19 clinical samples, and the test shows a sensitivity, specificity, and accuracy of 100% with a LOD of 20 copies/mL.<sup>101</sup> The high sensitivity of the test may attribute to the chemical augmentation using gold nanoparticles (AuNPs) to enhance the color intensity at the test band in the presence of the target (Figure 7C–E). This was achieved by using positively charged AuNPs to interact with the negatively charged streptavidin-coated AuNPs.<sup>101</sup>

**Fluorescence Sensors.** The fluorescence sensors rely on the detection of the emitted photon from a reporter which recognized the presence of the pathogen either through a molecular probe or in a label-free manner. Several nanoparticles have been used to construct fluorescence sensors including carbon dots (CDs),<sup>116,149</sup> quantum dots (QDs),<sup>126,150–152</sup> or up-conversion NPs.<sup>153</sup> Using multicolor QDs, Zhang *et al.*<sup>151</sup> showed the feasibility of detecting SARS-CoV-2 using a portable system. A smartphone-based portable device is used to read a barcode-like signal to track the SARS-CoV-2 infection.<sup>151</sup> QDs are characterized by their discrete fluorescence spectra, which enables the multiplex detection of analytes. AuNPs can act as a quencher for the QDs fluorescence that enables tracking the binding events at a molecular level.<sup>152</sup> Gold nanoparticles (AuNPs) and quantum



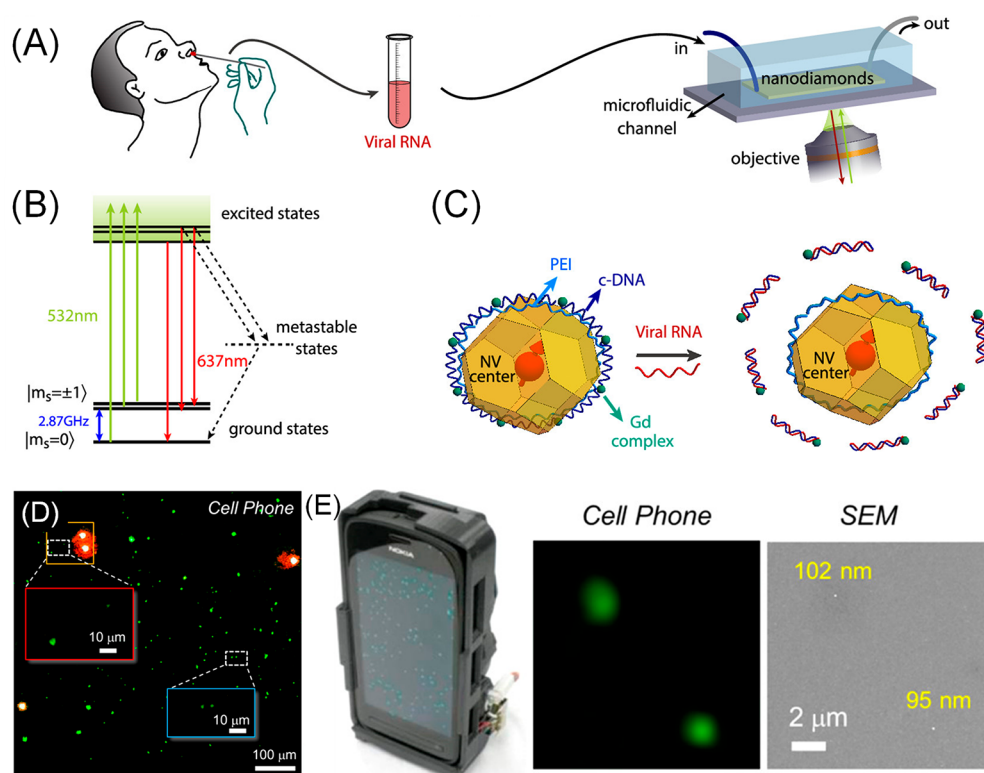


**Figure 8.** (A) Schematic representation of the SARS-CoV-2 diagnostic protocol. The test running procedure is envisioned to start with sample collection, followed by nucleic acid extraction. The test sample was then loaded into a microfluidic channel that contains functionalized nanodiamonds. The excitation of the nanodiamonds NV with a green laser resulted in a red fluorescence signal which can be recorded using a digital camera or confocal microscope. (B) Band-gap model represents the NV center and the optical transitions. (C) Schematic illustration of the magnetic noise quenching mechanism. A capturing cDNA sequence is adsorbed onto the surface of functionalized nanodiamond containing NV centers. These cDNAs are used as a capturing element, and they will cover the nanodiamond surface due to the cationic polyethylenimine (PEI) coating. To introduce strong magnetic noise,  $Gd^{3+}$  complex molecules can be connected to the cDNA structure. In the presence of target RNA, c-DNA will be hybridized with the RNA leading eventually to the detachment of a c-DNA- $Gd^{3+}$  complex from the nanodiamond surface. This can cause a weaker magnetic interaction between the  $Gd^{3+}$  complex and NV centers inside the nanodiamond. Reprinted with permission from ref 150. Copyright 2021 American Chemical Society. (D) Cell phone fluorescence image of Alexa-488-labeled virus particles. (E) The screen of the cell phone shows the fluorescence image of 1  $\mu m$  diameter green-fluorescent beads and image of fluorescent beads that have been used as location markers for scanning electron microscopy (SEM) comparison images. Reprinted with permission from ref 154. Copyright 2013 American Chemical Society.

dots (QDs) have played a role in studying the binding dynamic of the S-protein to the ACE-2 receptor. Gorshkov *et al.*<sup>152</sup> reported the use of a spike receptor-binding domain conjugated to quantum dots (ODs-RBD) to study the ACE receptor's neutralization.<sup>152</sup> The study reveals that the ACE-2 binds to the QD-RBD with high affinity to form a complex that enters cells through dyamin/clathrin-dependent receptor-mediated endocytosis.<sup>152</sup>

Quantum physics is a field that focuses on investigating matter and energy at a fundamental level. Recently, it has been shown to play a role in the emergence of a fast and less expensive test for the detection of COVID-19 and its variances. Li *et al.*<sup>150</sup> reported the use of nanodiamonds for the detection of SARS-CoV-2. The group validated theoretically that in the presence of SARS-CoV-2 RNA, the nitrogen-vacancy (NV) centers in nanodiamonds translate into an optical readout due to the generated magnetic noise signal.<sup>150</sup> Figure 8A depicts the workflow of the nanodiamonds-based sensor for the detection of SARS-CoV-2. The energy diagram of the nanodiamonds NV and the operation principle of the sensor are shown in Figure 8B–C.

Viruses are small organisms that can be investigated using several imaging techniques, among them is fluorescence

imaging. The visualization of viruses requires nanoscale optical imaging with a high signal-to-noise ratio. Labeling the virus with fluorescence nanoparticles or reporters allows the visualization of a single virus when investigated under a powerful imaging system. A field-portable fluorescence microscopy platform has been developed by Wei *et al.*<sup>154</sup> to visualize viruses up to the single-cell level. The system was installed on smartphones to enable imaging of the target virus using a phone camera module with lightweight compact optomechanical attachment. Figure 8D–E illustrates the imaging of a single virus particle using smartphone-based fluorescence microscopy.

Pinals *et al.*<sup>106</sup> developed a fluorescence-based antigen test for the detection of SARS-CoV-2. The sensor consists of a single-walled carbon nanotube (SWCNT) noncovalently functionalized with ACE2 receptors that are specific for SARS-CoV-2 proteins. The SWCNT was stabilized with single-stranded DNA to ensure the ACE2 stability. Thus, it avoids the disruption of the protein's natural conformation which may lead to losing its sensing ability for spike receptor-binding protein (S-RBD). The adsorption of the ACE2 receptors to the SWCNTs led to their fluorescence quenching. The sensor successfully detected SARS-CoV-2 within a time frame of 90

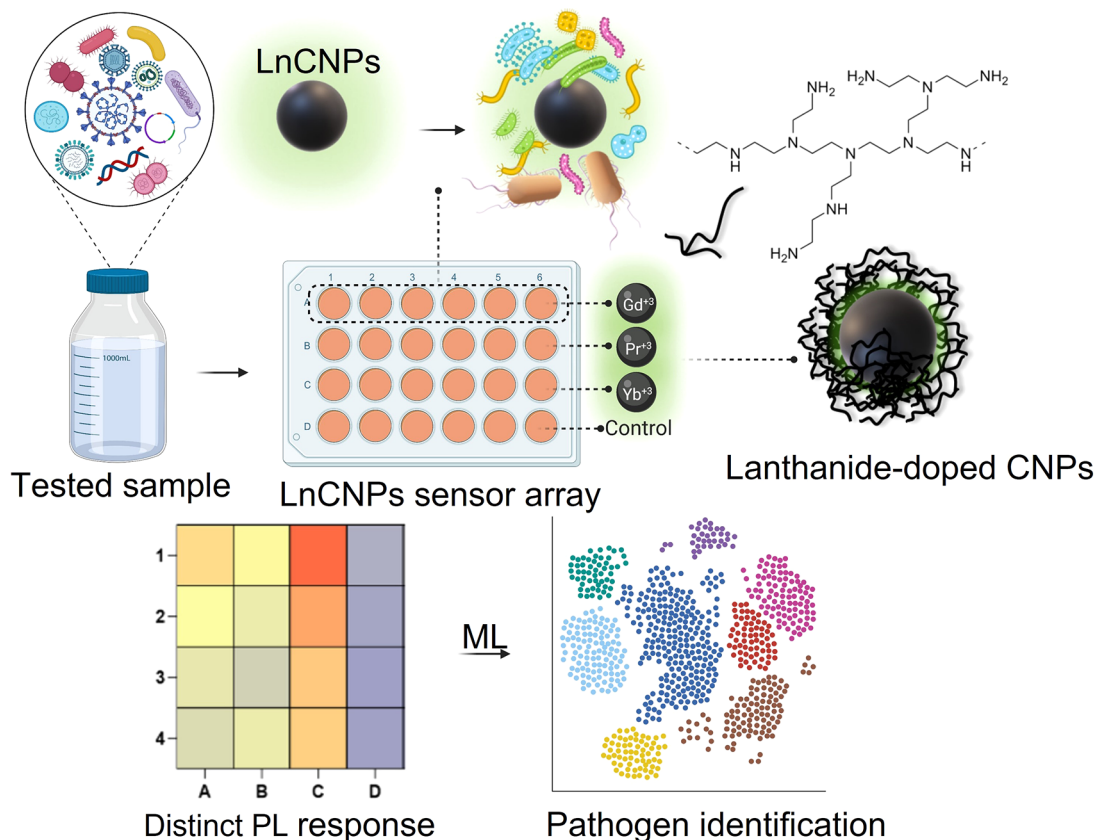


**Figure 9.** Illustration of the SARS-CoV-2 sensing mechanism using a carbon nanoparticles (CNPs)-based sensor array. Lanthanide-doped CNPs (LnCNPs) have been used as a building block of the sensor array. LnCNPs were found to interact selectively with different viruses and bacteria. This interaction leads to the generation of distinct photoluminescence signals for the diagnosis of SARS-CoV-2 and further separates it from other viruses and bacteria. With the help of a machine-learning-based pattern recognition algorithm, SARS-CoV-2 viral transmission is still wastewater that can be detected and discriminated from other pathogens using the LnCNP-based sensor array. Reprinted with permission from ref 158. Copyright 2022 American Chemical Society.

min with a two-fold increase in the fluorescence intensity. Exposing the sensor to 35 mg/L of SARS-CoV-2 virus-like particles exhibited a turn-off response of about 73% in a very short time.<sup>106</sup>

Approximately 40% of the subjects infected with COVID-19 shed virus RNA in their stool.<sup>155,156</sup> Thus, tracking the COVID-19 virus in sewage or wastewater may allow surveillance of the community level of both symptomatic and asymptomatic cases. Carbon nanoparticles (CNPs) are a class of photoluminescent material that exhibits a special optical characteristic.<sup>129,149,157</sup> Recently, CNPs have been used for the surveillance of SARS-CoV-2 in wastewater samples. The test takes advantage of the counterionic interaction of the lanthanide-doped CNPs to detect SARS-CoV-2 in a complex sample matrix with many biological interferences. The test uses a machine-learning algorithm to successfully detect COVID-19 and differentiate it from other viruses and bacteria with >95% accuracy as shown in Figure 9. The test has a turn-around time of 15 min and operates in a label-free manner allowing use in-field and across areas with limited resources.<sup>158</sup>

**Electrical and Electrochemical (EC) Sensors.** Electrochemical sensors have attracted large attention and industrial interest in a host of applications ranging from food safety, healthcare, precise agriculture, infectious disease diagnosis, and drug and food supply chains.<sup>98,159–161</sup> The electrochemical sensors are favorable due to their high sensitivity and accuracy; however, the type of recognition element used in the

electrochemical sensor determines the test cost and the level of complexity of the sample preprocessing, test time, and stability. The use of nanomaterials has enhanced the sensor stability, reducing the sample to assay time and improving sensitivity.<sup>100,162,163</sup> It has been demonstrated that the use of nanoparticles enhanced the change in the output electrical signal by 10 fold when compared to the same platform lacking nanoparticles (Figure 10A).<sup>100</sup> The sensor platform with the AuNPs coated with the capturing elements exhibits a higher change in the output voltage as compared to the same platform where the capturing elements are conjugated directly on the surface of the electrode.<sup>100</sup> The use of nanomaterials provides more surface interaction and thus enhances the electrical response.

The electrical sensors employed several transducing methods such as amperometry, potentiometry, impedimetry, calorimetry, chromatography, and mass-balance detection.<sup>100,137,164–166</sup> Electrical tests are favorable in many circumstances because they can be easily integrated with a smartphone readout and because of the ability to share data wirelessly with the primary care doctor or store it in the Cloud for future use.

Graphene has shown promise in developing field-effect transistor (FET)-based sensors. Seo *et al.*<sup>148</sup> reported the development of FET-based sensors for the detection of the SARS-CoV-2 virus in clinical samples. Graphene-based FET has been coated with antibodies specific for the SARS-CoV-2

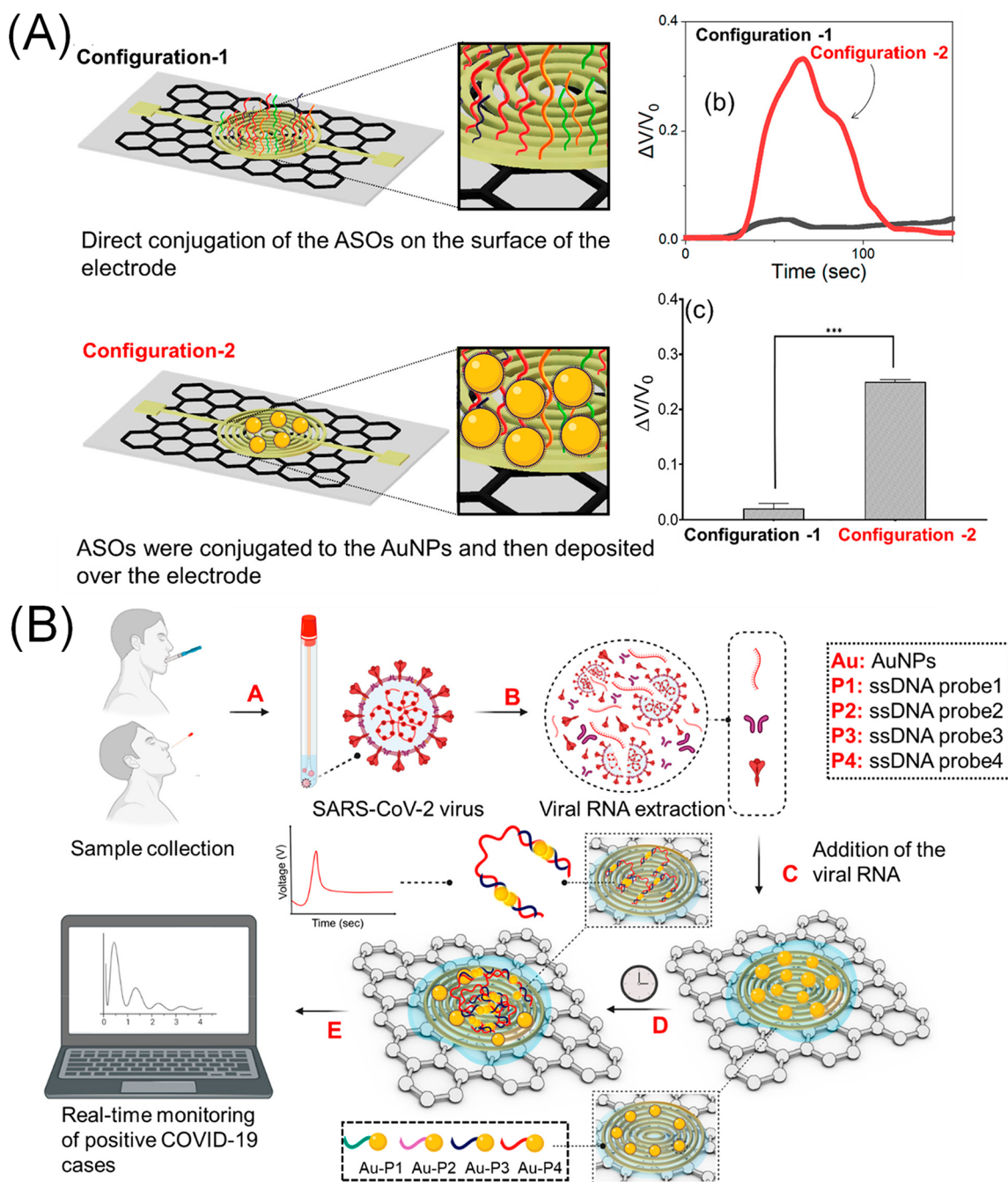


Figure 10. (A) Comparison of the electrical signal output in the presence and absence of AuNPs. (B) Schematic representation of the molecular detection of SARS-CoV-2 using a graphene-AuNPs-based electrochemical sensor. ASOs have been used as a recognition element for the detection of SARS-CoV-2 RNA. Reprinted with permission from ref 100. Copyright 2020 American Chemical Society.

spike protein. Graphene has been used because of its large specific area, high electron mobility and transfer rate, high charge-carrier mobility, and low level of electronic noise.<sup>167,168</sup> Further, graphene is facile to be modified, which allows efficient receptors immobilization. The developed FET-based sensor takes the advantage of the high carrier mobility of graphene for the sensitive detection of the SARS-CoV-2 virus with a LOD of  $2.42 \times 10^2$  copies/mL.<sup>148</sup>

The use of antibodies as a capturing element provides promise for virus diagnosis. However, they must be produced biologically rather than synthesized chemically, which makes them a costly option. ASO is a capturing element that shows promise in electrochemical sensing due to its inherent merits.

ASOs can be easily synthesized outside the body to be specific to the target sequence because they are designed to have a high binding energy and disruption energy at room temperature with low to moderate GC content (40–60%). ASOs are also cost-effective and easy to mass produce, enabling faster translation into a commercial product. It has been demonstrated that an electrochemical platform for COVID-19 diagnosis can be developed using a combination of 2D and 3D nanomaterial, i.e., graphene nanoplatelet and AuNPs.<sup>100</sup> Using AuNPs in combination with graphene as a base material offers high sensitivity. The platform was successful in diagnosing COVID-19 with 100% accuracy, specificity, and sensitivity with a LOD of 6.9 copies/ $\mu$ L. The test has a turn-



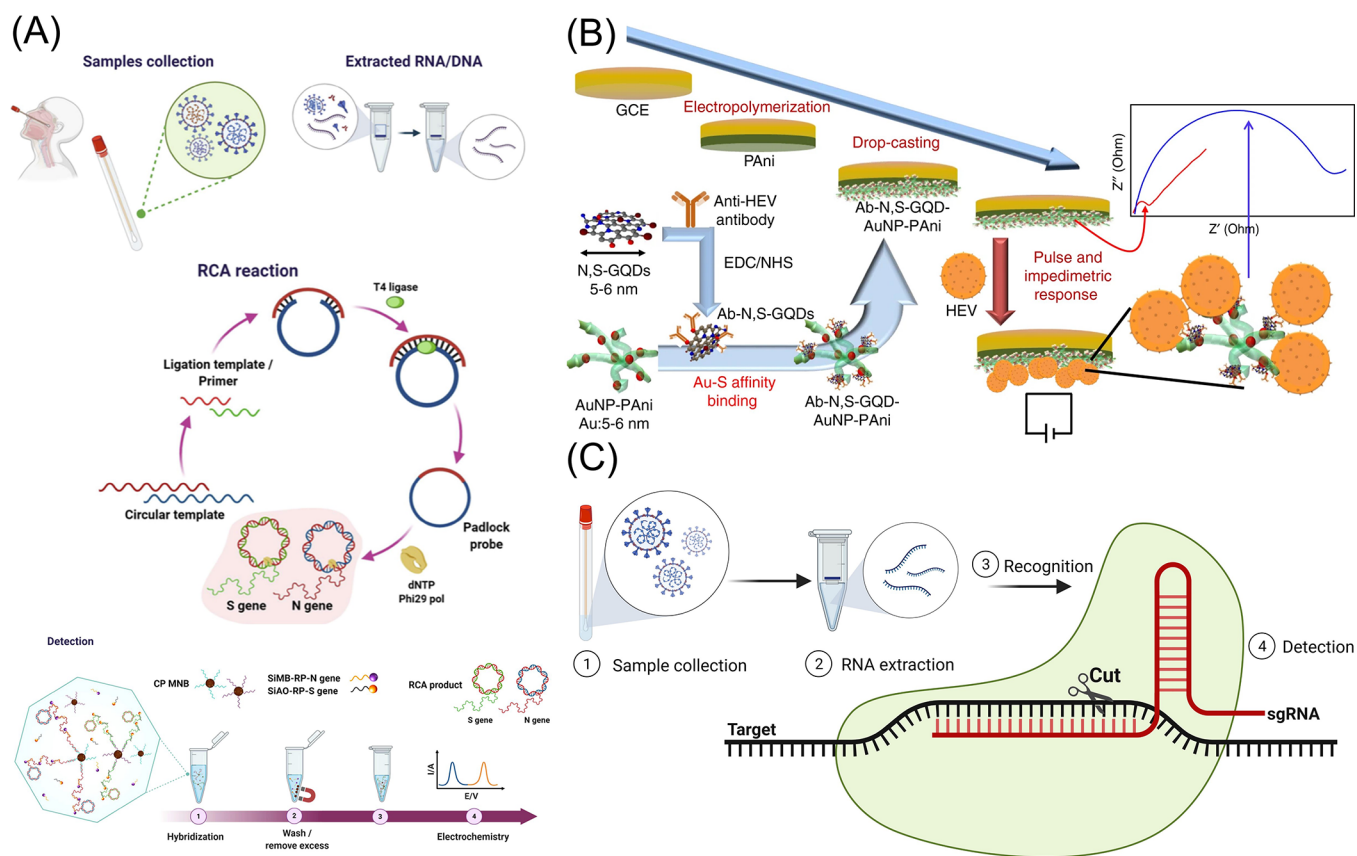


**Figure 11.** (A) Workflow of the RCA-based electrochemical biosensor for the diagnosis of COVID-19 using clinical samples. First, the sample is collected from the patient and undergoes RNA extraction. Next, the presence of SARS-CoV-2 RNA is recognized and amplified using RCA of the N and S genes. The RCA product will be captured and detected using an electrochemical biosensor. Reprinted with permission under a Creative Commons (CC-BY) from ref 169. Copyright 2021 Springer Nature. (B) Schematic illustration of the pulse-induced impedimetric sensing using the nanocomposite-loaded electrode. Reprinted with permission under a Creative Commons (CC-BY) from ref 137. Copyright 2019 Springer Nature. (C) Schematic representation of the CRISPR-enabled detection for pathogen gene.

around time of 5 min and does not involve NAA steps (Figure 10B).<sup>100</sup>

Combining electrochemical sensing with isothermal amplification has been reported for the sensitive detection of SARS-CoV-2. Chaibun *et al.*<sup>169</sup> reported an electrochemical-based approach for the detection of SARS-CoV-2 with good specificity and sensitivity. The test utilizes the rolling circle amplification (RCA) isothermal amplification technique to generate a concatemer containing multiple repeats of sequences that are complementary to the circular template. Silica nanoparticles labeled with redox molecules coated with capturing probes specific to the circular template have been used as an electrochemical reporter. Multiple silica nanoparticles would bind to the long RCA amplicon due to the multiple repeats of the target sequence. The RCA products/silica nanoparticles complex has been captured using magnetic nanoparticles coated with ssDNA capturing probe as shown in Figure 11A. The RCA-based electrochemical approach is successful in detecting SARS-CoV-2 with LOD of 1copy/ $\mu$ L and is sensitive to the mismatches in the target sequence, where two base mismatches of the target sequence showed a negative response.<sup>169</sup> The test's high sensitivity may be attributed to the use of the RCA technique to produce multiple copies of the same sequence. On the other hand, the use of silica NPs serves the purpose of a redox reporter, whereas the magnetic beads allow the removal of the unbonded silica NPs for high SNR.<sup>169</sup> The sensor sensitivity

can be further improved by applying an external electrical trigger to immobilize the virus. Chowdhury *et al.*<sup>137</sup> reported the development of a pulse-triggered electrochemical sensor for the detection of the virus with high sensitivity using a combination of nanomaterial and polymer complexes. The sensor was fabricated on a surface of a glassy carbon electrode using graphene QDs and AuNPs embedded in the polyaniline nanowire's structure as shown in Figure 11B. Introducing an external electrical pulse during the virus accumulation has been shown to enhance the platform sensitivity. The platform successfully detected the hepatitis E virus (HEV) in serum samples and its different genotypes including G1, G3, G7, and ferret HEV.<sup>137</sup>

Another type of recognition probe that showed promise is clustered regularly interspaced short palindromic repeats (CRISPR).<sup>170</sup> The recognition of the target sequence by CRISPR is highly specific with minimal off-target, making it an ideal candidate for COVID-19 detection. Cas12a technology was successful in identifying the presence of SARS-CoV-2 genetic material in  $\sim$ 50 min with a sensitivity of two copies per sample without cross-reactivity.<sup>171</sup> Several reports proved with the experimental evidence that a LOD as low as two copies can be achieved using a CRISPR-based platform.<sup>32,65</sup> The total testing time using the CRISPR-based platform varies based on the sensor platform utilized for the sensing purposes, ranging from 15 min to  $\sim$ 1 h.<sup>172–174</sup> The CRISPR-based sensor can be further adapted to detect the infection caused by several

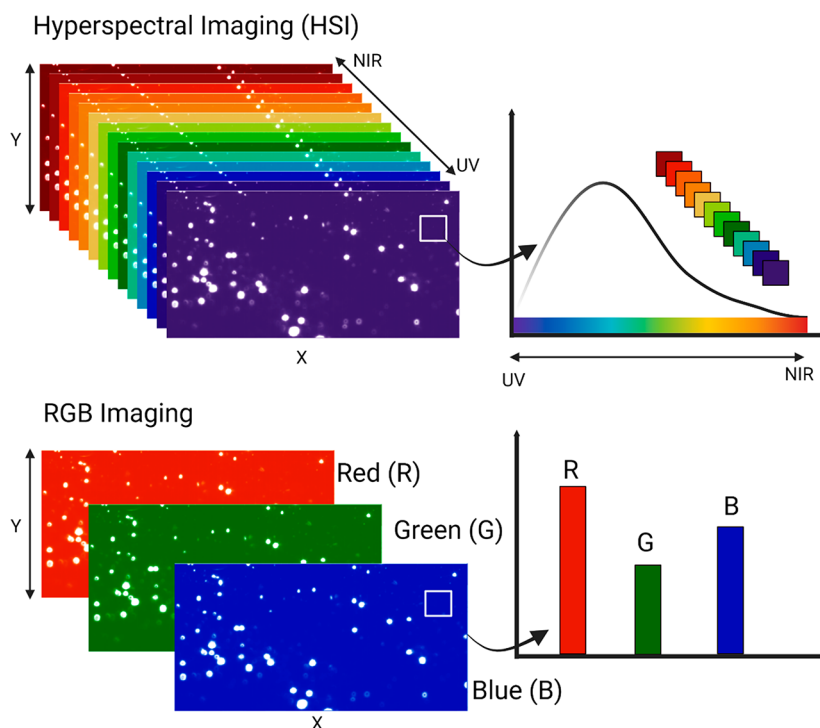


Figure 12. Schematic representation of the fundamental differences between hyperspectral imaging and conventional RGB imaging.

pathogens, which makes it an effective recognition element. The integration of CRISPR technology with an electronics chip sensor enables the sensitive detection of the target RNA/DNA successfully within 15 min and as sensitive as 1.7 fM.<sup>172</sup> Figure 11C depicts the schematic representation of the CRISPR-based detection.

The use of nanomaterials can advance the performance of the sensing technologies in virus identification. The integration of nanomaterials into a sensor device, e.g., quartz crystal microbalance, surface acoustic wave (SAW), or chemiresistors, led to many advancements in the field of sensing.<sup>175,176</sup> For quartz crystal microbalance (QCM), the relationship between the crystal resonance frequency and the overall mass is critical for the sensing application. The change in the crystal resonance frequency is directly proportional to the change in mass ( $\Delta m$ ) as shown in the following equation:

$$\Delta F = -\frac{2NF_0^2}{\sqrt{\rho\mu}} \frac{\Delta m}{A} \quad (2)$$

where  $N$  is the harmonic overtone,  $F_0$  fundamental resonance frequency,  $\rho$  is the crystal density,  $\mu$  is the elastic modulus of the quartz crystal, and  $A$  represents the surface area. QCM that has been modified with nanoporous materials attracted attention for the detection of volatile organic compounds (VOC). This has particular importance in the detection of COVID-19 indicative VOC biomarkers. Mesoporous silica nanoparticles (MSNs) are porous materials that have been used in modifying the QCM electrodes. The sensor exhibited good stability and enhanced sensitivity due to the presence of continuous porous networks that aid in the diffusion of the molecule.<sup>177,178</sup> Researchers have reported the use of amine-functionalized type mesoporous silica for the detection of hazardous vapors, an application that can be further expanded to detect VOC biomarkers.<sup>178</sup> Other materials including graphene, cobalt-containing mesoporous carbon, carbon nano-

tubes (CNTs), and metal–organic framework (MOF) have also been utilized to modify the QCM surface.<sup>175,176</sup> Different MOF structures have been evaluated for the detection of several VOCs including  $\text{CH}_3\text{OH}$ , isopropanol ( $i\text{-C}_3\text{H}_7\text{OH}$ ),  $\text{H}_2\text{O}$ , and  $\text{CH}_3\text{COCH}_3$  due to the variation in the adsorption and desorption process to the sensor surface.<sup>175</sup> Further, QCM has been used in the detection of microorganisms and viruses through a biorecognition element immobilized on its gold surface. The hybridization of the virus/microorganism antigen with its complementary bioreceptor changes the interfacial mass which leads to a shift in the resonance frequency. Thus, the amount of the target bound to the QCM surface can be quantified using the frequency shift. To detect several biomarkers or analytes, QCM-based sensors can be integrated with a microfluidic device where each well is differentially functionalized with bioreceptors specific for each target.<sup>179</sup>

Apart from QCM-based sensors, chemiresistor has been used as a sensing platform. Chemiresistors are mainly composed of a substrate, contact electrodes, and the detection area, which responds to the target analyte. Chemiresistors convert a microscopic event such as a chemical reaction or a binding event into a detectable electrical signal. For example, graphene oxide-based titanium oxide ( $\text{GO}/\text{TiO}_2$ ) coated chemiresistors exhibit a high sensitivity toward detecting a gas or VOC by retaining a more reactive site due to preventing the aggregation of the GO by  $\text{TiO}_2$ . A chitosan-based reduced graphene oxide (rGO) chemiresistor has been shown to effectively monitor acetone as a VOC. This sensor has been shown to capture a large quantity of gas due to its porous surface with a low dead volume. This allows the diffusion of the gas molecule by offering a large reactive site for better sensitivity and efficiency.<sup>180</sup>

**Microscopy and Spectroscopy-Based Tests.** Several microscopy techniques have revolutionized the sensing field including Raman spectroscopy,<sup>181–183</sup> Fourier transforms

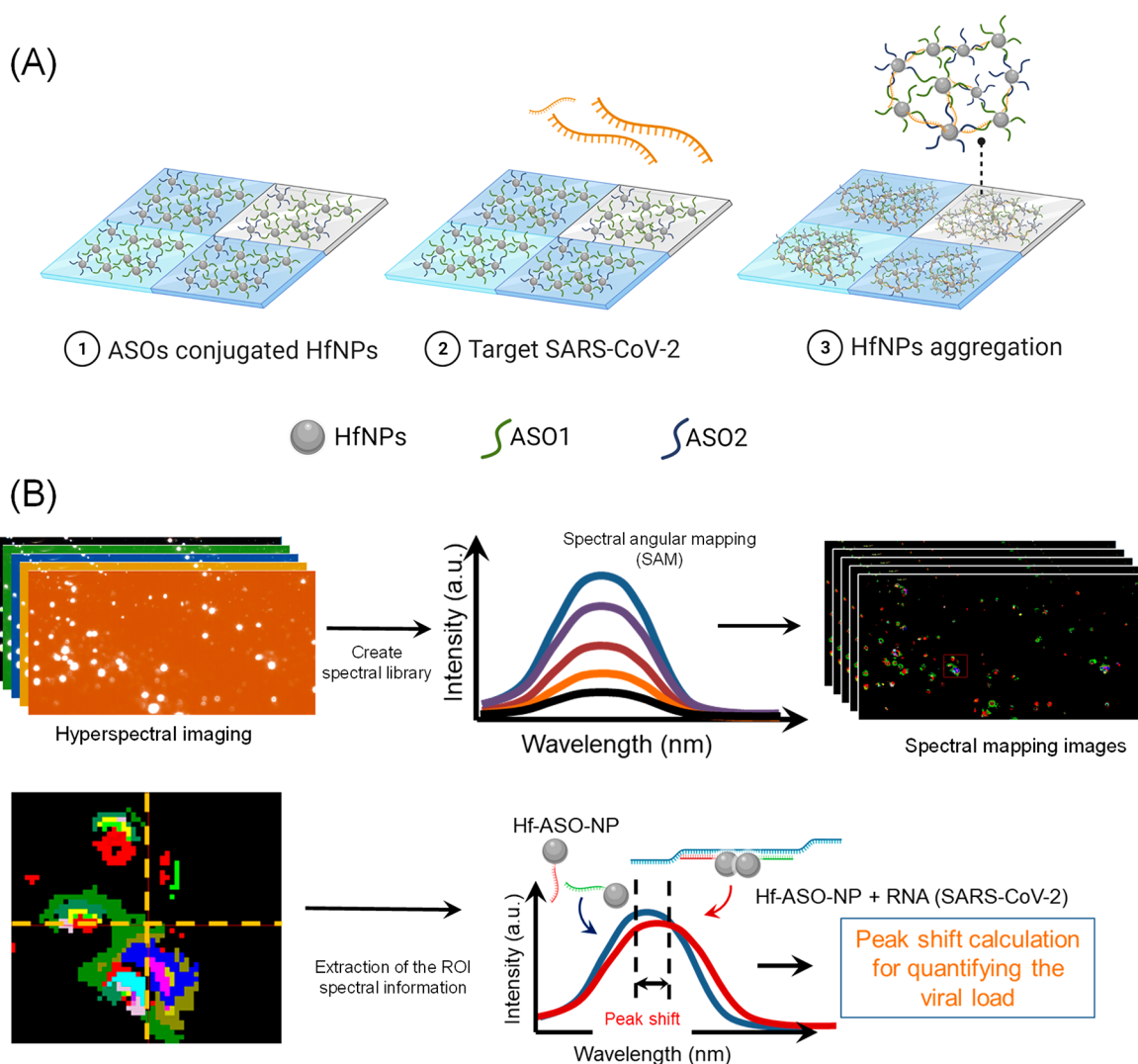


**Figure 13.** (A) Schematic representation of the sensing mechanism behind the HfNPs-based hyperspectral sensor. In the presence of SARS-CoV-2 RNA, a large aggregate of the HfNPs will be formed due to the hybridization of the ASO coating of the HfNPs with the target. The formation of the large aggregates shifts the hyperspectral signal of the HfNPs to the right. (B) Computational analysis of the capture hyperspectral signal to estimate viral load. Reprinted with permission from ref 99. Copyright 2021 American Chemical Society.

infrared spectroscopy (FT-IR),<sup>184–186</sup> and most recently hyperspectral spectroscopy.<sup>187–190</sup>

Raman-based spectroscopy is a well-known technique that can provide information about the chemical structure, crystallinity, phase, and molecular interaction of the sample under investigation.<sup>181–183</sup> Raman spectroscopy has been used extensively to detect pathogens, tumor margins, water contaminants, and several diseases.<sup>181–183</sup> Chen *et al.*<sup>191</sup> reported the development of a platform capable of detecting SARS-CoV-2 lysate using surface-enhanced Raman scattering (SERS) by an aptamer specific for the SARS-CoV-2 spike protein. A gold-grown nanopopcorn surface has been used to adsorb the aptamer for observing the change in the SERS peaks. The use of Raman spectroscopy enables the detection of SARS-CoV-2 lysate with a sensitivity of up to 10 PFU/mL in a short time (15 min).<sup>191</sup> The Raman-based test's sensitivity can be further improved by using ASOs as targeting probes. It has been shown that combining surface-enhanced Raman scattering with ASOs-capped AuNPs can lead to enhanced analytical and clinical performance. Using a machine-learning algorithm to analyze the Raman spectrum, the test was successful in

detecting SARS-CoV-2 with sensitivity and specificity of 100% and 90%, respectively. The system showed a limit of detection of 63 copies/mL of SARS-CoV-2 RNA concentration.<sup>192</sup>

Apart from Raman spectroscopy, the FT-IR technique has been used for the diagnosis of COVID-19. Kitane *et al.*<sup>193</sup> reported a label-free approach for the rapid detection of SARS-CoV-2 using the FT-IR spectroscopy technique. RNA extracted from samples collected from 280 patients was used to evaluate the system performance.<sup>193</sup> The system responses are in agreement with the gold standard, RT-PCR, with 97.8%, 97%, and 98.3% accuracy, sensitivity, and specificity, respectively.<sup>193</sup>

Recently, an imaging technique known as hyperspectral imaging (HSI) came into the spotlight, due to its ability to identify the target in a label-free manner.<sup>99,107,187–189,194–198</sup> HSI is a technique that captures thousands of images at different wavelengths across a continuous spectrum of light.<sup>187–189</sup> Thus, the value of each pixel is a continuous spectrum instead of three discrete intensities as in the case of regular RGB images (Figure 12). The data collected by the HSI system in each pixel can be viewed as a hypercube by

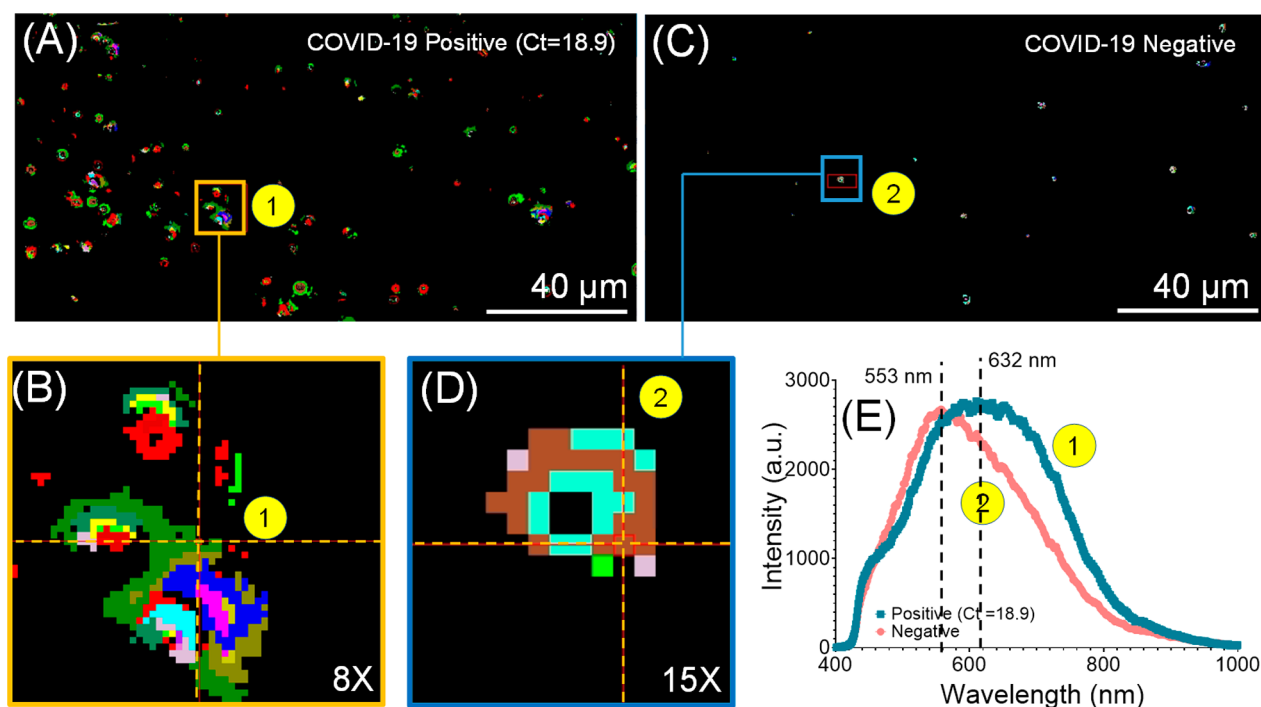


Figure 14. (A) Overlay of the hyperspectral map on the dark-field image of COVID-19 positive sample (Ct = 18.9). (B) Zoomed-in image of mapping in A. (C) The superimposed hyperspectral map on a dark-field image captured from a COVID-19 negative sample. (D) Zoomed-in image of C. (E) Predominant hyperspectral signature in both positive and negative COVID-19 samples. The positive sample showed a significant peak shift when compared with the negative sample. Reprinted with permission from ref 99. Copyright 2021 American Chemical Society.

analyzing a spectrum of light instead of assigning primary colors.

Alafeef *et al.*<sup>99</sup> recently reported the use of hyperspectral spectroscopy to diagnose COVID-19. The system relies on the change of the hyperspectral signature of the hafnium nanoparticles (HfNPs) coated with ASOs to generate a detectable signal in the presence of SARS-CoV-2 RNA as shown in Figure 13A. HfNPs conjugated to ASOs have been used as a recognition element to recognize its complementary sequence and thus lead to the aggregation of the HfNPs. The agglomeration of HfNPs led to a shift in the hyperspectral peak which has been analyzed to estimate the SARS-CoV-2 viral load as shown in Figure 13B. The workflow of the computational algorithm can be summarized as follows. First, hyperspectral imaging has been captured after the addition of the patient sample to the test chip containing HfNPs-ASOs. Next, the region of interest (ROI) has been defined and used to generate a spectral library. A powerful mapping algorithm known as the spectral angular mapping (SAM) algorithm has been applied to map the reference spectrum from the spectral library to each corresponding pixel. Next, the dominant spectrum has been identified by conducting a distribution analysis of the image's pixels. Finally, the peak shift of the predominant signal with respect to the HfNPs-ASOs spectrum is used to quantify the SARS-CoV-2 viral load.<sup>99</sup> The system performance has been evaluated using ~100 clinical samples, and the results have been benchmarked with the gold standard technique (RT-PCR). Figure 14 shows a representative image of the hyperspectral mapping of both confirmed positive and negative COVID-19 cases and the associated hyperspectral signals. The system showed an extraordinary sensitivity with a short turn-around time of a few minutes, and the ability to

extend its applicability to cover other viruses such as influenza.<sup>99</sup>

Nuclear magnetic resonance spectroscopy (NMR) is another approach used for the detection of viruses. The detection of the virus is possible through magnetic relaxation switching (MRS) of magnetic nanoparticles due to the aggregation of the NPs in the presence of the virus. Magnetic graphene quantum dots (MGQDs) have been utilized to detect SARS-CoV-2 by recording and analyzing MRS signals using NMR spectroscopy. The test is a one-pot reaction with no presample preparation.<sup>199,200</sup> Despite that the MRS-based assay exhibits a high sensitivity toward their target, its working mechanism remains poorly explained.<sup>199,200</sup> Further, the need for NMR spectroscopy limited the applicability of this diagnostic approach outside the laboratory setting. Further, a background in chemistry is required to operate the system and interpret the data, making the system unsuitable for field application.

## NEXT-GENERATION SEQUENCING

The detection of an organism without any prior information is hard to achieve using the previously mentioned techniques. To design a sensing platform for detecting specific pathogens, you need to know its genetic sequence and the associated cellular proteins. However, in the case of emerging viruses, next-generation sequencing (NGS) is the only option to read the genetic sequence of an unknown pathogen.<sup>201,202</sup>

The NGS enables the identification of pathogens and any emerging strains without any prior knowledge in an effective and unbiased way. The NGS involves a complex process of sample preparation, cluster generation, sequencing, and data analysis. Both NGS and PCR can provide a sensitive and



## Diagnosis of COVID-19 Using Breath Biopsy

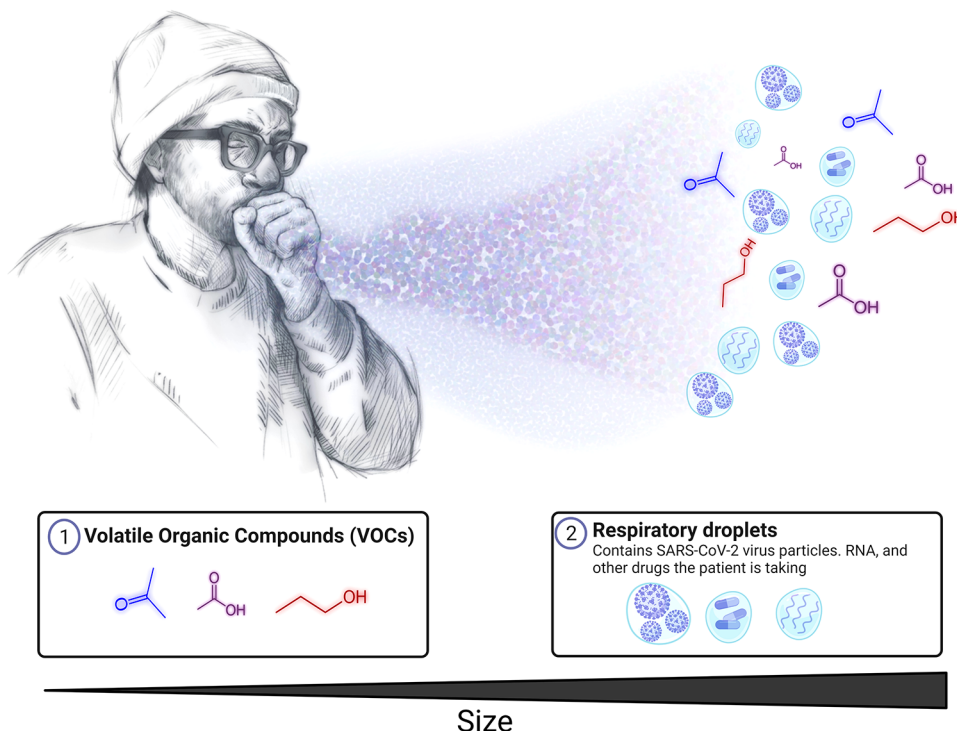


**Figure 15.** Diagnosis of COVID-19 using a breath biopsy. The exhaled air contains several components ranging from volatile organic compounds to virus particles, RNA, and drug metabolites.

accurate identification of emerging pathogens such as SARS-CoV-2 and its variants; however, PCR can only amplify known sequences, whereas NGS has a different level of discovery power by enabling effective sequencing of unknown sequences.

High-throughput sequencing is the most precise method for virus detection; however, the method cannot be adopted for clinical diagnostic application due to the time, cost, and level of the skill set needed as well as the sophisticated equipment required.<sup>201,202</sup>

### SARS-CoV-2 DIAGNOSIS USING MEDICAL IMAGING

Although RT-PCR is the standard technique to diagnose the infection of COVID-19, its positivity is low for both nasal swab (63%), and pharyngeal swab (32%).<sup>203,204</sup> Further, the RT-PCR test is still time-consuming and takes days to weeks for the results to be reported.<sup>205</sup> Therefore, suspected cases, with confirmed PCR results or without, need a second step of affirmation. The use of medical imaging for COVID-19 diagnosis is a supplementary step to confirm and monitor the viral infection and its spread in the lungs. Chest X-ray, computed tomography (CT), and magnetic resonance imaging (MRI) are medical imaging modalities that have been used to diagnose the infection by SARS-CoV-2 viruses. Revealing the presence of the infection can be fast using both chest X-ray and CT imaging, though the cost remains a major concern.<sup>206,207</sup> Moreover, COVID-19 diagnosis demands frequent testing of the subject in a short time, which raises major safety concerns.<sup>207–209</sup> On the other hand, MRI can help in the diagnosis of COVID-19, by detecting features of viral pneumonia, tissue damage, and lesions,<sup>209,210</sup> though once again the high running cost of MRI limits its wide deployment.

The real-time monitoring of the pathogen in body tissues can help us to understand the distributive behavior of the virus

particles. For preclinical studies, optical imaging offers striking benefits to visualize the virus distribution and kinetics within biological tissue. However, optical imaging has a low signal-to-noise ratio due to the tissue autofluorescence which limits its applicability. To overcome this limitation, the tissue can be imaged at a near-infrared second biological window (NIR-II) where tissue exhibits negligible autofluorescence. Moitra *et al.*<sup>102</sup> reported the use of QD-coated with a molecular probe that selectively targets the N-gene of SARS-CoV-2. QDs have been used to label SARS-CoV-2 to enable tracking of the virus distribution in deep tissue. The SARS-CoV-2 virus has been monitored using *ex-vivo* imaging, confirming the possibility to track the virus deeply in the tissue.<sup>102</sup>

### SARS-CoV-2 DIAGNOSIS USING VOLATILE ORGANIC COMPOUNDS

Noninvasive breath biopsy enables the diagnosis of respiratory infectious diseases in real-time. Breath biopsy obtained from COVID-19 patients contains viral particles or RNA released in a respiratory droplet, volatile organic compounds, and nonvolatile macromolecules like inflammatory mediators (Figure 15).<sup>211–214</sup> Breath-borne volatile organic compound (VOC) is a respiratory biomarker that helps in the diagnosis of COVID-19 and further enables the real-time noninvasive monitoring of lung tissue damage due to COVID-19 infection. Breath is a rich mixture of VOCs including carbohydrates, heterocyclic, alcohol, ketones, aldehydes, and esters.<sup>214–217</sup>

The use of a machine-learning algorithm to analyze the patient's VOC signature represents a powerful tool for the point-of-care screening of COVID-19. The composition of the VOC in the breath of COVID-19 patients is different from the same of healthy individuals. COVID-19 patients have shown elevated propanol levels in the exhaled air, and a low level of

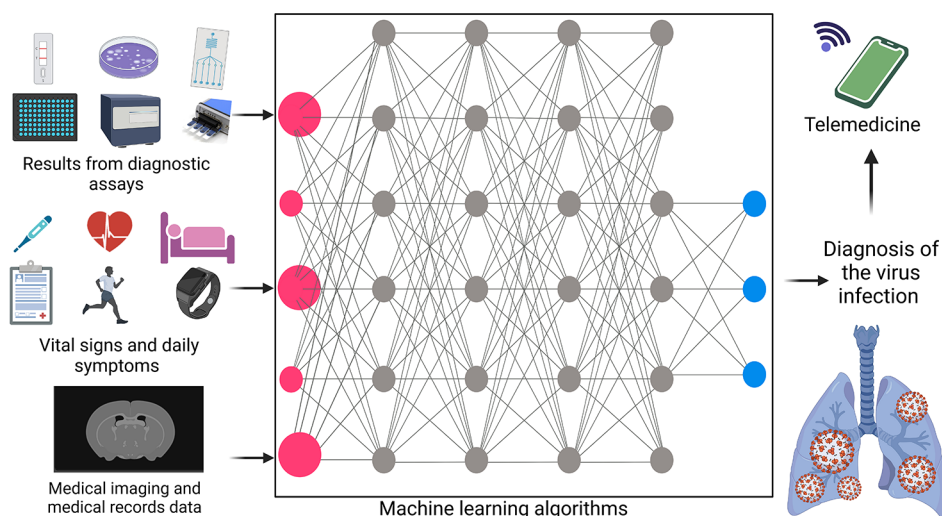


**Figure 16.** Schematic diagram of the potential use of machine learning in the analysis of big data to speed up the diagnosis of COVID-19 and help mitigate the virus spread.

acetone compared to the healthy subjects.<sup>218</sup> Furthermore, other VOCs including acetic acid and nonidentified VOCs also varied between the two groups.<sup>218</sup> Using a machine-learning algorithm to classify the VOCs data collected using a gas chromatograph (GC) and an ion mobility spectrometer (IMS), the COVID-19 patients have been differentiated from the normal cases with 90–100% accuracy.<sup>218</sup> Combining computational algorithms with a rapid sensing platform such as electrochemical or colorimetric tests allows for the detection and analysis of the VOCs in real-time for disease diagnosis. The VOC biomarkers if successful in diagnosing COVID-19 may solve the limitations of the current NAAT and alleviate the patient's discomfort associated with collecting throat/nasal swabs. Leong *et al.*<sup>219</sup> reported the design of a hand-held SERS-based breathalyzer to identify COVID-19 infected individuals in less than 5 min, achieving >95% sensitivity and specificity across 501 participants. Changes in the vibrational fingerprints have been observed due to the interaction between the metabolites present in the breath biopsy and the receptors used in the SERS-based breathalyzer. Using a computational algorithm such as partial least-squares discriminant analysis, these fingerprints have been classified accurately.<sup>219</sup>

In another attempt to diagnose COVID-19, electronic nose (eNoses) has been used to detect multiple targets by mimicking animal olfaction function. Using machine learning to analyze the body-odor data collected from a drive-through station using a chemical nose, the researcher was successful in diagnosing COVID-19 with fair accuracy.<sup>220</sup>

Shan *et al.*<sup>104</sup> reported the use of a nanomaterial-based sensor array for the detection of COVID-19-specific biomarkers from exhaled breath. The study evaluates the possibility of diagnosing COVID-19 in a clinical study conducted in Wuhan, China, with 140 participants. The participants consisted of three groups, 49 confirmed COVID-19 positive, 58 healthy subjects, and 33 subjects with non-COVID-19 pneumonia. The sensor array consists of AuNPs capped with different organic ligands which interact with the VOCs differentially. The VOCs diffuse into the sensing layer where they interact with the functional groups capping the AuNPs, which generate differential electrical signals. The electrical response was classified using the discriminant factor analysis (DFA) algorithm. The use of machine-learning

algorithms with nanotechnology-based approaches enabled the advancement of clinical decision support systems.<sup>221,222</sup>

The model was capable of differentiating COVID-19 infected from healthy subjects with 75%, 100%, and 61% accuracy, sensitivity, and specificity, respectively. COVID-19-infected subjects were differentiated from the subjects infected with non-COVID infected pneumonia with 95%, 100%, 90% accuracy, sensitivity, and specificity, respectively. However, the actual VOCs responsible for this differential signal were not explored in this study.<sup>104</sup>

SARS-CoV-2 has been also identified using exhaled breath condensate (EBC) through the detection of aerosolized VOCs and nonvolatile molecules (i.e., proteins, RNA, DNA, microorganisms, and viruses) in the condensate. The SARS-CoV-2 can be directly detected in the collected condensates using RT-PCR.<sup>223</sup> Ma *et al.*<sup>224</sup> illustrated that COVID-19 can be diagnosed by analyzing samples collected from EBC using an RT-PCR kit targeting both ORF1ab and N genes (Jiangsu Biopertectus Technologies, Nanjing, China). The use of the EBC system can be convenient and effective for the surveillance of the spread of COVID-19 in the community; however, it has suffered from a low positivity rate of around 26.9% ( $n = 52$ ).<sup>224</sup> Even though the EBC systems have a low positivity compared to nasal swab RT-PCR, it is still higher than the positivity rate in diagnosing COVID-19 using surface samples. A portable dehumidifier was used for the diagnosis of COVID-19 in a hospital ward.<sup>225</sup> However, further evaluation under controlled conditions is still needed to validate the effectiveness of the dehumidifier in diagnosing COVID-19 or any future emerging pathogens.<sup>225</sup> Despite breath biopsy being a convenient method to diagnose diseases, more studies are still needed to establish its effectiveness and identify the VOC biomarkers associated with each disease.

## ARTIFICIAL INTELLIGENCE FOR DIAGNOSIS OF INFECTIOUS DISEASES

Artificial intelligence is a tool that finds its way into a wide variety of applications from material science, and environmental applications, to smart health care systems.<sup>97,103,221,222,226–239</sup> Draz *et al.*<sup>240</sup> reported the development of nanoparticles-enabled smartphones for the detection of the virus using artificial intelligence.<sup>240</sup> The system consists



Table 5. Comparison of the Performance of the Four Main Technologies Used in the Diagnosis of COVID-19

|                                       | Technology                         | Target   | Specimen type  | Assay time              | LOD*   | Sensitivity and Specificity  |
|---------------------------------------|------------------------------------|--|--|-------------------------|--|--|
| VIRUS (DIRECT)                        | Nucleic acid test                  | Viral RNA (N-, S-, E-, ORF1ab, ORF3a, ORF7ab genes)  | Nasal swab, saliva, throat swab, oropharyngeal swab, nasopharyngeal swab | 2-4 hours               | 1-100 copies/reaction <sup>46</sup>  | sensitivity >83% and specificity >90%. <sup>46,243,244</sup>   |
|                                       | Antigen tests                      | Viral proteins (N, E, M, S proteins)   | Nasal swab, saliva, nasopharyngeal swab                                  | 15-30 min               | 2.07 × 10 <sup>6</sup> -2.86 × 10 <sup>7</sup> copies/swab <sup>245</sup><br>Or 1 × 10 <sup>6</sup> genome copies/ml <sup>27</sup> | Sensitivity -Symptomatic individual >65.3%<br>-Asymptomatic individual >44.0 and specificity >90%. <sup>28</sup> |
| ANTIBODIES                            | Serological tests                  | IgG, IgM antibodies  | Drawn blood or fingerstick   | 10-20 min <sup>46</sup> | 0.1 µg/mL <sup>41</sup>  | Sensitivity: 33.9-94.6%<br>Specificity: 91-100%. <sup>31,41</sup>  |
| VIRUS (INDIRECT) / INFECTION OUTCOMES | volatile organic compound analysis | VOC compounds (e.g., propanol, acetone)  | Breath biopsy  | 10-30 min               | NA   | Sensitivity 50%-99%<br>Specificity 75%-90%. <sup>246,247</sup>   |
|                                       | Imaging strategy                   | Chest X-ray (CXR): lung abnormality; lesions and masses.<br>US: pleural thickening, subpleural consolidation.<br>CT: ground-glass opacity (GGO). | Non-invasive imaging   | seconds to minutes      | NA   | CXR: sensitivity of 69%, US: sensitivity of 94% and specificity of 85%, CT: sensitivity of 98%. <sup>248</sup>   |

\*LOD value is assay dependent and the value in the table is a representative value based on the provided references.

of a microchip for capturing the virus using specifically designed platinum nanoprobe. The interaction between the platinum nanoprobe and the target virus in the presence of H<sub>2</sub>O<sub>2</sub> induces bubble formation. The bubble formation is mainly due to the formation of the platinum-virus complex which acts as a catalyst to decompose the H<sub>2</sub>O<sub>2</sub> into water and O<sub>2</sub> gas. The pattern of the formed bubbles has been captured using a smartphone camera in the presence of hepatitis B virus (HBV), hepatitis C virus (HCV), and Zika virus (ZIKV) and analyzed using a conventional neural network (CNN). The CNN algorithm was successful in the qualitative detection of the viral-infected samples with a sensitivity of 98.97% and a limit of detection of 250 copies/mL.<sup>240</sup>

Wearable devices that are continuously measuring the subject's vital signs have ample potential to track the onset of infectious diseases and more importantly mitigate the spread of COVID-19. A smartwatch is a widely deployable device that measures heart rate, sleep, ECG, and blood oxygen levels.<sup>241,242</sup> Machine learning enables real-time health monitoring and surveillance through analyzing the physiological parameters to actively predict the onset of COVID-19 in a retrospective manner by analyzing the data recorded using the wearable device. Studies showed that sleep duration is altered significantly by the onset of COVID-19; however, no information about the affected sleep stage was reported.<sup>242</sup> Furthermore, the analysis of smartwatch data from 3318 participants revealed that upon the onset of early infection,

subjects suffer from aberrant physiological and activity signals including heart rates and steps. The analysis of smartwatch data using a machine-learning algorithm can serve as an early alert for the onset of COVID-19 infection in both presymptomatic and asymptomatic infected individuals.<sup>240-242</sup> Machine learning can be used to analyze data collected from laboratory or point-of-care testing, recording the subjects' vital signs or through medical images. Figure 16 depicts a schematic representation of the workflow of using ML in the diagnosis of COVID-19.

## OUTLOOK AND FUTURE PERSPECTIVES

The COVID-19 pandemic is an ongoing global challenge that continues to impact the global economy and society. The effective control of SARS-CoV-2 requires the wide availability of rapid tests that can be used to identify positive cases on the spot to avoid the unnecessary quarantine of the negative cases and halt or reduce the silent spread of the virus. Monitoring unknown emerging pathogens is difficult; however, advanced sequencing techniques enable the identification of any unexpected viral threats. The pandemic has shed the light on the importance of various surveillance strategies including both at the individual and at the community levels which are key to responding to the pandemic. Table 5 summarizes the characteristics of the main technologies used for the diagnosis of COVID-19. Currently, disease confirmation and monitoring

are performed primarily with a NAAT test that detects SARS-CoV-2 RNA.<sup>22</sup>

COVID-19 highlights the importance of patient point-of-care tests to control the rapid spread of the virus; however, the available technologies have their inherent limitations. This is primarily due to the lack of an established target product profile (TPPs) to guide the process of developing diagnostic systems by outlining the targets and specifications for the performance and operational characteristics based on the user's need. TPPs should highlight the most important operational characteristics and test performance while outlining the lowest acceptable output for a characteristic. "Optimal" refers to the ideal target for operational characteristics, and thus the products have to meet at least all of the minimal characteristics and preferably as many of the optimal characteristics as possible. Certain key specifications need to be met for the development of the next generation of the point-of-care tests for pandemic preparedness. The test has to be easy to modify to target any newly identified pathogen, low-cost, with a short turnaround time. The sensitivity is a critical feature of the assay to reduce the false-negative incident depending on the viral load in the target specimen.<sup>21–23</sup> The steps required to prepare the sample, as well as the specimen type, play a critical role in the assay performance and usability. For example, the true positive rate of COVID-19 diagnosis using RT-PCR is high in the bronchoalveolar lavage fluid, followed by sputum, nasopharyngeal swabs, and low in pharyngeal swabs and stool samples as shown in Figure 1.<sup>21,22,243–249</sup> Unfortunately, because of the unexpected emergence of SARS-CoV-2, the luxury of having such a product profile does not exist. At the time of drafting this article, there have been over 351 million cases of confirmed COVID-19 cases worldwide, with over 51 million cases in the United States. There have been over 5.1 M deaths, with nearly 1 M occurring in the United States. A pandemic of this magnitude helped us to gain expertise in regulatory matters, as some tests seemed underregulated, which allowed flawed antigen tests to be sold. With increasing demand, the clinical laboratory performed a tremendous number of tests and validated new assays. We now have the valuable experience and gained knowledge to create initial TPPs with a comprehensive list of test performance and characteristics. For several of these characteristics though, only limited evidence is still available, and further opinion must be sought from the stakeholders. A comprehensive stakeholder opinion must be gathered by engaging a group of individuals from WHO, CDC, clinicians, chemists, and representatives of countries and diagnostics and pharmaceutical industries.

Nanotechnology plays a critical role in the advancement of the fabrication and manufacturing of miniaturized sensing technologies. The advancement in 2D and 3D-based nanomaterials is shown to satisfy the increasing demand for diagnostic tests with improved sensing performance. The major advantage of nanomaterials is that they provide a superior surface area/volume ratio in comparison to their bulk counterparts, which offers more sensitivity for the detection of biological or chemical molecules even at the trace of a single-molecule level. At the nanoscale, materials attain several unique optical, plasmonic, and electrical properties. For all these reasons, over the years, nanomaterials played a major role to advance the field of medical diagnostics, environmental monitoring, and many other sensing applications while offering high accuracy and sensitivity. The example of these sensing technologies may span from wearable sensors, and point-of-care sensors, to

implantable sensors. Nanotechnology-based biosensors exhibit high sensitivity, which allows the early detection and continuous monitoring of patient's health status in a personalized fashion. The use of nanotechnology in sensor design and fabrication tackles the current challenges in the diagnostic field in terms of scalability, mass-production, sensitivity, and multiplexing capability. For pandemic preparedness, a rapid response is highly anticipated. A flurry of recent works emphasize mounting interest in approaches that employ nanomaterials in diagnostic platforms. Compared with traditional approaches, nanotechnology offers ultrasensitivity for biological analytes with minimal cross-reactivity as characterized by their small size, low production cost, low power consumption, tailorable surface chemistry, and high surface-to-volume ratio. The recent pandemic also has witnessed an influx of federal funding which has helped researchers in that these materials could soon move toward clinical translation. Many of these materials can potentially be used in platform technologies with the anticipation that their modularity can be exploited for emerging pathogens. Thus, nanosensors have the potential to serve as a game-changer for pandemic preparedness.

It is understandable that because of the hard work of the research community during the pandemic we will control this virus, and with a strong vision, we will be better prepared for those pathogens that may emerge in the future.

## AUTHOR INFORMATION

### Corresponding Author

**Dipanjan Pan** – Department of Chemical, Biochemical and Environmental Engineering, University of Maryland Baltimore County, Interdisciplinary Health Sciences Facility, Baltimore, Maryland 21250, United States; Departments of Diagnostic Radiology and Nuclear Medicine and Pediatrics, Center for Blood Oxygen Transport and Hemostasis, University of Maryland Baltimore School of Medicine, Health Sciences Research Facility III, Baltimore, Maryland 21201, United States; Department of Bioengineering, the University of Illinois at Urbana–Champaign, Urbana, Illinois 61801, United States; [orcid.org/0000-0003-0175-4704](https://orcid.org/0000-0003-0175-4704); Email: [dipanjan@psu.edu](mailto:dipanjan@psu.edu)

### Author

**Maha Alafeef** – Department of Chemical, Biochemical and Environmental Engineering, University of Maryland Baltimore County, Interdisciplinary Health Sciences Facility, Baltimore, Maryland 21250, United States; Departments of Diagnostic Radiology and Nuclear Medicine and Pediatrics, Center for Blood Oxygen Transport and Hemostasis, University of Maryland Baltimore School of Medicine, Health Sciences Research Facility III, Baltimore, Maryland 21201, United States; Department of Bioengineering, the University of Illinois at Urbana–Champaign, Urbana, Illinois 61801, United States; Biomedical Engineering Department, Jordan University of Science and Technology, Irbid 22110, Jordan

Complete contact information is available at:

<https://pubs.acs.org/10.1021/acsnano.2c01697>

### Notes

The authors declare the following competing financial interest(s): Prof Pan is the founder or co-founder four university based start ups. None of these entities, however, supported this work.

## ACKNOWLEDGMENTS

The authors gratefully acknowledge the receipt of funding from the National Institute of Biomedical Imaging and Bioengineering (NIBIB) R03EB028026, R03 EB028026-02S2, and R03 EB028026-02S1, the University of Maryland, Baltimore (UMB), and the University of Maryland, Baltimore County (UMBC). Also, we would like to acknowledge Bisma Ali for her help in editing the manuscript. Some of the manuscript's figures have been created partially or fully using [biorender.com](https://biorender.com).

## VOCABULARY

nanomaterial = material with at least one dimension in the range of 1–100 nm

nanoparticle = a particle with a size or at least half number size distribution is lower than 100 nm

pandemic preparedness = a product development plan to prepare for any future health emergency caused by an infectious disease outbreak

biosensor = a device that utilizes a bioreceptor to detect the presence of the target analyte by generating a signal proportional to the target concentration

infectious disease = a disorder caused by a living organism such as bacteria, parasites, fungi, or virus. Some infectious diseases can pass from person to person

## REFERENCES

- (1) Kasibhatla, S. M.; Kinikar, M.; Limaye, S.; Kale, M. M.; Kulkarni-Kale, U. Understanding Evolution of SARS-CoV-2: A Perspective from Analysis of Genetic Diversity of RdRp Gene. *Journal of Medical Virology* **2020**, *92* (10), 1932–1937.
- (2) Asselah, T.; Durantel, D.; Pasmant, E.; Lau, G.; Schinazi, R. F. COVID-19: Discovery, Diagnostics and Drug Development. *Journal of Hepatology* **2021**, *74* (1), 168–184.
- (3) Velavan, T. P.; Meyer, C. G. The COVID-19 Epidemic. *Tropical Medicine & International Health* **2020**, *25* (3), 278–280.
- (4) Phan, T. Genetic Diversity and Evolution of SARS-CoV-2. *Infection, Genetics and Evolution* **2020**, *81*, 104260.
- (5) Huang, H.; Fan, C.; Li, M.; Nie, H.-L.; Wang, F.-B.; Wang, H.; Wang, R.; Xia, J.; Zheng, X.; Zuo, X.; Huang, J. COVID-19: A Call for Physical Scientists and Engineers. *ACS Nano* **2020**, *14* (4), 3747–3754.
- (6) Baloch, Z.; Ma, Z.; Ji, Y.; Ghanbari, M.; Pan, Q.; Aljabr, W. Unique Challenges to Control the Spread of COVID-19 in the Middle East. *Journal of Infection and Public Health* **2020**, *13* (9), 1247–1250.
- (7) Ruiz-Hitzky, E.; Darder, M.; Wicklein, B.; Ruiz-Garcia, C.; Martín-Sampedro, R.; del Real, G.; Aranda, P. Nanotechnology Responses to COVID-19. *Adv. Healthcare Mater.* **2020**, *9* (19), 2000979.
- (8) Budd, J.; Miller, B. S.; Manning, E. M.; Lampos, V.; Zhuang, M.; Edelstein, M.; Rees, G.; Emery, V. C.; Stevens, M. M.; Keegan, N.; Short, M. J.; Pillay, D.; Manley, E.; Cox, I. J.; Heymann, D.; Johnson, A. M.; McKendry, R. A. Digital Technologies in the Public-Health Response to COVID-19. *Nature Medicine* **2020**, *26* (8), 1183–1192.
- (9) Sanche, S.; Lin, Y. T.; Xu, C.; Romero-Severson, E.; Hengartner, N.; Ke, R. High Contagiousness and Rapid Spread of Severe Acute Respiratory Syndrome Coronavirus 2. *Emerging Infectious Disease Journal* **2020**, *26* (7), 1470.
- (10) Sah, P.; Fitzpatrick, M. C.; Zimmer, C. F.; Abdollahi, E.; Juden-Kelly, L.; Moghadas, S. M.; Singer, B. H.; Galvani, A. P. Asymptomatic SARS-CoV-2 Infection: A Systematic Review and Meta-Analysis. *Proc. Natl. Acad. Sci. U. S. A.* **2021**, *118* (34), No. e2109229118.
- (11) Sender, R.; Bar-On, Y. M.; Gleizer, S.; Bernshtein, B.; Flamholz, A.; Phillips, R.; Milo, R. The Total Number and Mass of SARS-CoV-2

Virions. *Proc. Natl. Acad. Sci. U. S. A.* **2021**, *118* (25), No. e2024815118.

(12) Valentin, J. Basic Anatomical and Physiological Data for Use in Radiological Protection: Reference Values: ICRP Publication 89: Approved by the Commission in September 2001. *Ann. ICRP* **2002**, *32* (3–4), 1–277.

(13) Kissler, S. M.; Fauver, J. R.; Mack, C.; Olesen, S. W.; Tai, C.; Shiue, K. Y.; Kalinich, C. C.; Jednak, S.; Ott, I. M.; Vogels, C. B. F.; Wohlgemuth, J.; Weisberger, J.; DiFiori, J.; Anderson, D. J.; Mancell, J.; Ho, D. D.; Grubaugh, N. D.; Grad, Y. H. Viral Dynamics of Acute SARS-CoV-2 Infection and Applications to Diagnostic and Public Health Strategies. *PLoS Biology* **2021**, *19* (7), No. e3001333.

(14) Bar-On, Y. M.; Flamholz, A.; Phillips, R.; Milo, R. SARS-CoV-2 (COVID-19) by the Numbers. *eLife* **2020**, *9*. DOI: 10.7554/eLife.57309.

(15) Shereen, M. A.; Khan, S.; Kazmi, A.; Bashir, N.; Siddique, R. COVID-19 Infection: Emergence, Transmission, and Characteristics of Human Coronaviruses. *Journal of Advanced Research* **2020**, *24*, 91–98.

(16) Carter, L. J.; Garner, L. V.; Smoot, J. W.; Li, Y.; Zhou, Q.; Saveson, C. J.; Sasso, J. M.; Gregg, A. C.; Soares, D. J.; Beskid, T. R.; Jervey, S. R.; Liu, C. Assay Techniques and Test Development for COVID-19 Diagnosis. *ACS Cent. Sci.* **2020**, *6* (5), 591–605.

(17) Fajnzylber, J.; Regan, J.; Coxen, K.; Corry, H.; Wong, C.; Rosenthal, A.; Worrall, D.; Giguel, F.; Piechocka-Trocha, A.; Atyeo, C.; Fischinger, S.; Chan, A.; Flaherty, K. T.; Hall, K.; Dougan, M.; Ryan, E. T.; Gillespie, E.; Chishti, R.; Li, Y.; et al. SARS-CoV-2 Viral Load Is Associated with Increased Disease Severity and Mortality. *Nat. Commun.* **2020**, *11* (1), 5493.

(18) Iwamura, A. P. D.; Tavares da Silva, M. R.; Hümmelgen, A. L.; Soeiro Pereira, P. v; Falcai, A.; Grumach, A. S.; Goudouris, E.; Neto, A. C.; Prando, C. Immunity and Inflammatory Biomarkers in COVID-19: A Systematic Review. *Reviews in Medical Virology* **2021**, *31* (4), No. e2199.

(19) Rodriguez-Smith, J. J.; Verweyen, E. L.; Clay, G. M.; Esteban, Y. M.; de Loizaga, S. R.; Baker, E. J.; Do, T.; Dhakal, S.; Lang, S. M.; Grom, A. A.; Grier, D.; Schuler, G. S. Inflammatory Biomarkers in COVID-19-Associated Multisystem Inflammatory Syndrome in Children, Kawasaki Disease, and Macrophage Activation Syndrome: A Cohort Study. *Lancet Rheumatology* **2021**, *3* (8), e574–e584.

(20) Laing, A. G.; Lorenc, A.; del Molino del Barrio, I.; Das, A.; Fish, M.; Monin, L.; Muñoz-Ruiz, M.; McKenzie, D. R.; Hayday, T. S.; Francos-Quijorna, I.; Kamdar, S.; Joseph, M.; Davies, D.; Davis, R.; Jennings, A.; Zlatareva, I.; Vantourout, P.; Wu, Y.; Sofra, V.; et al. A Dynamic COVID-19 Immune Signature Includes Associations with Poor Prognosis. *Nature Medicine* **2020**, *26* (10), 1623–1635.

(21) Kim, Y.-g.; Yun, S. G.; Kim, M. Y.; Park, K.; Cho, C. H.; Yoon, S. Y.; Nam, M. H.; Lee, C. K.; Cho, Y.-J.; Lim, C. S. Comparison between Saliva and Nasopharyngeal Swab Specimens for Detection of Respiratory Viruses by Multiplex Reverse Transcription-PCR. *Journal of Clinical Microbiology* **2017**, *55* (1), 226–233.

(22) Tastanova, A.; Stoffel, C. I.; Dzung, A.; Cheng, P. F.; Bellini, E.; Johansen, P.; Duda, A.; Nobbe, S.; Lienhard, R.; Bosshard, P. P.; Levesque, M. P. A Comparative Study of Real-Time RT-PCR-Based SARS-CoV-2 Detection Methods and Its Application to Human-Derived and Surface Swabbed Material. *Journal of Molecular Diagnostics* **2021**, *23* (7), 796–804.

(23) Garg, A.; Ghoshal, U.; Patel, S. S.; Singh, D. v; Arya, A. K.; Vasanth, S.; Pandey, A.; Srivastava, N. Evaluation of Seven Commercial RT-PCR Kits for COVID-19 Testing in Pooled Clinical Specimens. *Journal of Medical Virology* **2021**, *93* (4), 2281–2286.

(24) Lucira COVID-19 All-In-One Test Kit - IFU. U.S. Food and Drug. <https://www.fda.gov/media/143808/> (accessed 2022-02-04).

(25) Wolff-Duchek, M.; Bergmann, F.; Jorda, A.; Weber, M.; Müller, M.; Seitz, T.; Zoufaly, A.; Strassl, R.; Zeitlinger, M.; Herkner, H.; Schnidar, H.; Anderle, K.; Derhaschnig, U. Sensitivity and Specificity of SARS-CoV-2 Rapid Antigen Detection Tests Using Oral, Anterior Nasal, and Nasopharyngeal Swabs: A Diagnostic Accuracy Study. *Microbiology Spectrum* **2022**, *10* (1), No. e02029-21.



- (26) Deearain, J. M.; Tran, T.; Batty, M.; Yoga, Y.; Druce, J.; Mackenzie, C.; Taiaroa, G.; Taouk, M.; Chea, S.; Zhang, B.; Prestedge, J.; Ninan, M.; Carville, K.; Fielding, J.; Catton, M.; Williamson, D. A. Assessment of Twenty-Two SARS-CoV-2 Rapid Antigen Tests against SARS-CoV-2: A Laboratory Evaluation Study. *medRxiv* **2021**, 2021.12.15.21267691.
- (27) Cubas-Atienzar, A. L.; Kontogianni, K.; Edwards, T.; Wooding, D.; Buist, K.; Thompson, C. R.; Williams, C. T.; Patterson, E. I.; Hughes, G. L.; Baldwin, L.; Escadafal, C.; Sacks, J. A.; Adams, E. R. Limit of Detection in Different Matrices of 19 Commercially Available Rapid Antigen Tests for the Detection of SARS-CoV-2. *Sci. Rep.* **2021**, *11* (1), 18313.
- (28) Jegerlehner, S.; Suter-Riniker, F.; Jent, P.; Bittel, P.; Nagler, M. Diagnostic Accuracy of a SARS-CoV-2 Rapid Antigen Test in Real-Life Clinical Settings. *International Journal of Infectious Diseases* **2021**, *109*, 118–122.
- (29) Gremmels, H.; Winkel, B. M. F.; Schuurman, R.; Rosingh, A.; Rigtter, N. A. M.; Rodriguez, O.; Ubijaaan, J.; Wensing, A. M. J.; Bonten, M. J. M.; Hofstra, L. M. Real-Life Validation of the Panbio™ COVID-19 Antigen Rapid Test (Abbott) in Community-Dwelling Subjects with Symptoms of Potential SARS-CoV-2 Infection. *EClinicalMedicine* **2021**, *31*, 100677.
- (30) Serre-Miranda, C.; Nobrega, C.; Roque, S.; Canto-Gomes, J.; Silva, C. S.; Vieira, N.; Barreira-Silva, P.; Alves-Peixoto, P.; Cotter, J.; Reis, A.; Formigo, M.; Sarmiento, H.; Pires, O.; Carvalho, A.; Petrovskiy, D. Y.; Diéguez, L.; Sousa, J. C.; Sousa, N.; Capela, C.; et al. Performance Assessment of 11 Commercial Serological Tests for SARS-CoV-2 on Hospitalised COVID-19 Patients. *International Journal of Infectious Diseases* **2021**, *104*, 661–669.
- (31) *EUA Authorized Serology Test Performance*. U.S. Food and Drug Administration. <https://www.fda.gov/medical-devices/coronavirus-disease-2019-covid-19-emergency-use-authorizations-medical-devices/eua-authorized-serology-test-performance> (accessed 2022-03-04).
- (32) Hahn, S. M. *Coronavirus (COVID-19) Update: FDA Authorizes First Antigen Test to Help in the Rapid Detection of the Virus that Causes COVID-19 in Patients*. U.S. Food and Drug Administration. <https://www.fda.gov/news-events/press-announcements/coronavirus-covid-19-update-fda-authorizes-first-antigen-test-help-rapid-detection-virus-causes> (accessed 2022-02-04).
- (33) Udugama, B.; Kadhiresan, P.; Kozlowski, H. N.; Malekjahani, A.; Osborne, M.; Li, V. Y. C.; Chen, H.; Mubareka, S.; Gubbay, J. B.; Chan, W. C. W. Diagnosing COVID-19: The Disease and Tools for Detection. *ACS Nano* **2020**, *14* (4), 3822–3835.
- (34) Moitra, P.; Alafeef, M.; Dighe, K.; Frieman, M. B.; Pan, D. Selective Naked-Eye Detection of SARS-CoV-2 Mediated by N Gene Targeted Antisense Oligonucleotide Capped Plasmonic Nanoparticles. *ACS Nano* **2020**, *14* (6), 7617–7627.
- (35) Kendall, E. A.; Arinaminpathy, N.; Sacks, J. A.; Manabe, Y. C.; Dittrich, S.; Schumacher, S. G.; Dowdy, D. W. Antigen-Based Rapid Diagnostic Testing or Alternatives for Diagnosis of Symptomatic COVID-19: A Simulation-Based Net Benefit Analysis. *Epidemiology* **2021**, *32* (6), 811.
- (36) Pray, I. W.; Ford, L.; Cole, D.; Lee, C.; Bigouette, J. P.; Glen, G. R.; Bushman, D.; Delahoy, M. J.; Currie, D.; Cherney, B.; Kirby, M.; Fajardo, G.; Caudill, M.; Langolf, K.; Kahrs, J.; Kelly, P.; Pitts, C.; Lim, A.; Aulik, N.; Tamin, A.; Harcourt, J. L.; Queen, K.; Zhang, J.; Whitaker, B.; Browne, H.; Medrzycki, M.; Shewmaker, P.; Folster, Banka, B. Performance of an Antigen-Based Test for Asymptomatic and Symptomatic SARS-CoV-2 Testing at Two University Campuses-Wisconsin, September-October 2020. *MMWR Morb Mortal Wkly Rep.* **2022**, *69*, 1642–1647.
- (37) Kahn, M.; Schuierer, L.; Bartenschlager, C.; Zellmer, S.; Frey, R.; Freitag, M.; Dhillon, C.; Heier, M.; Ebigbo, A.; Denzel, C.; Temizel, S.; Messmann, H.; Wehler, M.; Hoffmann, R.; Kling, E.; Römmele, C. Performance of Antigen Testing for Diagnosis of COVID-19: A Direct Comparison of a Lateral Flow Device to Nucleic Acid Amplification Based Tests. *BMC Infectious Diseases* **2021**, *21* (1), 798.
- (38) Baro, B.; Rodo, P.; Ouchi, D.; Bordoy, A. E.; Saya Amaro, E. N.; Salsench, S. v.; Molinos, S.; Alemany, A.; Ubals, M.; Corbacho-Monné, M.; Millat-Martinez, P.; Marks, M.; Clotet, B.; Prat, N.; Estrada, O.; Vilar, M.; Ara, J.; Vall-Mayans, M.; G-Beiras, C.; et al. Performance Characteristics of Five Antigen-Detecting Rapid Diagnostic Test (Ag-RDT) for SARS-CoV-2 Asymptomatic Infection: A Head-to-Head Benchmark Comparison. *Journal of Infection* **2021**, *82* (6), 269–275.
- (39) Kim, S.; Yee, E.; Miller, E. A.; Hao, Y.; Tay, D. M. Y.; Sung, K.-J.; Jia, H.; Johnson, J. M.; Saeed, M.; Mace, C. R.; Yuksel Yurt, D.; Sikes, H. D. Developing a SARS-CoV-2 Antigen Test Using Engineered Affinity Proteins. *ACS Appl. Mater. Interfaces* **2021**, *13* (33), 38990–39002.
- (40) Peroni, L. A.; Toscaro, J. M.; Canateli, C.; Tonoli, C. C. C.; de Olivera, R. R.; Benedetti, C. E.; Coimbra, L. D.; Pereira, A. B.; Marques, R. E.; Proença-Modena, J. L.; Lima, G. C.; Viana, R.; Borges, J. B.; Lin-Wang, H. T.; Abboud, C. S.; Gun, C.; Franchini, K. G.; Bajgelman, M. C. Serological Testing for COVID-19, Immunological Surveillance, and Exploration of Protective Antibodies. *Front. Immunol.* **2021**, *12* DOI: 10.3389/fimmu.2021.635701
- (41) Trombetta, B. A.; Kandigian, S. E.; Kitchen, R. R.; Grauwet, K.; Webb, P. K.; Miller, G. A.; Jennings, C. G.; Jain, S.; Miller, S.; Kuo, Y.; Sweeney, T.; Gilboa, T.; Norman, M.; Simmons, D. P.; Ramirez, C. E.; Bedard, M.; Fink, C.; Ko, J.; de León Peralta, E. J.; et al. Evaluation of Serological Lateral Flow Assays for Severe Acute Respiratory Syndrome Coronavirus-2. *BMC Infectious Diseases* **2021**, *21* (1), 580.
- (42) Brangel, P.; Sobarzo, A.; Parolo, C.; Miller, B. S.; Howes, P. D.; Gelkop, S.; Lutwama, J. J.; Dye, J. M.; McKendry, R. A.; Lobel, L.; Stevens, M. M. A Serological Point-of-Care Test for the Detection of IgG Antibodies against Ebola Virus in Human Survivors. *ACS Nano* **2018**, *12* (1), 63–73.
- (43) Jones, H. *Importance of diagnostic testing for COVID-19*. <https://www.id-hub.com/2020/04/02/the-importance-of-diagnostic-testing-for-covid-19/>.
- (44) Wirz, O. F.; Röltgen, K.; Stevens, B. A.; Pandey, S.; Sahoo, M. K.; Tolentino, L.; Verghese, M.; Nguyen, K.; Hunter, M.; Snow, T. T.; Singh, A. R.; Blish, C. A.; Cochran, J. R.; Zehnder, J. L.; Nadeau, K. C.; Pinsky, B. A.; Pham, T. D.; Boyd, S. D. Use of Outpatient-Derived COVID-19 Convalescent Plasma in COVID-19 Patients Before Seroconversion. *Front. Immunol.* **2021**, *12* DOI: 10.3389/fimmu.2021.739037
- (45) Carter, J. A.; Freedenberg, A. T.; Romeiser, J. L.; Talbot, L. R.; Browne, N. J.; Cosgrove, M. E.; Shevik, M. E.; Generale, L. M.; Rago, M. G.; Caravella, G. A.; Ahmed, T.; Mamone, L. J.; Bennett-Guerrero, E.; The Stony Brook Medicine COVID Plasma Trial Group. Impact of Serological and PCR Testing Requirements on the Selection of COVID-19 Convalescent Plasma Donors. *Transfusion (Paris)* **2021**, *61* (5), 1461–1470.
- (46) Kubina, R.; Dziedzic, A. Molecular and Serological Tests for COVID-19. A Comparative Review of SARS-CoV-2 Coronavirus Laboratory and Point-of-Care Diagnostics. *Diagnostics* **2020**, *10* (6), 434.
- (47) Wölfel, R.; Corman, V. M.; Guggemos, W.; Seilmaier, M.; Zange, S.; Müller, M. A.; Niemeyer, D.; Jones, T. C.; Vollmar, P.; Rothe, C.; Hoelscher, M.; Bleicker, T.; Brünink, S.; Schneider, J.; Ehmman, R.; Zwirgmaier, K.; Drosten, C.; Wendtner, C. Virological Assessment of Hospitalized Patients with COVID-2019. *Nature* **2020**, *581* (7809), 465–469.
- (48) Lew, T. T. S.; Aung, K. M. M.; Ow, S. Y.; Amrun, S. N.; Sutarlie, L.; Ng, L. F. P.; Su, X. Epitope-Functionalized Gold Nanoparticles for Rapid and Selective Detection of SARS-CoV-2 IgG Antibodies. *ACS Nano* **2021**, *15* (7), 12286–12297.
- (49) Fulford, T. S.; Van, H.; Gherardin, N. A.; Zheng, S.; Ciula, M.; Drummer, H. E.; Redmond, S.; Tan, H.-X.; Boo, I.; Center, R. J.; Li, F.; Grimley, S. L.; Wines, B. D.; Nguyen, T. H. O.; Mordant, F. L.; Ellenberg, P.; Rowntree, L. C.; Kedzierski, L.; Cheng, A. C. A Point-of-Care Lateral Flow Assay for Neutralising Antibodies against SARS-CoV-2. *eBioMedicine* **2021**, *74*, 103729.

- (50) Ahmadi, A.; Mirzaeizadeh, Z.; Omidfar, K. Simultaneous Detection of SARS-CoV-2 IgG/IgM Antibodies, Using Gold Nanoparticles-Based Lateral Flow Immunoassay. *Monoclonal Antibodies in Immunodiagnosis and Immunotherapy* **2021**, *40* (5), 210–218.
- (51) Parolo, C.; de la Escosura-Muñiz, A.; Merkoçi, A. Enhanced Lateral Flow Immunoassay Using Gold Nanoparticles Loaded with Enzymes. *Biosens. Bioelectron.* **2013**, *40* (1), 412–416.
- (52) Huang, C.; Wen, T.; Shi, F.-J.; Zeng, X.-Y.; Jiao, Y.-J. Rapid Detection of IgM Antibodies against the SARS-CoV-2 Virus via Colloidal Gold Nanoparticle-Based Lateral-Flow Assay. *ACS Omega* **2020**, *5* (21), 12550–12556.
- (53) Payandehpeyman, J.; Parvini, N.; Moradi, K.; Hashemian, N. Detection of SARS-CoV-2 Using Antibody–Antigen Interactions with Graphene-Based Nanomechanical Resonator Sensors. *ACS Applied Nano Materials* **2021**, *4* (6), 6189–6200.
- (54) della Ventura, B.; Cennamo, M.; Minopoli, A.; Campanile, R.; Bolletti Censi, S.; Terracciano, D.; Portella, G.; Velotta, R. Colorimetric Test for Fast Detection of SARS-CoV-2 in Nasal and Throat Swabs. *ACS Sensors* **2020**, *5* (10), 3043–3048.
- (55) Bender, J. K.; Meyer, E. D.; Sandfort, M.; Matysiak-Klose, D.; Bojara, G.; Hellenbrand, W. Low Sensitivity of Rapid Antigen Tests to Detect Severe Acute Respiratory Syndrome Coronavirus 2 Infections Before and on the Day of Symptom Onset in Nursing Home Staff and Residents, Germany, January–March 2021. *Journal of Infectious Diseases* **2021**, *224* (11), 1987–1989.
- (56) Demuth, S.; Damaschek, S.; Schildgen, O.; Schildgen, V. Low Sensitivity of SARS-CoV-2 Rapid Antigen Self-Tests under Laboratory Conditions. *New Microbes and New Infections* **2021**, *43*, 100916.
- (57) Kashiwagi, K.; Ishii, Y.; Aoki, K.; Yagi, S.; Maeda, T.; Miyazaki, T.; Yoshizawa, S.; Aoyagi, K.; Tateda, K. Immunochromatographic Test for the Detection of SARS-CoV-2 in Saliva. *Journal of Infection and Chemotherapy* **2021**, *27* (2), 384–386.
- (58) Asai, N.; Sakanashi, D.; Ohashi, W.; Nakamura, A.; Kawamoto, Y.; Miyazaki, N.; Ohno, T.; Yamada, A.; Chida, S.; Shibata, Y.; Kato, H.; Shiota, A.; Hagihara, M.; Koita, I.; Yamagishi, Y.; Suematsu, H.; Ohta, H.; Mikamo, H. Efficacy and Validity of Automated Quantitative Chemiluminescent Enzyme Immunoassay for SARS-CoV-2 Antigen Test from Saliva Specimen in the Diagnosis of COVID-19. *Journal of Infection and Chemotherapy* **2021**, *27* (7), 1039–1042.
- (59) Dramé, M.; Tabue Teguo, M.; Proye, E.; Hequet, F.; Hentzien, M.; Kanagaratnam, L.; Godaert, L. Should RT-PCR Be Considered a Gold Standard in the Diagnosis of COVID-19? *Journal of Medical Virology* **2020**, *92* (11), 2312–2313.
- (60) Filippis, C.; Binder, F.; Lickfeld, M.; Schröder, A. K.; Klemens, J. M.; Saschenbrecker, S.; Steller, U. Novel PCR Test to Differentiate Between Infections with SARS-CoV-2, Influenza A and B. *International Journal of Infectious Diseases* **2022**, *116*, S43–S44.
- (61) Sahajpal, N. S.; Mondal, A. K.; Ananth, S.; Njau, A.; Jones, K.; Ahluwalia, P.; Oza, E.; Ross, T. M.; Kota, V.; Kothandaraman, A.; Fulzele, S.; Hegde, M.; Chaubey, A.; Rojiani, A. M.; Kolhe, R. Clinical Validation of a Multiplex PCR-Based Detection Assay Using Saliva or Nasopharyngeal Samples for SARS-Cov-2, Influenza A and B. *Sci. Rep.* **2022**, *12* (1), 3480.
- (62) Aziz, N. A.; Othman, J.; Lugova, H.; Suleiman, A. Malaysia's Approach in Handling COVID-19 Onslaught: Report on the Movement Control Order (MCO) and Targeted Screening to Reduce Community Infection Rate and Impact on Public Health and Economy. *Journal of Infection and Public Health* **2020**, *13* (12), 1823–1829.
- (63) Cheong, J.; Yu, H.; Lee, C. Y.; Lee, J.; Choi, H.-J.; Lee, J.-H.; Lee, H.; Cheon, J. Fast Detection of SARS-CoV-2 RNA via the Integration of Plasmonic Thermocycling and Fluorescence Detection in a Portable Device. *Nature Biomedical Engineering* **2020**, *4* (12), 1159–1167.
- (64) Yeol Lee, C.; Degani, I.; Cheong, J.; Weissleder, R.; Lee, J.-H.; Cheon, J.; Lee, H. Development of Integrated Systems for On-Site Infection Detection. *Acc. Chem. Res.* **2021**, *54* (21), 3991–4000.
- (65) Varlamov, D. A.; Blagodatskikh, K. A.; Smirnova, E. v.; Kramarov, V. M.; Ignatov, K. B. Combinations of PCR and Isothermal Amplification Techniques Are Suitable for Fast and Sensitive Detection of SARS-CoV-2 Viral RNA. *Front. Bioeng. Biotechnol.* **2020**, *8* DOI: 10.3389/fbioe.2020.604793
- (66) Shirato, K.; Nao, N.; Matsuyama, S.; Takeda, M.; Kageyama, T. An Ultra-Rapid Real-Time RT-PCR Method Using the PCR1100 to Detect Severe Acute Respiratory Syndrome Coronavirus-2. *Japanese Journal of Infectious Diseases* **2021**, *74* (1), 29–34.
- (67) SARS-CoV-2 Viral Mutations: Impact on COVID-19 Tests. U.S. Food and Drug Administration. <https://www.fda.gov/medical-devices/coronavirus-covid-19-and-medical-devices/sars-cov-2-viral-mutations-impact-covid-19-tests> (accessed 2022-02-04).
- (68) Amaral, C.; Antunes, W.; Moe, E.; Duarte, A. G.; Lima, L. M. P.; Santos, C.; Gomes, I. L.; Afonso, G. S.; Vieira, R.; Teles, H. S. S.; Reis, M. S.; da Silva, M. A. R.; Henriques, A. M.; Fevereiro, M.; Ventura, M. R.; Serrano, M.; Pimentel, C. A Molecular Test Based on RT-LAMP for Rapid, Sensitive and Inexpensive Colorimetric Detection of SARS-CoV-2 in Clinical Samples. *Sci. Rep.* **2021**, *11* (1), 16430.
- (69) Huang, X.; Tang, G.; Ismail, N.; Wang, X. Developing RT-LAMP Assays for Rapid Diagnosis of SARS-CoV-2 in Saliva. *eBioMedicine* **2022**, *75*, 103736.
- (70) Huang, W. E.; Lim, B.; Hsu, C.-C.; Xiong, D.; Wu, W.; Yu, Y.; Jia, H.; Wang, Y.; Zeng, Y.; Ji, M.; Chang, H.; Zhang, X.; Wang, H.; Cui, Z. RT-LAMP for Rapid Diagnosis of Coronavirus SARS-CoV-2. *Microbial Biotechnology* **2020**, *13* (4), 950–961.
- (71) Huang, P.; Wang, H.; Cao, Z.; Jin, H.; Chi, H.; Zhao, J.; Yu, B.; Yan, F.; Hu, X.; Wu, F.; Jiao, C.; Hou, P.; Xu, S.; Zhao, Y.; Feng, N.; Wang, J.; Sun, W.; Wang, T.; Gao, Y.; et al. A Rapid and Specific Assay for the Detection of MERS-CoV. *Front. Microbiol.* **2018**. DOI: 10.3389/fmicb.2018.01101
- (72) Broughton, J. P.; Deng, X.; Yu, G.; Fasching, C. L.; Servellita, V.; Singh, J.; Miao, X.; Streithorst, J. A.; Granados, A.; Sotomayor-Gonzalez, A.; Zorn, K.; Gopez, A.; Hsu, E.; Gu, W.; Miller, S.; Pan, C.-Y.; Guevara, H.; Wadford, D. A.; Chen, J. S.; et al. CRISPR–Cas12-Based Detection of SARS-CoV-2. *Nat. Biotechnol.* **2020**, *38* (7), 870–874.
- (73) Fowler, V. L.; Howson, E. L. A.; Madi, M.; Mioulet, V.; Caiusi, C.; Pauszek, S. J.; Rodriguez, L. L.; King, D. P. Development of a Reverse Transcription Loop-Mediated Isothermal Amplification Assay for the Detection of Vesicular Stomatitis New Jersey Virus: Use of Rapid Molecular Assays to Differentiate between Vesicular Disease Viruses. *Journal of Virological Methods* **2016**, *234*, 123–131.
- (74) Ganguli, A.; Mostafa, A.; Berger, J.; Aydin, M. Y.; Sun, F.; Ramirez, S. A. S. d.; Valera, E.; Cunningham, B. T.; King, W. P.; Bashir, R. Rapid Isothermal Amplification and Portable Detection System for SARS-CoV-2. *Proc. Natl. Acad. Sci. U. S. A.* **2020**, *117* (37), 22727–22735.
- (75) Ramachandran, A.; Huyke, D. A.; Sharma, E.; Sahoo, M. K.; Huang, C.; Banaei, N.; Pinsky, B. A.; Santiago, J. G. Electric Field-Driven Microfluidics for Rapid CRISPR-Based Diagnostics and Its Application to Detection of SARS-CoV-2. *Proc. Natl. Acad. Sci. U. S. A.* **2020**, *117* (47), 29518–29525.
- (76) Rolando, J. C.; Jue, E.; Schoepp, N. G.; Ismagilov, R. F. Real-Time, Digital LAMP with Commercial Microfluidic Chips Reveals the Interplay of Efficiency, Speed, and Background Amplification as a Function of Reaction Temperature and Time. *Anal. Chem.* **2019**, *91* (1), 1034–1042.
- (77) Song, J.; El-Tholoth, M.; Li, Y.; Graham-Wooten, J.; Liang, Y.; Li, J.; Li, W.; Weiss, S. R.; Collman, R. G.; Bau, H. H. Single- and Two-Stage, Closed-Tube, Point-of-Care, Molecular Detection of SARS-CoV-2. *Anal. Chem.* **2021**, *93* (38), 13063–13071.
- (78) Khan, M.; Wang, R.; Li, B.; Liu, P.; Weng, Q.; Chen, Q. Comparative Evaluation of the LAMP Assay and PCR-Based Assays for the Rapid Detection of Alternaria Solani. *Frontiers Microbiol.* **2018**, *9* DOI: 10.3389/fmicb.2018.02089



- (79) Alafeef, M.; Moitra, P.; Dighe, K.; Pan, D. RNA-Extraction-Free Nano-Amplified Colorimetric Test for Point-of-Care Clinical Diagnosis of COVID-19. *Nat. Protoc.* **2021**, *16* (6), 3141–3162.
- (80) Carter, J. G.; Orueta Iturbe, L.; Duprey, J.-L. H. A.; Carter, I. R.; Southern, C. D.; Rana, M.; Whalley, C. M.; Bosworth, A.; Beggs, A. D.; Hicks, M. R.; Tucker, J. H. R.; Dafforn, T. R. Ultrarapid Detection of SARS-CoV-2 RNA Using a Reverse Transcription-Free Exponential Amplification Reaction, RTF-EXPAR. *Proc. Natl. Acad. Sci. U. S. A.* **2021**, *118* (35), No. e2100347118.
- (81) Woo, C. H.; Jang, S.; Shin, G.; Jung, G. Y.; Lee, J. W. Sensitive Fluorescence Detection of SARS-CoV-2 RNA in Clinical Samples via One-Pot Isothermal Ligation and Transcription. *Nature Biomedical Engineering* **2020**, *4* (12), 1168–1179.
- (82) L'Helgouach, N.; Champigneux, P.; Schneider, F. S.; Molina, L.; Espeut, J.; Alali, M.; Baptiste, J.; Cardeur, L.; Dubuc, B.; Foulongne, V.; Galtier, F.; Makinson, A.; Marin, G.; Picot, M.-C.; Prieux-Lejeune, A.; Quenot, M.; Robles, F. C.; Salvétat, N.; Vetter, D.; et al. EasyCOV: LAMP Based Rapid Detection of SARS-CoV-2 in Saliva. *medRxiv* **2020**, 2020.05.30.20117291.
- (83) Wang, L.; Qian, C.; Wu, H.; Qian, W.; Wang, R.; Wu, J. Technical Aspects of Nicking Enzyme Assisted Amplification. *Analyst* **2018**, *143* (6), 1444–1453.
- (84) Ménéová, P.; Raindlová, V.; Hocek, M. Scope and Limitations of the Nicking Enzyme Amplification Reaction for the Synthesis of Base-Modified Oligonucleotides and Primers for PCR. *Bioconjugate Chem.* **2013**, *24* (6), 1081–1093.
- (85) Gorzalski, A. J.; Tian, H.; Laverdure, C.; Morzunov, S.; Verma, S. C.; VanHooser, S.; Pandori, M. W. High-Throughput Transcription-Mediated Amplification on the Hologic Panther Is a Highly Sensitive Method of Detection for SARS-CoV-2. *Journal of Clinical Virology* **2020**, *129*, 104501.
- (86) Nakajima, N.; Kitamori, Y.; Ohnaka, S.; Mitoma, Y.; Mizuta, K.; Wakita, T.; Shimizu, H.; Arita, M. Development of a Transcription-Reverse Transcription Concerted Reaction Method for Specific Detection of Human Enterovirus 71 from Clinical Specimens. *Journal of Clinical Microbiology* **2012**, *50* (5), 1764–1768.
- (87) McCalla, S. E.; Ong, C.; Sarma, A.; Opal, S. M.; Artenstein, A. W.; Tripathi, A. A Simple Method for Amplifying RNA Targets (SMART). *Journal of Molecular Diagnostics* **2012**, *14* (4), 328–335.
- (88) Hogan, C. A.; et al. Comparison of the Accula SARS-CoV-2 Test with a Laboratory-Developed Assay for Detection of SARS-CoV-2 RNA in Clinical Nasopharyngeal Specimens. *J. Clinical Microbiol.* **2022**, *58*, No. e01072-20.
- (89) Sun, Y.; Ge, L.; Udhane, S. S.; Langenheim, J. F.; Rau, M. J.; Patton, M. D.; Gallan, A. J.; Felix, J. C.; Rui, H. Sensitive and Specific Immunohistochemistry Protocol for Nucleocapsid Protein from All Common SARS-CoV-2 Virus Strains in Formalin-Fixed, Paraffin Embedded Tissues. *Methods Protocols* **2021**, *4*, 47.
- (90) el Jamal, S. M.; Pujadas, E.; Ramos, I.; Bryce, C.; Grimes, Z. M.; Amanat, F.; Tsankova, N. M.; Mussa, Z.; Olson, S.; Salem, F.; Miorin, L.; Aydilto, T.; Schotsaert, M.; Albrecht, R. A.; Liu, W.-C.; Marjanovic, N.; Francoeur, N.; Sebra, R.; Sealfon, S. C.; et al. Tissue-Based SARS-CoV-2 Detection in Fatal COVID-19 Infections: Sustained Direct Viral-Induced Damage Is Not Necessary to Drive Disease Progression. *Human Pathology* **2021**, *114*, 110–119.
- (91) Hepp, C.; Shiaelis, N.; Robb, N. C.; Vaughan, A.; Matthews, P. C.; Stoesser, N.; Crook, D.; Kapanidis, A. N. Viral Detection and Identification in 20 min by Rapid Single-Particle Fluorescence in-Situ Hybridization of Viral RNA. *Sci. Rep.* **2021**, *11* (1), 19579.
- (92) Carossino, M.; Ip, H. S.; Richt, J. A.; Shultz, K.; Harper, K.; Loynachan, A. T.; del Piero, F.; Balasuriya, U. B. R. Detection of SARS-CoV-2 by RNAscope® in Situ Hybridization and Immunohistochemistry Techniques. *Arch. Virol.* **2020**, *165* (10), 2373–2377.
- (93) Massoth, L. R.; Desai, N.; Szabolcs, A.; Harris, C. K.; Neyaz, A.; Crotty, R.; Chebib, I.; Rivera, M. N.; Sholl, L. M.; Stone, J. R.; Ting, D. T.; Deshpande, V. Comparison of RNA In Situ Hybridization and Immunohistochemistry Techniques for the Detection and Localization of SARS-CoV-2 in Human Tissues. *American Journal of Surgical Pathology* **2021**, *45* (1), 14.
- (94) Jansen, G. J.; Wiersma, M.; van Wamel, W. J. B.; Wijnberg, I. D. Direct Detection of SARS-CoV-2 Antisense and Sense Genomic RNA in Human Saliva by Semi-Autonomous Fluorescence in Situ Hybridization: A Proxy for Contagiousness? *PLoS One* **2021**, *16* (8), No. e0256378.
- (95) Jesse, S.; Borisevich, A. Y.; Fowlkes, J. D.; Lupini, A. R.; Rack, P. D.; Unocic, R. R.; Sumpster, B. G.; Kalinin, S. V.; Belianinov, A.; Ovchinnikova, O. S. Directing Matter: Toward Atomic-Scale 3D Nanofabrication. *ACS Nano* **2016**, *10* (6), 5600–5618.
- (96) A Matter of Scale. *Nat. Nanotechnol.* **2016**, *11* (9), 733..
- (97) Alafeef, M.; Dighe, K.; Pan, D. Label-Free Pathogen Detection Based on Yttrium-Doped Carbon Nanoparticles up to Single-Cell Resolution. *ACS Appl. Mater. Interfaces* **2019**, *11* (46), 42943–42955.
- (98) Alafeef, M.; Moitra, P.; Pan, D. Nano-Enabled Sensing Approaches for Pathogenic Bacterial Detection. *Biosens. Bioelectron.* **2020**, *165*, 112276.
- (99) Alafeef, M.; Moitra, P.; Dighe, K.; Pan, D. Hyperspectral Mapping for the Detection of SARS-CoV-2 Using Nanomolecular Probes with Yoctomole Sensitivity. *ACS Nano* **2021**, *15* (8), 13742–13758.
- (100) Alafeef, M.; Dighe, K.; Moitra, P.; Pan, D. Rapid, Ultrasensitive, and Quantitative Detection of SARS-CoV-2 Using Antisense Oligonucleotides Directed Electrochemical Biosensor Chip. *ACS Nano* **2020**, *14* (12), 17028–17045.
- (101) Dighe, K.; Moitra, P.; Alafeef, M.; Gunaseelan, N.; Pan, D. A Rapid RNA Extraction-Free Lateral Flow Assay for Molecular Point-of-Care Detection of SARS-CoV-2 Augmented by Chemical Probes. *Biosens. Bioelectron.* **2022**, *200*, 113900.
- (102) Moitra, P.; Alafeef, M.; Dighe, K.; Sheffield, Z.; Dahal, D.; Pan, D. Synthesis and Characterisation of N-Gene Targeted NIR-II Fluorescent Probe for Selective Localisation of SARS-CoV-2. *Chem. Commun.* **2021**, *57* (51), 6229–6232.
- (103) Srivastava, I.; Khan, M. S.; Dighe, K.; Alafeef, M.; Wang, Z.; Banerjee, T.; Ghonge, T.; Grove, L. M.; Bashir, R.; Pan, D. On-Chip Electrical Monitoring of Real-Time “Soft” and “Hard” Protein Corona Formation on Carbon Nanoparticles. *Small Methods* **2020**, *4* (7), 2000099.
- (104) Shan, B.; Broza, Y. Y.; Li, W.; Wang, Y.; Wu, S.; Liu, Z.; Wang, J.; Gui, S.; Wang, L.; Zhang, Z.; Liu, W.; Zhou, S.; Jin, W.; Zhang, Q.; Hu, D.; Lin, L.; Zhang, Q.; Li, W.; Wang, J.; Liu, H.; Pan, Y.; Haick, H. Multiplexed Nanomaterial-Based Sensor Array for Detection of COVID-19 in Exhaled Breath. *ACS Nano* **2020**, *14* (9), 12125–12132.
- (105) Mahar, B.; Laslau, C.; Yip, R.; Sun, Y. Development of Carbon Nanotube-Based Sensors—A Review. *IEEE Sensors Journal* **2007**, *7* (2), 266–284.
- (106) Pinals, R. L.; Ledesma, F.; Yang, D.; Navarro, N.; Jeong, S.; Pak, J. E.; Kuo, L.; Chuang, Y.-C.; Cheng, Y.-W.; Sun, H.-Y.; Landry, M. P. Rapid SARS-CoV-2 Spike Protein Detection by Carbon Nanotube-Based Near-Infrared Nanosensors. *Nano Lett.* **2021**, *21* (5), 2272–2280.
- (107) Mehta, N.; Sahu, S. P.; Shaik, S.; Devireddy, R.; Gartia, M. R. Dark-Field Hyperspectral Imaging for Label Free Detection of Nano-Bio-Materials. *WIREs Nanomedicine and Nanobiotechnology* **2021**, *13* (1), No. e1661.
- (108) Iravani, S. Nano- and Biosensors for the Detection of SARS-CoV-2: Challenges and Opportunities. *Materials Advances* **2020**, *1* (9), 3092–3103.
- (109) O'Brien, M.; Rundell, Z. C.; Nemeč, M. D.; Langan, L. M.; Back, J. A.; Lugo, J. N. A Comparison of Four Commercially Available RNA Extraction Kits for Wastewater Surveillance of SARS-CoV-2 in a College Population. *Science of The Total Environment* **2021**, *801*, 149595.
- (110) Campos, K. R.; Sacchi, C. T.; Gonçalves, C. R.; Pagnoca, É. V. R. G.; dos S. Dias, A.; Fukasawa, L. O.; Caterino-de-Araujo, A. COVID-19 Laboratory Diagnosis: Comparative Analysis of Different RNA Extraction Methods for SARS-CoV-2 Detection by Two Amplification Protocols. *Revista do Instituto de Medicina Tropical de São Paulo* **2021**, *63*, e52.



- (111) Saha, K.; Agasti, S. S.; Kim, C.; Li, X.; Rotello, V. M. Gold Nanoparticles in Chemical and Biological Sensing. *Chem. Rev.* **2012**, *112* (5), 2739–2779.
- (112) Pramanik, A.; Gao, Y.; Patibandla, S.; Mitra, D.; McCandless, M. G.; Fassero, L. A.; Gates, K.; Tandon, R.; Chandra Ray, P. The Rapid Diagnosis and Effective Inhibition of Coronavirus Using Spike Antibody Attached Gold Nanoparticles. *Nanoscale Advances* **2021**, *3* (6), 1588–1596.
- (113) Wang, J.; Drelich, A. J.; Hopkins, C. M.; Mecozzi, S.; Li, L.; Kwon, G.; Hong, S. Gold Nanoparticles in Virus Detection: Recent Advances and Potential Considerations for SARS-CoV-2 Testing Development. *WIREs Nanomedicine and Nanobiotechnology* **2022**, *14* (1), No. e1754.
- (114) Soh, J. H.; Lin, Y.; Rana, S.; Ying, J. Y.; Stevens, M. M. Colorimetric Detection of Small Molecules in Complex Matrixes via Target-Mediated Growth of Aptamer-Functionalized Gold Nanoparticles. *Anal. Chem.* **2015**, *87* (15), 7644–7652.
- (115) Chandra, A.; Singh, N. Bacterial Growth Sensing in Microgels Using PH-Dependent Fluorescence Emission. *Chem. Commun.* **2018**, *54* (13), 1643–1646.
- (116) Nandi, S.; Ritenberg, M.; Jelinek, R. Bacterial Detection with Amphiphilic Carbon Dots. *Analyst* **2015**, *140* (12), 4232–4237.
- (117) Singh, P.; Kakkar, S.; Bharti, B.; Kumar, R.; Bhalla, V. Rapid and Sensitive Colorimetric Detection of Pathogens Based on Silver–Urease Interactions. *Chem. Commun.* **2019**, *55* (33), 4765–4768.
- (118) Ratnarathorn, N.; Chailapakul, O.; Henry, C. S.; Dungchai, W. Simple Silver Nanoparticle Colorimetric Sensing for Copper by Paper-Based Devices. *Talanta* **2012**, *99*, 552–557.
- (119) Zhang, Y.; Yuan, S.; Day, G.; Wang, X.; Yang, X.; Zhou, H.-C. Luminescent Sensors Based on Metal–Organic Frameworks. *Coord. Chem. Rev.* **2018**, *354*, 28–45.
- (120) Udourioh, G. A.; Solomon, M. M.; Epelle, E. I. Metal Organic Frameworks as Biosensing Materials for COVID-19. *Cell Mol. Bioeng* **2021**, *14* (6), 535–553.
- (121) Wang, Y.; Zhao, Z.; Li, G.; Yan, Y.; Hao, C. A 2D Covalent Organic Framework as a Sensor for Detecting Formaldehyde. *J. Mol. Model.* **2018**, *24* (7), 153.
- (122) Wang, L.; Liang, H.; Xu, M.; Wang, L.; Xie, Y.; Song, Y. Ratiometric Electrochemical Biosensing Based on Double-Enzymes Loaded on Two-Dimensional Dual-Pore COFETTA-TPAL. *Sens. Actuators, B* **2019**, *298*, 126859.
- (123) Feng, C.; Zhao, P.; Wang, L.; Yang, T.; Wu, Y.; Ding, Y.; Hu, A. Fluorescent Electronic Tongue Based on Soluble Conjugated Polymeric Nanoparticles for the Discrimination of Heavy Metal Ions in Aqueous Solution. *Polym. Chem.* **2019**, *10* (18), 2256–2262.
- (124) Ferhan, A. R.; Kim, D.-H. Nanoparticle Polymer Composites on Solid Substrates for Plasmonic Sensing Applications. *Nano Today* **2016**, *11* (4), 415–434.
- (125) Schroeder, V.; Savagatrup, S.; He, M.; Lin, S.; Swager, T. M. Carbon Nanotube Chemical Sensors. *Chem. Rev.* **2019**, *119*, 599–663, DOI: 10.1021/acs.chemrev.8b00340.
- (126) Yue, Z.; Lisdat, F.; Parak, W. J.; Hickey, S. G.; Tu, L.; Sabir, N.; Dorfs, D.; Bigall, N. C. Quantum-Dot-Based Photoelectrochemical Sensors for Chemical and Biological Detection. *ACS Appl. Mater. Interfaces* **2013**, *5* (8), 2800–2814.
- (127) Zhang, Y.; Wang, T.-H. Quantum Dot Enabled Molecular Sensing and Diagnostics. *Theranostics* **2012**, *2* (7), 631–654.
- (128) Pan, D. Theranostic Nanomedicine with Functional Nanoarchitecture. *Mol. Pharmaceutics* **2013**, *10* (3), 781–782.
- (129) Srivastava, I.; Misra, S. K.; Ostadhosseini, F.; Daza, E.; Singh, J.; Pan, D. Surface Chemistry of Carbon Nanoparticles Functionally Select Their Uptake in Various Stages of Cancer Cells. *Nano Research* **2017**, *10* (10), 3269–3284.
- (130) Khan, M. S.; Misra, S. K.; Dighe, K.; Wang, Z.; Schwartz-Duval, A. S.; Sar, D.; Pan, D. Electrically-Receptive and Thermally-Responsive Paper-Based Sensor Chip for Rapid Detection of Bacterial Cells. *Biosens. Bioelectron.* **2018**, *110*, 132–140.
- (131) Mukherjee, P.; Misra, S. K.; Gryka, M. C.; Chang, H.-H.; Tiwari, S.; Wilson, W. L.; Scott, J. W.; Bhargava, R.; Pan, D. Tunable Luminescent Carbon Nanospheres with Well-Defined Nanoscale Chemistry for Synchronized Imaging and Therapy. *Small* **2015**, *11* (36), 4691–4703.
- (132) Pan, D.; Pramanik, M.; Wickline, S. A.; Wang, L. v.; Lanza, G. M. Recent Advances in Colloidal Gold Nanobeacons for Molecular Photoacoustic Imaging. *Contrast Media & Molecular Imaging* **2011**, *6* (5), 378–388.
- (133) Owyung, R. E.; Panzer, M. J.; Sonkusale, S. R. Colorimetric Gas Sensing Washable Threads for Smart Textiles. *Sci. Rep.* **2019**, *9* (1), 5607.
- (134) Yang, M.; Liu, X.; Luo, Y.; Pearlstein, A. J.; Wang, S.; Dillow, H.; Reed, K.; Jia, Z.; Sharma, A.; Zhou, B.; Pearlstein, D.; Yu, H.; Zhang, B. Machine Learning-Enabled Non-Destructive Paper Chromogenic Array Detection of Multiplexed Viable Pathogens on Food. *Nature Food* **2021**, *2* (2), 110–117.
- (135) Peng, H.; Chen, I. A. Rapid Colorimetric Detection of Bacterial Species through the Capture of Gold Nanoparticles by Chimeric Phages. *ACS Nano* **2019**, *13* (2), 1244–1252.
- (136) Linic, S.; Chavez, S.; Elias, R. Flow and Extraction of Energy and Charge Carriers in Hybrid Plasmonic Nanostructures. *Nat. Mater.* **2021**, *20* (7), 916–924.
- (137) Chowdhury, A. D.; Takemura, K.; Li, T.-C.; Suzuki, T.; Park, E. Y. Electrical Pulse-Induced Electrochemical Biosensor for Hepatitis E Virus Detection. *Nat. Commun.* **2019**, *10* (1), 3737.
- (138) Kaushik, A. K.; Dhau, J. S.; Gohel, H.; Mishra, Y. K.; Kateb, B.; Kim, N.-Y.; Goswami, D. Y. Electrochemical SARS-CoV-2 Sensing at Point-of-Care and Artificial Intelligence for Intelligent COVID-19 Management. *ACS Applied Bio Materials* **2020**, *3* (11), 7306–7325.
- (139) Asai, K.; Yamamoto, T.; Nagashima, S.; Ogata, G.; Hibino, H.; Einaga, Y. An Electrochemical Aptamer-Based Sensor Prepared by Utilizing the Strong Interaction between a DNA Aptamer and Diamond. *Analyst* **2020**, *145* (2), 544–549.
- (140) Zhen, J.; Liang, G.; Chen, R.; Jia, W. Label-Free Hairpin-like Aptamer and EIS-Based Practical, Biostable Sensor for Acetamiprid Detection. *PLoS One* **2020**, *15* (12), No. e0244297.
- (141) Vanova, V.; Mitrevska, K.; Milosavljevic, V.; Hynek, D.; Richtera, L.; Adam, V. Peptide-Based Electrochemical Biosensors Utilized for Protein Detection. *Biosens. Bioelectron.* **2021**, *180*, 113087.
- (142) Ucar, A.; González-Fernández, E.; Staderini, M.; Avlonitis, N.; Murray, A. F.; Bradley, M.; Mount, A. R. Miniaturisation of a Peptide-Based Electrochemical Protease Activity Sensor Using Platinum Microelectrodes. *Analyst* **2020**, *145* (3), 975–982.
- (143) Lin, Z.-T.; DeMarr, V.; Bao, J.; Wu, T. Molecularly Imprinted Polymer-Based Biosensors: For the Early, Rapid Detection of Pathogens, Biomarkers, and Toxins in Clinical, Environmental, or Food Samples. *IEEE Nanotechnology Magazine* **2018**, *12* (1), 6–13.
- (144) Onur, P.; Tom, K. S.; Andrew, M.; F, C. V.; Alberto, S. Molecularly Selective Nanoporous Membrane-Based Wearable Organic Electrochemical Device for Noninvasive Cortisol Sensing. *Sci. Adv.* **2022**, *4* (7), No. eaar2904.
- (145) Qiu, G.; Gai, Z.; Tao, Y.; Schmitt, J.; Kullak-Ublick, G. A.; Wang, J. Dual-Functional Plasmonic Photothermal Biosensors for Highly Accurate Severe Acute Respiratory Syndrome Coronavirus 2 Detection. *ACS Nano* **2020**, *14* (5), 5268–5277.
- (146) Long, Q.-X.; Liu, B.-Z.; Deng, H.-J.; Wu, G.-C.; Deng, K.; Chen, Y.-K.; Liao, P.; Qiu, J.-F.; Lin, Y.; Cai, X.-F.; Wang, D.-Q.; Hu, Y.; Ren, J.-H.; Tang, N.; Xu, Y.-Y.; Yu, L.-H.; Mo, Z.; Gong, F.; Zhang, X.-L.; et al. Antibody Responses to SARS-CoV-2 in Patients with COVID-19. *Nature Medicine* **2020**, *26* (6), 845–848.
- (147) Jiang, Y.; Hu, M.; Liu, A.-A.; Lin, Y.; Liu, L.; Yu, B.; Zhou, X.; Pang, D.-W. Detection of SARS-CoV-2 by CRISPR/Cas12a-Enhanced Colorimetry. *ACS Sensors* **2021**, *6* (3), 1086–1093.
- (148) Seo, G.; Lee, G.; Kim, M. J.; Baek, S.-H.; Choi, M.; Ku, K. B.; Lee, C.-S.; Jun, S.; Park, D.; Kim, H. G.; Kim, S.-J.; Lee, J.-O.; Kim, B. T.; Park, E. C.; Kim, S. I. Rapid Detection of COVID-19 Causative Virus (SARS-CoV-2) in Human Nasopharyngeal Swab Specimens Using Field-Effect Transistor-Based Biosensor. *ACS Nano* **2020**, *14* (4), 5135–5142.

- (149) Ding, H.; Yu, S.-B.; Wei, J.-S.; Xiong, H.-M. Full-Color Light-Emitting Carbon Dots with a Surface-State-Controlled Luminescence Mechanism. *ACS Nano* **2016**, *10* (1), 484–491.
- (150) Li, C.; Soleyman, R.; Kohandel, M.; Cappellaro, P. SARS-CoV-2 Quantum Sensor Based on Nitrogen-Vacancy Centers in Diamond. *Nano Lett.* **2022**, *22* (1), 43–49.
- (151) Zhang, Y.; Malekjahani, A.; Udugama, B. N.; Kadhiresan, P.; Chen, H.; Osborne, M.; Franz, M.; Kucera, M.; Plenderleith, S.; Yip, L.; Bader, G. D.; Tran, V.; Gubbay, J. B.; McGeer, A.; Mubareka, S.; Chan, W. C. W. Surveillance and Tracking COVID-19 Patients Using a Portable Quantum Dot Smartphone Device. *Nano Lett.* **2021**, *21* (12), 5209–5216.
- (152) Gorshkov, K.; Susumu, K.; Chen, J.; Xu, M.; Pradhan, M.; Zhu, W.; Hu, X.; Breger, J. C.; Wolak, M.; Oh, E. Quantum Dot-Conjugated SARS-CoV-2 Spike Pseudo-Virions Enable Tracking of Angiotensin Converting Enzyme 2 Binding and Endocytosis. *ACS Nano* **2020**, *14* (9), 12234–12247.
- (153) Huang, L.-J.; Yu, R.-Q.; Chu, X. DNA-Functionalized Upconversion Nanoparticles as Biosensors for Rapid, Sensitive, and Selective Detection of Hg<sup>2+</sup> in Complex Matrices. *Analyst* **2015**, *140* (15), 4987–4990.
- (154) Wei, Q.; Qi, H.; Luo, W.; Tseng, D.; Ki, S. J.; Wan, Z.; Gorocs, Z.; Bentolila, L. A.; Wu, T.-T.; Sun, R.; Ozcan, A. Fluorescent Imaging of Single Nanoparticles and Viruses on a Smart Phone. *ACS Nano* **2013**, *7* (10), 9147–9155.
- (155) Parasa, S.; Desai, M.; Thoguluva Chandrasekar, V.; Patel, H. K.; Kennedy, K. F.; Roesch, T.; Spadaccini, M.; Colombo, M.; Gabbadini, R.; Artifon, E. L. A.; Repici, A.; Sharma, P. Prevalence of Gastrointestinal Symptoms and Fecal Viral Shedding in Patients With Coronavirus Disease 2019: A Systematic Review and Meta-Analysis. *JAMA Network Open* **2020**, *3* (6), No. e2011335.
- (156) Kirby, A. E.; Walters, M. S.; Jennings, W. C.; Fugitt, R.; LaCross, N.; Mattioli, M.; Marsh, Z. A.; Roberts, V. A.; Mercante, J. W.; Yoder, J.; Hill, V. R. Using Wastewater Surveillance Data to Support the COVID-19 Response — United States, 2020–2021. *MMWR Morb Mortal Wkly Rep.* **2021**, *70*, 1242.
- (157) Srivastava, I.; Misra, S. K.; Tripathi, I.; Schwartz-Duval, A.; Pan, D. In Situ Time-Dependent and Progressive Oxidation of Reduced State Functionalities at the Nanoscale of Carbon Nanoparticles for Polarity-Driven Multiscale Near-Infrared Imaging. *Advanced Biosystems* **2018**, *2* (3), 1800009.
- (158) Alafeef, M.; Dighe, K.; Moitra, P.; Pan, D. Monitoring the Viral Transmission of SARS-CoV-2 in Still Waterbodies Using a Lanthanide-Doped Carbon Nanoparticle-Based Sensor Array. *ACS Sustainable Chem. Eng.* **2022**, *10* (1), 245–258.
- (159) Chen, X.; Wan, H.; Guo, R.; Wang, X.; Wang, Y.; Jiao, C.; Sun, K.; Hu, L. A Double-Layered Liquid Metal-Based Electrochemical Sensing System on Fabric as a Wearable Detector for Glucose in Sweat. *Microsystems & Nanoengineering* **2022**, *8* (1), 48.
- (160) Li, R.; Qi, H.; Ma, Y.; Deng, Y.; Liu, S.; Jie, Y.; Jing, J.; He, J.; Zhang, X.; Wheatley, L.; Huang, C.; Sheng, X.; Zhang, M.; Yin, L. A Flexible and Physically Transient Electrochemical Sensor for Real-Time Wireless Nitric Oxide Monitoring. *Nat. Commun.* **2020**, *11* (1), 3207.
- (161) Liu, X.; Huang, L.; Qian, K. Nanomaterial-Based Electrochemical Sensors: Mechanism, Preparation, and Application in Biomedicine. *Advanced NanoBiomed Research* **2021**, *1* (6), 2000104.
- (162) Abdel-Karim, R.; Reda, Y.; Abdel-Fattah, A. Review—Nanostructured Materials-Based Nanosensors. *J. Electrochem. Soc.* **2020**, *167* (3), 037554.
- (163) Holzinger, M.; le Goff, A.; Cosnier, S. Nanomaterials for Biosensing Applications: A Review. *Front. Chem.* **2014**, *2* DOI: 10.3389/fchem.2014.00063
- (164) Zupančič, U.; Jolly, P.; Estrela, P.; Moschou, D.; Ingber, D. E. Graphene Enabled Low-Noise Surface Chemistry for Multiplexed Sepsis Biomarker Detection in Whole Blood. *Adv. Funct. Mater.* **2021**, *31* (16), 2010638.
- (165) Mazouzi, Y.; Sallem, F.; Farina, F.; Loiseau, A.; Rocha Tartaglia, N.; Fontaine, M.; Parikh, A.; Salmain, M.; Neri, C.; Boujday, S. Biosensing Extracellular Vesicle Subpopulations in Neurodegenerative Disease Conditions. *ACS Sensors* **2022**, *7*, 1657–1665.
- (166) Honda, H.; Kusaka, Y.; Wu, H.; Endo, H.; Tsuya, D.; Ohnuki, H. Toward a Practical Impedimetric Biosensor: A Micro-Gap Parallel Plate Electrode Structure That Suppresses Unexpected Device-to-Device Variations. *ACS Omega* **2022**, *7* (13), 11017–11022.
- (167) Lee, J.-H.; Park, S.-J.; Choi, J.-W. Electrical Property of Graphene and Its Application to Electrochemical Biosensing. *Nanomaterials* **2019**, *9*, 297.
- (168) Ghiasi, T. S.; Kaverzin, A. A.; Dismukes, A. H.; de Wal, D. K.; Roy, X.; van Wees, B. J. Electrical and Thermal Generation of Spin Currents by Magnetic Bilayer Graphene. *Nat. Nanotechnol.* **2021**, *16* (7), 788–794.
- (169) Chaibun, T.; Puenpa, J.; Ngamdee, T.; Boonapatcharoen, N.; Athamanolap, P.; O'Mullane, A. P.; Vongpunsawad, S.; Poovorawan, Y.; Lee, S. Y.; Lertanantawong, B. Rapid Electrochemical Detection of Coronavirus SARS-CoV-2. *Nat. Commun.* **2021**, *12* (1), 802.
- (170) Hsu, P. D.; Lander, E. S.; Zhang, F. Development and Applications of CRISPR-Cas9 for Genome Engineering. *Cell* **2014**, *157* (6), 1262–1278.
- (171) Huang, Z.; Tian, D.; Liu, Y.; Lin, Z.; Lyon, C. J.; Lai, W.; Fusco, D.; Drouin, A.; Yin, X.; Hu, T.; Ning, B. Ultra-Sensitive and High-Throughput CRISPR-powered COVID-19 Diagnosis. *Biosens. Bioelectron.* **2020**, *164*, 112316.
- (172) Hajian, R.; Balderston, S.; Tran, T.; deBoer, T.; Etienne, J.; Sandhu, M.; Wauford, N. A.; Chung, J.-Y.; Nokes, J.; Athaiya, M.; Paredes, J.; Peytavi, R.; Goldsmith, B.; Murthy, N.; Conboy, I. M.; Aran, K. Detection of Unamplified Target Genes via CRISPR–Cas9 Immobilized on a Graphene Field-Effect Transistor. *Nature Biomedical Engineering* **2019**, *3* (6), 427–437.
- (173) Rahimi, H.; Salehiabar, M.; Barsbay, M.; Ghaffarlou, M.; Kavetskiy, T.; Sharafi, A.; Davaran, S.; Chauhan, S. C.; Danafar, H.; Kaboli, S.; Nosrati, H.; Yallapu, M. M.; Conde, J. CRISPR Systems for COVID-19 Diagnosis. *ACS Sensors* **2021**, *6* (4), 1430–1445.
- (174) Javalkote, V. S.; Kancharla, N.; Bhadra, B.; Shukla, M.; Soni, B.; Sapre, A.; Goodin, M.; Bandyopadhyay, A.; Dasgupta, S. CRISPR-Based Assays for Rapid Detection of SARS-CoV-2. *Methods* **2022**, *203*, 594–603.
- (175) Kosuru, L.; Bouchaala, A.; Jaber, N.; Younis, M. I. Humidity Detection Using Metal Organic Framework Coated on QCM. *J. Sensors* **2016**, *2016*, 4902790.
- (176) Torad, N. L.; Zhang, S.; Amer, W. A.; Ayad, M. M.; Kim, M.; Kim, J.; Ding, B.; Zhang, X.; Kimura, T.; Yamauchi, Y. Advanced Nanoporous Material-Based QCM Devices: A New Horizon of Interfacial Mass Sensing Technology. *Advanced Materials Interfaces* **2019**, *6* (20), 1900849.
- (177) Grunewald, C.; Schmutde, M.; Noufele, C. N.; Graf, C.; Risse, T. Ordered Structures of Functionalized Silica Nanoparticles on Gold Surfaces: Correlation of Quartz Crystal Microbalance with Structural Characterization. *Anal. Chem.* **2015**, *87* (20), 10642–10649.
- (178) Zhu, Y.; Li, H.; Zheng, Q.; Xu, J.; Li, X. Amine-Functionalized SBA-15 with Uniform Morphology and Well-Defined Mesostructure for Highly Sensitive Chemosensors To Detect Formaldehyde Vapor. *Langmuir* **2012**, *28* (20), 7843–7850.
- (179) Thies, J.-W.; Thürmann, B.; Vierheller, A.; Dietzel, A. Particle-Based Microfluidic Quartz Crystal Microbalance (QCM) Biosensing Utilizing Mass Amplification and Magnetic Bead Convection. *Micromachines* **2018**, *9*, 194.
- (180) Lee, E.; Lee, D.; Yoon, J.; Yin, Y.; Lee, Y. N.; Upreti, S.; Yoon, Y. S.; Kim, D.-J. Enhanced Gas-Sensing Performance of GO/TiO<sub>2</sub> Composite by Photocatalysis. *Sensors* **2018**, *18*, 3334.
- (181) Ember, K. J. I.; Hoeve, M. A.; McAughtrie, S. L.; Bergholt, M. S.; Dwyer, B. J.; Stevens, M. M.; Faulds, K.; Forbes, S. J.; Campbell, C. J. Raman Spectroscopy and Regenerative Medicine: A Review. *npj Regenerative Medicine* **2017**, *2* (1), 12.
- (182) Downes, A.; Elfick, A. Raman Spectroscopy and Related Techniques in Biomedicine. *Sensors* **2010**, *10*, 1871.



- (183) Saletnik, A.; Saletnik, B.; Puchalski, C. Overview of Popular Techniques of Raman Spectroscopy and Their Potential in the Study of Plant Tissues. *Molecules* **2021**, *26*, 1537.
- (184) Berthomieu, C.; Hienerwadel, R. Fourier Transform Infrared (FTIR) Spectroscopy. *Photosynthesis Research* **2009**, *101* (2), 157–170.
- (185) Vogt, S.; Löffler, K.; Dinkelacker, A. G.; Bader, B.; Autenrieth, I. B.; Peter, S.; Liese, J. Fourier-Transform Infrared (FTIR) Spectroscopy for Typing of Clinical Enterobacter Cloacae Complex Isolates. *Front. Microbiol.* **2019**, *10* DOI: 10.3389/fmicb.2019.02582
- (186) Baker, M. J.; Trevisan, J.; Bassan, P.; Bhargava, R.; Butler, H. J.; Dorling, K. M.; Fielden, P. R.; Fogarty, S. W.; Fullwood, N. J.; Heys, K. A.; Hughes, C.; Lasch, P.; Martin-Hirsch, P. L.; Obinaju, B.; Sockalingum, G. D.; Sulé-Suso, J.; Strong, R. J.; Walsh, M. J.; Wood, B. R.; et al. Using Fourier Transform IR Spectroscopy to Analyze Biological Materials. *Nat. Protoc.* **2014**, *9* (8), 1771–1791.
- (187) Hadoux, X.; Hui, F.; Lim, J. K. H.; Masters, C. L.; Pébay, A.; Chevalier, S.; Ha, J.; Loi, S.; Fowler, C. J.; Rowe, C.; Villemagne, V. L.; Taylor, E. N.; Fluke, C.; Soucy, J.-P.; Lesage, F.; Sylvestre, J.-P.; Rosa-Neto, P.; Mathotaarachchi, S.; Gauthier, S.; et al. Non-Invasive in Vivo Hyperspectral Imaging of the Retina for Potential Biomarker Use in Alzheimer's Disease. *Nat. Commun.* **2019**, *10* (1), 4227.
- (188) Li, H.; Liu, W.; Dong, B.; Kaluzny, J. v; Fawzi, A. A.; Zhang, H. F. Snapshot Hyperspectral Retinal Imaging Using Compact Spectral Resolving Detector Array. *Journal of Biophotonics* **2017**, *10* (6–7), 830–839.
- (189) Chandran Suja, V.; Sentmanat, J.; Hofmann, G.; Scales, C.; Fuller, G. G. Hyperspectral Imaging for Dynamic Thin Film Interferometry. *Sci. Rep.* **2020**, *10* (1), 11378.
- (190) Misra, S. K.; Ostadhossein, F.; Daza, E.; Johnson, E. v; Pan, D. Hyperspectral Imaging Offers Visual and Quantitative Evidence of Drug Release from Zwitterionic-Phospholipid-Nanocarbon When Concurrently Tracked in 3D Intracellular Space. *Adv. Funct. Mater.* **2016**, *26* (44), 8031–8041.
- (191) Chen, H.; Park, S.-G.; Choi, N.; Kwon, H.-J.; Kang, T.; Lee, M.-K.; Choo, J. Sensitive Detection of SARS-CoV-2 Using a SERS-Based Aptasensor. *ACS Sensors* **2021**, *6* (6), 2378–2385.
- (192) Moitra, P.; Chaichi, A.; Abid Hasan, S. M.; Dighe, K.; Alafeef, M.; Prasad, A.; Gartia, M. R.; Pan, D. Probing the Mutation Independent Interaction of DNA Probes with SARS-CoV-2 Variants through a Combination of Surface-Enhanced Raman Scattering and Machine Learning. *Biosens. Bioelectron.* **2022**, *208*, 114200.
- (193) Kitane, D. L.; Loukman, S.; Marchoudi, N.; Fernandez-Galiana, A.; el Ansari, F. Z.; Jouali, F.; Badir, J.; Gala, J.-L.; Bertsimas, D.; Azami, N.; Lakbita, O.; Moudam, O.; Benhida, R.; Fekkak, J. A Simple and Fast Spectroscopy-Based Technique for COVID-19 Diagnosis. *Sci. Rep.* **2021**, *11* (1), 16740.
- (194) Aboughaleb, I. H.; Aref, M. H.; El-Sharkawy, Y. H. Hyperspectral Imaging for Diagnosis and Detection of Ex-Vivo Breast Cancer. *Photodiagnosis and Photodynamic Therapy* **2020**, *31*, 101922.
- (195) Lu, G.; Little, J. v; Wang, X.; Zhang, H.; Patel, M. R.; Griffith, C. C.; El-Deiry, M. W.; Chen, A. Y.; Fei, B. Detection of Head and Neck Cancer in Surgical Specimens Using Quantitative Hyperspectral Imaging. *Clin. Cancer Res.* **2017**, *23* (18), 5426–5436.
- (196) Wang, X.; Cui, Y.; Irudayaraj, J. Single-Cell Quantification of Cytosine Modifications by Hyperspectral Dark-Field Imaging. *ACS Nano* **2015**, *9* (12), 11924–11932.
- (197) Halicek, M.; Fabelo, H.; Ortega, S.; Callico, G. M.; Fei, B. In-Vivo and Ex-Vivo Tissue Analysis through Hyperspectral Imaging Techniques: Revealing the Invisible Features of Cancer. *Cancers* **2019**, *11*, 756.
- (198) Fei, B.; Lu, G.; Wang, X.; Zhang, H.; Little, J. v; Patel, M. R.; Griffith, C. C.; El-Deiry, M. W.; Chen, A. Y. Label-Free Reflectance Hyperspectral Imaging for Tumor Margin Assessment: A Pilot Study on Surgical Specimens of Cancer Patients. *J. Biomed Opt* **2017**, *22* (8), 1–7.
- (199) Min, C.; Shao, H.; Liang, M.; Yoon, T.-J.; Weissleder, R.; Lee, H. Mechanism of Magnetic Relaxation Switching Sensing. *ACS Nano* **2012**, *6* (8), 6821–6828.
- (200) Li, Y.; Ma, P.; Tao, Q.; Krause, H. J.; Yang, S.; Ding, G.; Dong, H.; Xie, X. Magnetic Graphene Quantum Dots Facilitate Closed-Tube One-Step Detection of SARS-CoV-2 with Ultra-Low Field NMR Relaxometry. *Sens. Actuators, B* **2021**, *337*, 129786.
- (201) Bloom, J. S.; Sathe, L.; Munugala, C.; Jones, E. M.; Gasperini, M.; Lubock, N. B.; Yarza, F.; Thompson, E. M.; Kovary, K. M.; Park, J.; Marquette, D.; Kay, S.; Lucas, M.; Love, T.; Sina Boeshaghi, A.; Brandenburg, O. F.; Guo, L.; Boocock, J.; Hochman, M.; Simpkins, S. W.; Lin, I.; LaPierre, N.; Hong, D.; Zhang, Y.; Oland, G.; Choe, B. J.; Chandrasekaran, S.; Hilt, E. E.; Butte, M. J.; Damoiseaux, R.; Kravitz, C.; Cooper, A. R.; Yin, Y.; Pachter, L.; Garner, O. B.; Flint, J.; Eskin, E.; Luo, C.; Kosuri, S.; Kruglyak, L.; Arboleda, V. A. Massively Scaled-up Testing for SARS-CoV-2 RNA via next-Generation Sequencing of Pooled and Barcoded Nasal and Saliva Samples. *Nature Biomedical Engineering* **2021**, *5* (7), 657–665.
- (202) Aynaud, M.-M.; Hernandez, J. J.; Barutcu, S.; Braunschweig, U.; Chan, K.; Pearson, J. D.; Trcka, D.; Prosser, S. L.; Kim, J.; Barrios-Rodiles, M.; Jen, M.; Song, S.; Shen, J.; Bruce, C.; Hazlett, B.; Poutanen, S.; Attisano, L.; Bremner, R.; Blencowe, B. J.; et al. A Multiplexed, next Generation Sequencing Platform for High-Throughput Detection of SARS-CoV-2. *Nat. Commun.* **2021**, *12* (1), 1405.
- (203) Sethuraman, N.; Jeremiah, S. S.; Ryo, A. Interpreting Diagnostic Tests for SARS-CoV-2. *JAMA* **2020**, *323* (22), 2249–2251.
- (204) Wang, W.; Xu, Y.; Gao, R.; Lu, R.; Han, K.; Wu, G.; Tan, W. Detection of SARS-CoV-2 in Different Types of Clinical Specimens. *JAMA* **2020**, *323* (18), 1843–1844.
- (205) Gunson, R. N.; Collins, T. C.; Carman, W. F. Practical Experience of High Throughput Real Time PCR in the Routine Diagnostic Virology Setting. *Journal of Clinical Virology* **2006**, *35* (4), 355–367.
- (206) Hosseiny, M.; Kooraki, S.; Gholamrezanezhad, A.; Reddy, S.; Myers, L. Radiology Perspective of Coronavirus Disease 2019 (COVID-19): Lessons From Severe Acute Respiratory Syndrome and Middle East Respiratory Syndrome. *American Journal of Roentgenology* **2020**, *214* (5), 1078–1082.
- (207) Wong, H. Y. F.; Lam, H. Y. S.; Fong, A. H.-T.; Leung, S. T.; Chin, T. W.-Y.; Lo, C. S. Y.; Lui, M. M.-S.; Lee, J. C. Y.; Chiu, K. W.-H.; Chung, T. W.-H.; Lee, E. Y. P.; Wan, E. Y. F.; Hung, I. F. N.; Lam, T. P. W.; Kuo, M. D.; Ng, M.-Y. Frequency and Distribution of Chest Radiographic Findings in Patients Positive for COVID-19. *Radiology* **2020**, *296* (2), E72–E78.
- (208) Dennie, C.; Hague, C.; Lim, R. S.; Manos, D.; Memauri, B. F.; Nguyen, E. T.; Taylor, J. Canadian Society of Thoracic Radiology/Canadian Association of Radiologists Consensus Statement Regarding Chest Imaging in Suspected and Confirmed COVID-19. *Canadian Association of Radiologists Journal* **2020**, *71* (4), 470–481.
- (209) Ojha, V.; Verma, M.; Pandey, N. N.; Mani, A.; Malhi, A. S.; Kumar, S.; Jagia, P.; Roy, A.; Sharma, S. Cardiac Magnetic Resonance Imaging in Coronavirus Disease 2019 (COVID-19): A Systematic Review of Cardiac Magnetic Resonance Imaging Findings in 199 Patients. *Journal of Thoracic Imaging* **2021**, *36* (2), 73.
- (210) Vasilev, Y. A.; Sergunova, K. A.; Bazhin, A. v; Masri, A. G.; Vasileva, Y. N.; Semenov, D. S.; Kudryavtsev, N. D.; Panina, O. Y.; Khoruzhaya, A. N.; Zinchenko, V. v; Akhmad, E. S.; Petraikin, A. v; Vladzimirskyy, A. v; Midaev, A. v; Morozov, S. P. Chest MRI of Patients with COVID-19. *Magn. Reson. Imaging* **2021**, *79*, 13–19.
- (211) Yang, H.-Y.; Wang, Y.-C.; Peng, H.-Y.; Huang, C.-H. Breath Biopsy of Breast Cancer Using Sensor Array Signals and Machine Learning Analysis. *Sci. Rep.* **2021**, *11* (1), 103.
- (212) Ferrandino, G.; Orf, I.; Smith, R.; Calcagno, M.; Thind, A. K.; Debram-Beecham, I.; Williams, M.; Gandelman, O.; de Saedeleer, A.; Kibble, G.; Lydon, A. M.; Mayhew, C. A.; Allsworth, M.; Boyle, B.; van der Schee, M. P.; Allison, M.; Hoare, M.; Snowdon, V. K. Breath Biopsy Assessment of Liver Disease Using an Exogenous Volatile Organic Compound—Toward Improved Detection of Liver Impairment. *Clinical and Translational Gastroenterology* **2020**, *11* (9), e00239.



- (213) Moria, L.; Sondra, T.; M, P. J.; Orna, B.; Omry, K.; Jotham, S. Pathophysiology of SARS-CoV-2 Infection in the Upper Respiratory Tract and Its Relation to Breath Volatile Organic Compounds. *mSystems* **2022**, *6* (4), No. e00104-21.
- (214) Fenske, J. D.; Paulson, S. E. Human Breath Emissions of VOCs. *J. Air Waste Manage Assoc* **1999**, *49* (5), 594–598.
- (215) Phillips, M.; Gleeson, K.; Hughes, J. M. B.; Greenberg, J.; Cataneo, R. N.; Baker, L.; McVay, W. P. Volatile Organic Compounds in Breath as Markers of Lung Cancer: A Cross-Sectional Study. *Lancet* **1999**, *353* (9168), 1930–1933.
- (216) Miekisch, W.; Schubert, J. K.; Noeldge-Schomburg, G. F. E. Diagnostic Potential of Breath Analysis—Focus on Volatile Organic Compounds. *Clin. Chim. Acta* **2004**, *347* (1), 25–39.
- (217) Giovannini, G.; Haick, H.; Garoli, D. Detecting COVID-19 from Breath: A Game Changer for a Big Challenge. *ACS Sensors* **2021**, *6* (4), 1408–1417.
- (218) Chen, H.; Qi, X.; Zhang, L.; Li, X.; Ma, J.; Zhang, C.; Feng, H.; Yao, M. COVID-19 Screening Using Breath-Borne Volatile Organic Compounds. *J. Breath Res.* **2021**. DOI: 10.1088/1752-7163/ac2e57.
- (219) Leong, S. X.; Leong, Y. X.; Tan, E. X.; Sim, H. Y. F.; Koh, C. S. L.; Lee, Y. H.; Chong, C.; Ng, L. S.; Chen, J. R. T.; Pang, D. W. C.; Nguyen, L. B. T.; Boong, S. K.; Han, X.; Kao, Y.-C.; Chua, Y. H.; Phan-Quang, G. C.; Phang, I. Y.; Lee, H. K.; Abdad, M. Y.; Tan, N. S.; Ling, X. Y. Noninvasive and Point-of-Care Surface-Enhanced Raman Scattering (SERS)-Based Breathalyzer for Mass Screening of Coronavirus Disease 2019 (COVID-19) under 5 min. *ACS Nano* **2022**, *16* (2), 2629–2639.
- (220) Snitz, K.; Andelman-Gur, M.; Pinchover, L.; Weissgross, R.; Weissbrod, A.; Mishor, E.; Zoller, R.; Linetsky, V.; Medhanie, A.; Shushan, S.; Jaffe, E.; Sobel, N. Proof of Concept for Real-Time Detection of SARS CoV-2 Infection with an Electronic Nose. *PLoS One* **2021**, *16* (6), No. e0252121.
- (221) Broza, Y. Y.; Haick, H. Biodiagnostics in an Era of Global Pandemics—From Biosensing Materials to Data Management. *VIEW* **2022**, *3* (2), 20200164.
- (222) Haick, H.; Tang, N. Artificial Intelligence in Medical Sensors for Clinical Decisions. *ACS Nano* **2021**, *15* (3), 3557–3567.
- (223) Lamote, K.; Janssens, E.; Schillebeeckx, E.; Lapperre, T. S.; de Winter, B. Y.; van Meerbeeck, J. P. The Scent of COVID-19: Viral (Semi-)Volatiles as Fast Diagnostic Biomarkers? *Journal of Breath Research* **2020**, *14* (4), 042001.
- (224) Ma, J.; Qi, X.; Chen, H.; Li, X.; Zhang, Z.; Wang, H.; Sun, L.; Zhang, L.; Guo, J.; Morawska, L.; Grinshpun, S. A.; Biswas, P.; Flagan, R. C.; Yao, M. Coronavirus Disease 2019 Patients in Earlier Stages Exhaled Millions of Severe Acute Respiratory Syndrome Coronavirus 2 Per Hour. *Clinical Infectious Diseases* **2021**, *72* (10), e652–e654.
- (225) Moitra, P.; Alafeef, M.; Dighe, K.; Ray, P.; Chang, J.; Thole, A.; Punshon-Smith, B.; Tolosa, M.; Ramamurthy, S. S.; Ge, X.; Frey, D. D.; Pan, D.; Rao, G. Rapid and Low-Cost Sampling for Detection of Airborne SARS-CoV-2 in Dehumidifier Condensate. *Biotechnol. Bioeng.* **2021**, *118* (8), 3029–3036.
- (226) Alafeef, M. Smartphone-Based Photoplethysmographic Imaging for Heart Rate Monitoring. *Journal of Medical Engineering & Technology* **2017**, *41* (5), 387–395.
- (227) Alafeef, M.; Fraiwan, M. On the Diagnosis of Idiopathic Parkinson's Disease Using Continuous Wavelet Transform Complex Plot. *Journal of Ambient Intelligence and Humanized Computing* **2019**, *10* (7), 2805–2815.
- (228) Alafeef, M.; Fraiwan, M. Smartphone-Based Respiratory Rate Estimation Using Photoplethysmographic Imaging and Discrete Wavelet Transform. *Journal of Ambient Intelligence and Humanized Computing* **2020**, *11* (2), 693–703.
- (229) Hadoush, H.; Alafeef, M.; Abdulhay, E. Brain Complexity in Children with Mild and Severe Autism Spectrum Disorders: Analysis of Multiscale Entropy in EEG. *Brain Topography* **2019**, *32* (5), 914–921.
- (230) Alafeef, M.; Srivastava, I.; Pan, D. Machine Learning for Precision Breast Cancer Diagnosis and Prediction of the Nanoparticle Cellular Internalization. *ACS Sensors* **2020**, *5* (6), 1689–1698.
- (231) Hadoush, H.; Alafeef, M.; Abdulhay, E. Automated Identification for Autism Severity Level: EEG Analysis Using Empirical Mode Decomposition and Second Order Difference Plot. *Behavioural Brain Research* **2019**, *362*, 240–248.
- (232) Abdulhay, E.; Alafeef, M.; Hadoush, H.; Arunkumar, N. Resting State EEG-Based Diagnosis of Autism via Elliptic Area of Continuous Wavelet Transform Complex Plot. *Journal of Intelligent & Fuzzy Systems* **2020**, *39*, 8599–8607.
- (233) Abdulhay, E.; Alafeef, M.; Hadoush, H.; N, A. Autism Diagnosis via Correlation between Vectors of Direct Quadrature Instantaneous Frequency of EEG Analytic Normalized Intrinsic Mode Functions. *Expert Systems* **2022**, *39* (3), No. e12801.
- (234) Alafeef, M.; Fraiwan, M.; Alkhalaf, H.; Audat, Z. Shannon Entropy and Fuzzy C-Means Weighting for AI-Based Diagnosis of Vertebral Column Diseases. *Journal of Ambient Intelligence and Humanized Computing* **2020**, *11* (6), 2557–2566.
- (235) Abdulhay, E.; Alafeef, M.; Abdelhay, A.; Al-Bashir, A. Classification of Normal, Ictal and Inter-Ictal EEG via Direct Quadrature and Random Forest Tree. *Journal of Medical and Biological Engineering* **2017**, *37* (6), 843–857.
- (236) Hadoush, H.; Nazzal, M.; Almasri, N. A.; Khalil, H.; Alafeef, M. Therapeutic Effects of Bilateral Anodal Transcranial Direct Current Stimulation on Prefrontal and Motor Cortical Areas in Children with Autism Spectrum Disorders: A Pilot Study. *Autism Research* **2020**, *13* (5), 828–836.
- (237) Abdulhay, E.; Alafeef, M.; Alzghoul, L.; al Momani, M.; al Abdi, R.; Arunkumar, N.; Munoz, R.; de Albuquerque, V. H.C. Computer-Aided Autism Diagnosis via Second-Order Difference Plot Area Applied to EEG Empirical Mode Decomposition. *Neural Computing and Applications* **2020**, *32* (15), 10947–10956.
- (238) Zheng, Y.; Tang, N.; Omar, R.; Hu, Z.; Duong, T.; Wang, J.; Wu, W.; Haick, H. Smart Materials Enabled with Artificial Intelligence for Healthcare Wearables. *Adv. Funct. Mater.* **2021**, *31* (51), 2105482.
- (239) Einoch-Amor, R.; Broza, Y. Y.; Haick, H. Detection of Single Cancer Cells in Blood with Artificially Intelligent Nanoarray. *ACS Nano* **2021**, *15* (4), 7744–7755.
- (240) S, D. M.; Anish, V.; Aradana, M.; Kumar, K. M.; Prudhvi, T.; Aparna, S.; Sanchana, K.; Vinish, Y.; Wenyu, L.; G, Y. X.; T, C. R.; Hadi, S. Virus Detection Using Nanoparticles and Deep Neural Network-Enabled Smartphone System. *Sci. Adv.* **2022**, *6* (51), No. eabd5354.
- (241) Alavi, A.; Bogu, G. K.; Wang, M.; Rangan, E. S.; Brooks, A. W.; Wang, Q.; Higgs, E.; Celli, A.; Mishra, T.; Metwally, A. A.; Cha, K.; Knowles, P.; Alavi, A. A.; Bhasin, R.; Panchamukhi, S.; Celis, D.; Aditya, T.; Honkala, A.; Rolnik, B.; et al. Real-Time Alerting System for COVID-19 and Other Stress Events Using Wearable Data. *Nature Medicine* **2022**, *28* (1), 175–184.
- (242) Mishra, T.; Wang, M.; Metwally, A. A.; Bogu, G. K.; Brooks, A. W.; Bahmani, A.; Alavi, A.; Celli, A.; Higgs, E.; Dagan-Rosenfeld, O.; Fay, B.; Kirkpatrick, S.; Kellogg, R.; Gibson, M.; Wang, T.; Hunting, E. M.; Mamic, P.; Ganz, A. B.; Rolnik, B.; et al. Pre-Symptomatic Detection of COVID-19 from Smartwatch Data. *Nature Biomedical Engineering* **2020**, *4* (12), 1208–1220.
- (243) Subsoontorn, P.; Lohitnavy, M.; Kongkaew, C. The Diagnostic Accuracy of Isothermal Nucleic Acid Point-of-Care Tests for Human Coronaviruses: A Systematic Review and Meta-Analysis. *Sci. Rep.* **2020**, *10* (1), 22349.
- (244) Kostoulas, P.; Eusebi, P.; Hartnack, S. Diagnostic Accuracy Estimates for COVID-19 Real-Time Polymerase Chain Reaction and Lateral Flow Immunoassay Tests With Bayesian Latent-Class Models. *American Journal of Epidemiology* **2021**, *190* (8), 1689–1695.
- (245) Corman, V. M.; Haage, V. C.; Bleicker, T.; Schmidt, M. L.; Mühlemann, B.; Zuchowski, M.; Jo, W. K.; Tscheak, P.; Möncke-Buchner, E.; Müller, M. A.; Krumbholz, A.; Drexler, J. F.; Drosten, C. Comparison of Seven Commercial SARS-CoV-2 Rapid Point-of-Care

Antigen Tests: A Single-Centre Laboratory Evaluation Study. *Lancet Microbe* **2021**, *2* (7), e311–e319.

(246) Liangou, A.; Tasoglou, A.; Huber, H. J.; Wistrom, C.; Brody, K.; Menon, P. G.; Bebekoski, T.; Menschel, K.; Davidson-Fiedler, M.; DeMarco, K.; Salphale, H.; Wistrom, J.; Wistrom, S.; Lee, R. J. A Method for the Identification of COVID-19 Biomarkers in Human Breath Using Proton Transfer Reaction Time-of-Flight Mass Spectrometry. *eClinicalMedicine* **2021**, *42*, 101207.

(247) Ruskiewicz, D. M.; Sanders, D.; O'Brien, R.; Hempel, F.; Reed, M. J.; Riepe, A. C.; Bailie, K.; Brodrick, E.; Darnley, K.; Ellerkmann, R.; Mueller, O.; Skarysz, A.; Truss, M.; Wortelmann, T.; Yordanov, S.; Thomas, C. L. P.; Schaaf, B.; Eddleston, M. Diagnosis of COVID-19 by Analysis of Breath with Gas Chromatography-Ion Mobility Spectrometry - a Feasibility Study. *eClinicalMedicine* **2020**, *29*. DOI: 10.1016/j.eclinm.2020.100609.

(248) Varadarajan, V.; Shabani, M.; Ambale Venkatesh, B.; Lima, J. A. C. Role of Imaging in Diagnosis and Management of COVID-19: A Multiorgan Multimodality Imaging Review. *Front. Med.* **2021**, *8* DOI: 10.3389/fmed.2021.765975

(249) Vandenberg, O.; Martiny, D.; Rochas, O.; van Belkum, A.; Kozlakidis, Z. Considerations for Diagnostic COVID-19 Tests. *Nature Reviews Microbiology* **2021**, *19* (3), 171–183.

## Recommended by ACS

### Diagnostic, Prognostic, and Therapeutic Use of Radiopharmaceuticals in the Context of SARS-CoV-2

Roger M. Pallares and Rebecca J. Abergel

JANUARY 15, 2021  
ACS PHARMACOLOGY & TRANSLATIONAL SCIENCE

READ 

### COVID-19 Diagnostics: Past, Present, and Future

Alexis Scholtz, Andrea M. Armani, *et al.*

SEPTEMBER 15, 2021  
ACS PHOTONICS

READ 

### Diagnosing COVID-19: The Disease and Tools for Detection

Buddhisha Udugama, Warren C. W. Chan, *et al.*

MARCH 30, 2020  
ACS NANO

READ 

### Developing nations face COVID-19 diagnostic challenges

Mark Peplow, special to C&EN.

JULY 13, 2020  
C&EN GLOBAL ENTERPRISE

READ 

Get More Suggestions >